LA-6201-MS
Informal Report

c. 3

UC-32
Reporting Date: January 1976
Issued: February 1976

TIMEX : A Time-Dependent Explicit Discrete Ordinates Program for the Solution of Multigroup Transport Equations with Delayed Neutrons

by

T. R. Hill
Wm. H. Reed

los alamos
scientific laboratory
of the University of California
LOS ALAMOS, NEW MEXICO 87545

An Affirmative Action/Equal Opportunity Employer

UNITED STATES
ENERGY RESEARCH AND DEVELOPMENT ADMINISTRATION
CONTRACT W-7405-ENG. 36

In the interest of prompt distribution, this report was not edited by the Technical Information staff.

Printed in the United States of America. Available from
National Technical Information Service
U.S. Department of Commerce
5285 Port Royal Road
Springfield, VA 22151
Price: Printed Copy $6.00 Microfiche $2.25

TABLE OF CONTENTS

	Page
ABSTRACT	1
I. INTRODUCTION	2
II. THEORY	2
A. The Analytic Transport Equation	3
1. Particular Forms of the Divergence Operator	3
2. Spherical Harmonics Expansion of the Source Term	3
B. Energy, Time, and Angular Approximations	6
1. Multigroup Equations	6
2. Discretization of the Time Variable	7
3. Discrete Ordinates Equations	8
a. Plane Geometry	8
b. Cylindrical Geometry	9
c. Spherical Geometry	10
d. Diamond Difference Assumption and Starting Directions	10
C. Discretization of the Spatial Variable	10
D. Solution Algorithms	14
1. Boundary Conditions	14
2. Sweep of the Space-Angle Mesh	15
3. Negative Flux Fixup	15
4. Adjoint Problems	16
5. Acceleration Methods	16
a. Exponential Extrapolation	16
b. Within-group Fine-Mesh Rebalance	18
c. Outer Rebalance	19
6. First-Collision Source	20
7. Moving Boundaries	22
III. A GUIDE TO USER APPLICATION	22
A. Overall Program Flow	22
B. Details of Program Options	22
1. Cross Sections	22
a. Input Formats	22
b. Cross-Section Mixing	24
c. Anisotropic Cross Sections	24
d. Adjoint Cross Sections	25
e. Cross-Section Checking	25
f. Fission Fractions	25
g. (n,2n) Reactions	25
h. Fine-Mesh Density Factors	25
i. Delayed Neutron Parameters	26
2. Geometry and Boundary Condition Specifications	26
a. Spatial Mesh	26
b. Boundary Conditions	26

TABLE OF CONTENTS (continued)

		Page
	c. Buckling Absorption	27
3.	Angular Quadrature Coefficient Specifications	27
4.	Source Options	28
5.	Source Input Options	28
6.	Initial Condition Specification	29
7.	Flux Dumps and Restart Procedures	29
8.	Adjoint Computations	30
9.	Edit Options	30
10.	Time-Zone Control Parameters	31
11.	Movie Option	32
C.	Data Input Rules	32
D.	Description of Input Data	33
1.	Job Title Cards	33
2.	Input of Control Numbers	33
3.	Problem-Dependent Data	35
4.	Zone-Edit Input	37
5.	Time-Zone Control Input	38
E.	Output Description for a Test Problem	38
IV.	PROGRAMMING INFORMATION	57
A.	Program Structure	57
1.	Role and Function of Subprograms	57
2.	Relation of Problem Variables and Program Mnemonics	57
3.	Definition of Variables in Common Blocks	57
4.	Machine-Dependent Subprograms	67
	a. LCM System Routines	67
	b. General System Routines	67
B.	External and Internal Data Files	67
C.	Hardware Requirements	67
D.	Software Requirements	67
1.	CDC Machines	67
2.	TIMEX for the IBM-360	69
E.	Programming Considerations	69
1.	Storage Management	69
	a. Variable Dimensioning	69
	b. Allocation of Large Core Memory (LCM)	69
	c. Computation of Required Storage	70
	d. Temporary Storage Requirements	71
	e. Overstorage of Data in Core	71
2.	Restart Tape Composition	71
3.	Standard Interface Files	71
F.	Time-Dependent Sources and Cross Sections	71
G.	TIMEX Problems with Feedback	72
REFERENCES		72

LIST OF FIGURES

		Page
Figure 1	Coordinates in plane geometry.	4
Figure 2	Coordinates in cylindrical geometry.	4
Figure 3	Coordinates in spherical geometry.	4
Figure 4	Ordering of S_6 directions in plane and spherical geometries.	8
Figure 5	Ordering of S_6 directions in cylindrical geometry	9
Figure 6	Ordering of S_4 directions in two-angle plane geometry.	9
Figure 7	Linear discontinuous representation of the angular flux in the i^{th} mesh cell.	11
Figure 8	Angular flux nodal values for the i,m (space, angle) mesh cell.	12
Figure 9	Simplified logical flow diagram for TIMEX.	23

LIST OF TABLES

		Page
Table I	Forms of $\nabla \cdot \underline{\Omega}\psi$	4
Table II	Tabular Array of Spherical Harmonics: P_n^{ℓ}	6
Table III	Spherical Harmonics Storage: Cylindrical Geometry	6
Table IV	Spherical Harmonics Storage: Two-Angle Plane Geometry	6
Table V	Table of Geometric Functions	14
Table VI	Analytic Uncollided Flux	21
Table VII	Time-Zone Control Parameters	32
Table VIII	Options for Special Read Formats in LOAD	33
Table IX	Function of TIMEX Subroutines	57
Table X	Relation of Problem Variables to Program Mnemonics	59
Table XI	Contents of Blank Common Block IA	60
Table XII	Contents of Named Common Block/UNITS/	67
Table XIII	TIMEX File Requirements	68
Table XIV	LCM Storage Parameters	70

TIMEX:
A TIME-DEPENDENT EXPLICIT DISCRETE ORDINATES PROGRAM FOR THE SOLUTION OF MULTIGROUP TRANSPORT EQUATIONS WITH DELAYED NEUTRONS

by

T. R. Hill and Wm. H. Reed

ABSTRACT

1. Program Identification: TIMEX

2. Computer for which Program is Designed: CDC 7600, IBM-360

3. Description of Function: TIMEX solves the time-dependent, one-dimensional multigroup transport equation with delayed neutrons in plane, cylindrical, spherical, and two-angle plane geometries. Both regular and adjoint, inhomogeneous and homogeneous problems subject to vacuum, reflective, periodic, white, albedo or inhomogeneous boundary flux conditions are solved. General anisotropic scattering is allowed and anisotropic inhomogeneous sources are permitted.

4. Method of Solution: The discrete ordinates approximation for the angular variable is used with the diamond (central) difference approximation for the angular extrapolation in curved geometries. A linear discontinuous finite element representation for the angular flux in each spatial mesh cell is used. Negative fluxes are eliminated by a local set-to-zero and correct algorithm. The time variable is differenced by an explicit technique that is unconditionally stable so that arbitrarily large time steps can be taken. Because no iteration is performed the method is exceptionally fast in terms of computing time per time step. Two acceleration methods, exponential extrapolation and rebalance, are utilized to improve the accuracy of the time differencing scheme.

5. Restrictions: Variable dimensioning is used so that any combination of problem parameters leading to a container array less than MAXCOR can be accommodated. On CDC machines MAXCOR can be about 25 000 words and peripheral storage is used for most group-dependent data.

6. Running Time: The running time for TIMEX is highly problem-dependent, but varies almost linearly with the total number of unknowns and time steps. A 16-group, 30 interval mesh, S_2, six delayed neutron groups calculation of the decay of a point burst in a Pu-Be sphere requires 4½ min. on the CDC 7600 for 200 time steps.

7. Unusual Features of the Program: Provision is made for creation of standard interface output files for angular fluxes and angle-integrated fluxes. Standard interface input files for S_N constants, inhomogeneous sources, cross sections, and initial angular fluxes may be read. A special angular flux file is available to provide exact initial conditions. All binary operations are localized in subroutines REED and RITE. Flexible edit options, including restart capability, are provided.

8. Machine Requirements: Five interface units (use of interface units is optional), five output units, and two system input/output units are required. A large bulk memory is desirable, but may be replaced by disk, drum, or tape storage.

9. Related Programs: The ONETRAN program may be utilized to provide compatible initial conditions to TIMEX.

10. Material Available: Source deck, test problems, results of executed test problems, and this report are available from the Argonne Code Center and the Oak Ridge Radiation Shielding Information Center.

I. INTRODUCTION

TIMEX is a program designed to solve the time-dependent one-dimensional multigroup transport equation with delayed neutrons in plane, cylindrical, spherical, and two-angle plane geometries. The program solves both regular and adjoint, homogeneous and inhomogeneous, time-dependent problems subject to a variety of boundary conditions.

TIMEX utilizes a discontinuous linear finite elment scheme for discretization of the spatial variable that interacts extremely well with the differencing of the time variable.[1] The ONETRAN[2] steady-state code may be used to provide compatible initial conditions to TIMEX.

The TIMEX code produces meaningful results in both wave and diffusion situations. Wave situations are characterized by spatial discontinuities in the neutron flux that propagate with the velocity of the neutrons and are important over short time intervals. A diffusion situation occurs when scattering is important and when the neutron flux is smooth and varies slowly. A typical time-dependent transport problem can involve a progression through a wave-like regime in the initial stages of a problem to a diffusion situation after all of the wavefronts have dissipated.

An instantaneous point source of neutrons in a sphere represents the ultimate in wavefront behavior. Here the solution is a series of shells of neutrons propagating outward with velocities characteristic of each energy group. Inside the outermost shell lies a continuum of neutrons that have suffered one or more collisions. To treat such a difficult problem, a first-collision source option is included in TIMEX. Under this option an analytic representation of the uncollided flux is used to generate a source to the collided flux, which is calculated numerically by the code. This approach improves the accuracy of the code in the above situation. A first-collision source is also available to treat instantaneous plane sources in slabs and line sources in cylinders. The major features of TIMEX include:

(1) direct and adjoint capability,

(2) plane, cylindrical, spherical, and two-angle plane geometry options,

(3) arbitrary anisotropic scattering order,

(4) two different sets of built-in S_N constants,

(5) vacuum, reflective, periodic, white, albedo, and inhomogeneous boundary conditions,

(6) optional print suppress of large input arrays,

(7) core dump and restart capability at selected time steps,

(8) flexible input of initial conditions,

(9) flexible input of isotropic or anisotropic inhomogeneous distributed sources and boundary sources,

(10) user choice of a single fission spectrum, zone-dependent fission spectra, a single fission matrix, or zone-dependent fission matrices,

(11) optional input of initial flux condition, inhomogeneous distributed and boundary sources, S_N constants, and cross sections from standard interface files,[3]

(12) optional FIDO format[4] input of cross sections,

(13) detailed editing capability,

(14) ability to load new system properties (cross sections, sources, radii, velocities, densities, etc.) at selected times,

(15) energy-group-dependent time step sizes,

(16) optional specification of a pointwise density for cross-section spatial dependence,

(17) a group-at-a-time storage of fluxes and cross sections to permit execution of exceptionally large problems,

(18) use of either or both acceleration devices (rebalance and exponential extrapolation) to improve accuracy, and

(19) zone-dependent delayed neutron properties.

The next section of this report contains the theoretical development of all methods and approximations used in TIMEX. Section III is a user's guide for preparation of TIMEX input and Sec. IV contains detailed programming information to facilitate local modification of the code. The contents of this report follow the guidelines[5] for documentation of digital computer programs accepted as an American Nuclear Society standard.

II. THEORY

In this section, the time, energy, angular, and spatial variables of the transport equation are discretized to obtain a set of linear algebraic equations. The exact transport equation is discussed and the spherical harmonics expansion of the scattering sources is performed in Sec. II.A. The multigroup treatment of the energy variable, the

finite differencing of the time variable, and the discrete ordinates approximation of the angular variable are treated in Sec. II.B. Section II.C. is devoted to a discussion of the discontinuous linear finite element scheme used to discretize the spatial variable. The solution algorithms used to solve the set of algebraic equations are presented in Sec. II.D.

A. The Analytic Transport Equation

The form of the time-dependent inhomogeneous transport equation used in TIMEX is

$$\frac{1}{v}\frac{\partial\psi}{\partial t} + \nabla\cdot(\underline{\Omega}\psi) + \sigma(r,E)\,\psi(r,E,\underline{\Omega},t) = \iint dE'\,d\underline{\Omega}'\,\sigma_s(r,E'\to E,\underline{\Omega}\cdot\underline{\Omega}')\,\psi(r,E',\underline{\Omega}',t)$$
$$+\frac{1}{4\pi}(1-\beta)\iint dE'\,d\underline{\Omega}'\,\chi^p(r,E'\to E)\,\nu\sigma_f(r,E')\,\psi(r,E',\underline{\Omega}',t) + Q(r,E,\underline{\Omega},t)$$
$$+\sum_{k=1}^{IGD}\lambda_k(r)\,\chi_k^d(r,E)\,C_k(r,t) \qquad (1a)$$

where ψ is the particle flux (particle number density times their speed) defined such that $\psi\,dE\,dV d\underline{\Omega}$ is the flux of particles in the volume element dV about r, in the energy range dE about E at time t. Similarly, $Q\,dV\,dE\,d\underline{\Omega}$ is the number of particles in the same element of phase space emitted by sources independent of ψ. The macroscopic total interaction cross section is denoted by σ, the macroscopic scattering transfer probability (from energy E' to E through a scattering angle with cosine $\underline{\Omega}\cdot\underline{\Omega}'$) by σ_s, and the macroscopic fission cross section by σ_f. All of these quantities may be space- and energy-dependent. The number of particles emitted isotropically ($1/4\pi$) per fission is ν, and the fraction of these liberated in the range dE about E from fissions in dE' about E' is $\chi^p(r,E'\to E)$, the prompt fission spectrum. The total fraction of the fission neutrons which are prompt is $(1-\beta)$. The k'th delayed neutron precursor concentration is $C_k(r,t)$ with decay constant λ_k. The fraction of the neutrons from the k'th delayed neutron group emitted in energy range dE about E is $\chi_k^d(r,E)$, the delayed neutron fission spectrum.

The delayed neutron precursor concentrations satisfy the equation

$$\frac{d\,C_k(r,t)}{dt} = -\lambda_k(r)\,C_k(r,t) + \beta_k\int dE'\,\nu\sigma_f(r,E')\int d\underline{\Omega}'\,\psi(r,E',\underline{\Omega}',t) \qquad k = 1, 2, \ldots, IGD, \qquad (1b)$$

where β_k is the delayed neutron fraction from the k^{th} precursor group, with

$$\beta = \sum_{k=1}^{IGD}\beta_k$$ being the total delayed neutron fraction.

The homogeneous transport equation is written in the same manner as Eq. (1a) except that Q is zero. Both Eqs. (1a) and (1b) are subject to specified initial conditions $\psi(r,E,\underline{\Omega},t=0)$, and $C_k(r,t=0)$.

1. Particular Forms of the Divergence Operator

The form of $\nabla\cdot\underline{\Omega}\psi$ for the three geometries treated by TIMEX is given in Table I in terms of the coordinate systems sketched in Figs. 1-3. In the standard plane geometry, the angular flux is assumed independent of the azimuthal angle ϕ so that the angular dependence can be reduced to the μ interval (-1,+1). TIMEX also permits the two-angle option in plane geometry where no assumptions of symmetry are imposed. Here the complete unit sphere of angular directions must be considered. In cylindrical geometry, the angular flux is assumed symmetric in the ξ angular cosine and symmetric about the $\phi = 0^o$-180^o plane. Thus, only one-quarter of the unit sphere must be considered in the angular dependence. In spherical geometry, the angular flux is also assumed independent of the azimuthal angle ϕ so that the angular dependence is reduced to the μ interval of (-1,+1).

2. Spherical Harmonics Expansion of the Source Term

In the TIMEX program, the scattering transfer probability is assumed to be represented by a finite Legendre polynomial expansion of the

TABLE I

FORMS OF $\nabla \cdot \Omega\psi$

Geometry	Dependence of	Definition of Variables	$\nabla \cdot \Omega\psi$
Plane	$\psi(x,\mu,t)$	$\mu=\hat{e}_x\cdot\Omega$	$\mu\frac{\partial\psi}{\partial x}$
	or		
	$\psi(x,\mu,\phi,t)$	$\xi=(1-\mu^2)^{\frac{1}{2}}\cos\phi$	
		$\eta=(1-\mu^2)^{\frac{1}{2}}\sin\phi$	
Cylindrical	$\psi(r,\mu,\eta,t)$	$\mu=\hat{e}_r\cdot\Omega$	
		$\xi=\hat{e}_z\cdot\Omega$	$\frac{\mu}{r}\frac{\partial(r\psi)}{\partial r}-\frac{1}{r}\frac{\partial(\eta\psi)}{\partial\phi}$
		$\eta=(1-\xi^2)^{\frac{1}{2}}\sin\phi$	
		$\mu=(1-\xi^2)^{\frac{1}{2}}\cos\phi$	
Spherical	$\psi(r,\mu,t)$	$\mu=\hat{e}_r\cdot\Omega$	$\frac{\mu}{r^2}\frac{\partial(r^2\psi)}{\partial r}$
			$+\frac{1}{r}\frac{\partial[(1-\mu^2)\psi]}{\partial\mu}$

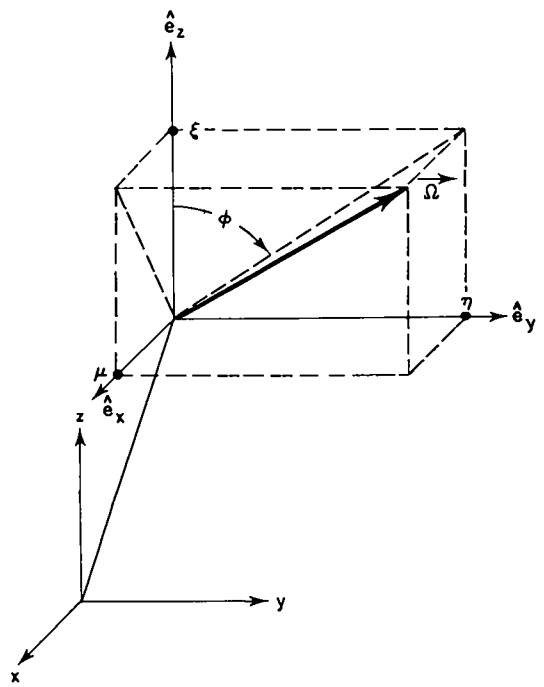

Fig. 1. Coordinates in plane geometry.

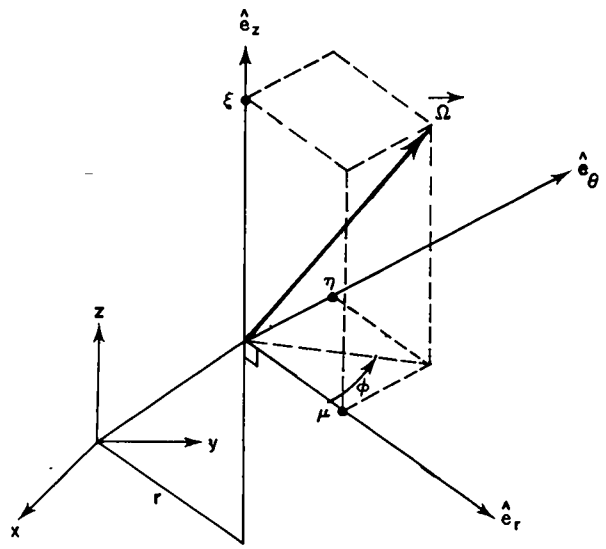

Fig. 2. Coordinates in cylindrical geometry.

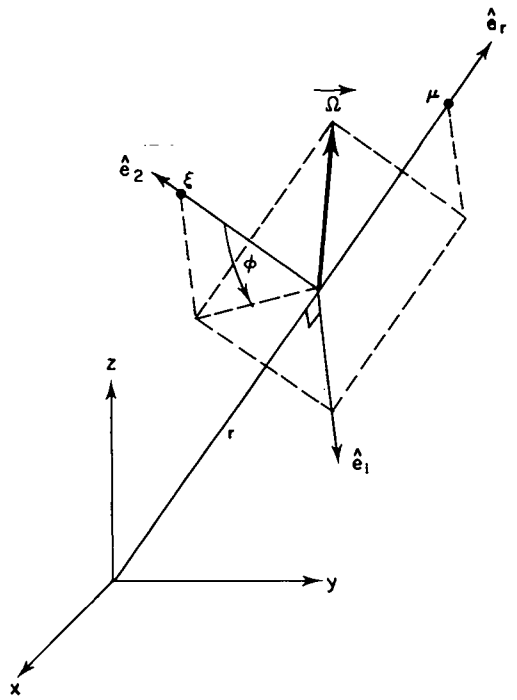

Fig. 3. Coordinates in spherical geometry.

order ISCT

$$\sigma_s(r,E'\to E,\underline{\Omega}\cdot\underline{\Omega}') = \sum_{n=0}^{ISCT} \frac{2n+1}{4\pi}\,\sigma_s^n(r,E'\to E)\,P_n(\underline{\Omega}\cdot\underline{\Omega}'). \quad (2)$$

If this expansion is inserted into Eq. (1a), and the addition theorem for spherical harmonics used to expand $P_n(\underline{\Omega}\cdot\underline{\Omega}')$, the scattering term may be written after integration of Eq. (1a) over the azimuthal angle for one-angle plane and spherical geometries as

$$\iint dE'\, d\underline{\Omega}'\, \sigma_s(r, E' \to E, \underline{\Omega} \cdot \underline{\Omega}')\psi(r, E', \underline{\Omega}', t) = \int dE' \sum_{n=0}^{ISCT} (2n+1)\, \sigma_s^n(r, E' \to E)\, P_n(\mu)\, \phi_n(r, E', t), \tag{3}$$

where the moments of the angular flux are defined

$$\phi_n(r, E, t) = \int_{-1}^{1} \frac{d\mu}{2}\, P_n(\mu)\, \psi(r, E, \mu, t). \tag{4}$$

For cylindrical and two-angle plane geometries, the scattering term becomes more complicated, since the associated Legendre polynomials from the addition theorem cannot be integrated out. Dropping the spatial, time, and energy variables, this term is

$$\iint dE'\, d\underline{\Omega}'\, \sigma_s(\underline{\Omega} \cdot \underline{\Omega}')\, \psi(\underline{\Omega}') = \sum_{n=0}^{ISCT} \frac{2n+1}{4\pi}\, \sigma_s^n \Bigg[P_n(\xi) \int_{-1}^{1} d\xi' \int_{0}^{2\pi} d\phi'\, P_n(\xi')\, \psi(\xi', \phi')$$

$$+ 2 \sum_{\ell=1}^{n} \frac{(n-\ell)!}{(n+\ell)!}\, P_n^{\ell}(\xi) \int_{-1}^{1} d\xi' \int_{0}^{2\pi} d\phi'\, P_n^{\ell}(\xi')\, \cos \ell(\phi - \phi')\, \psi(\xi', \phi') \Bigg], \tag{5}$$

where for two-angle plane geometry the variable ξ is replaced by μ. Using the trigonometric relation

$$\cos \ell(\phi - \phi') = \cos \ell \phi \cos \ell \phi' + \sin \ell \phi \sin \ell \phi', \tag{6}$$

Eq. (5) may be written

$$= \sum_{n=0}^{ISCT} (2n+1)\, \sigma_s^n \Bigg\{ P_n(\xi)\, \phi_n + \sum_{\ell=1}^{n} \sqrt{2\frac{(n-\ell)!}{(n+\ell)!}}\, [P_n^{\ell}(\xi) \cos \ell \phi\, \phi_n^{\ell} + P_n^{\ell}(\xi) \sin \ell \phi\, \phi_n^{\ell}] \Bigg\}, \tag{7}$$

where the moments of the angular flux are defined

$$\phi_n = \int_{-1}^{1} d\xi' \int_{0}^{2\pi} d\phi'\, P_n(\xi')\, \psi(\xi', \phi')/4\pi \tag{8}$$

and

$$\phi_n^{\ell} = \sqrt{2\frac{(n-\ell)!}{(n+\ell)!}} \int_{-1}^{1} d\xi' \int_{0}^{2\pi} d\phi'\, P_n^{\ell}(\xi') \begin{Bmatrix} \cos \ell \phi' \\ \sin \ell \phi' \end{Bmatrix} \psi(\xi', \phi')/4\pi, \tag{9}$$

and where either the sin or cos of Eq. (9) is chosen depending on its coefficient (sin or cos) in Eq. (7).

A tabular array of the $P_n^{\ell}(\xi)$ Legendre functions is shown in Table II. In cylindrical geometry, the angular flux is assumed symmetric in ξ so that the odd flux moments ($n - \ell$ odd) vanish. Likewise, the angular flux is assumed symmetric in ϕ so that the sine moments of the flux vanish. Thus, in cylindrical geometry, only the moments indicated in Table III are required. In the two-angle plane geometry, no assumptions of symmetry are made on the angular flux. Thus the complete array of spherical harmonics, as indicated in Table IV, is required.

In all cases, the scattering term may be written in the general form

$$S.T. = \int_{0}^{\infty} dE' \sum_{n=1}^{NM} (2n-1)\, \sigma_s^n(r, E' \to E)\, R_n(\underline{\Omega})\, \phi_n(r, E', t), \tag{10}$$

where NM is the number of flux moments given by

$$NM = \begin{cases} ISCT+1 & \text{for plane and spherical geometry,} \\ (ISCT+2)^2/4 & \text{for cylindrical geometry, or} \\ (ISCT+1)^2 & \text{for two-angle plane geometry,} \end{cases}$$

$R_n(\underline{\Omega})$ is a spherical harmonic appropriate to that geometry, and ϕ_n is the corresponding angular flux moment. For cylindrical and two-angle plane geometry, the two-dimensional arrays of spherical harmonic moments are stored as one-dimensional arrays, indexed in the order shown in Tables III and IV.

In similar fashion, the inhomogeneous source term of Eq. (1) is expanded in spherical harmonics

TABLE II

TABULAR ARRAY OF SPHERICAL HARMONICS: P_n^ℓ

n \ ℓ →				
	P_0	-	-	-	-
	P_1	P_1^1	-	-	-
	P_2	P_2^1	P_2^2	-	-
	P_3	P_3^1	P_3^2	P_3^3	-
	P_4	P_4^1	P_4^2	P_4^3	P_4^4

$$\text{Inhomogeneous Source} = \sum_{n=1}^{NMQ} (2n-1)\, R_n(\underline{\Omega})\, Q_n(r,E,t), \tag{11}$$

where the number of source moments NMQ is related to the order of source anisotropy IQAN by

$$NMQ = \begin{cases} IQAN+1 & \text{for plane and spherical geometry,} \\ (IQAN+2)^2/4 & \text{for cylindrical geometry, or} \\ (IQAN+1)^2 & \text{for two-angle plane geometry,} \end{cases}$$

and $Q_n(r,E,t)$ is the corresponding source moment.

B. Energy, Time, and Angular Approximations

In this section the multigroup approximation for the energy variable, the discretization of the time variable, and the discrete ordinates approximation for the angular variable are given.

1. Multigroup Equations

The energy domain of interest is assumed to be partitioned into IGM intervals of width ΔE_g, g = 1, 2, ..., IGM. By convention, increasing g represents decreasing energy. If we integrate Eq. (1) over ΔE_g after making the spherical harmonic expansion of Eqs. (10) and (11), we can write

TABLE III

SPHERICAL HARMONICS STORAGE: CYLINDRICAL GEOMETRY

1.	P_0		-		-		-	-
	x	2.	$P_1^1 \cos\phi$		-		-	-
3.	P_2		x	4.	$P_2^2 \cos 2\phi$		-	-
	x	5.	$P_3^1 \cos\phi$		x	6.	$P_3^3 \cos 3\phi$	-
7.	P_4		x	8.	$P_4^2 \cos 2\phi$		x	9. $P_4^4 \cos 4\phi$

x - storage not required.

TABLE IV

SPHERICAL HARMONICS STORAGE: TWO-ANGLE PLANE GEOMETRY

1.	P_0		-		-		-		-
2.	P_1	3. 4.	$P_1^1 \cos\phi$ $P_1^1 \sin\varphi$		-		-		-
5.	P_2	6. 7.	$P_2^1 \cos\phi$ $P_2^1 \sin\phi$	8. 9.	$P_2^2 \cos 2\phi$ $P_2^2 \sin 2\phi$		-		-
10.	P_3	11. 12.	$P_3^1 \cos\phi$ $P_3^1 \sin\phi$	13. 14.	$P_3^2 \cos 2\phi$ $P_3^2 \sin 2\phi$	15. 16.	$P_3^3 \cos 3\phi$ $P_3^3 \sin 3\phi$		-
17.	P_4	18. 19.	$P_4^1 \cos\phi$ $P_4^1 \sin\phi$	20. 21.	$P_4^2 \cos 2\phi$ $P_4^2 \sin 4\phi$	22. 23.	$P_4^3 \cos 3\phi$ $P_4^3 \sin 4\phi$	24. 25.	$P_4^4 \cos 4\phi$ $P_4^4 \sin 4\phi$

$$\frac{1}{v_g}\frac{\partial \psi_g}{\partial t} + \nabla \cdot (\underline{\Omega}\,\psi_g) + \sigma_g\,\psi_g(r,\underline{\Omega},t) = \sum_{h=1}^{IGM}\sum_{n=1}^{NM}(2n-1)\,\sigma^n_{s,h\to g}\,R_n(\underline{\Omega})\,\phi_{nh}(r,t)$$

$$+ (1-\beta)\sum_{h=1}^{IGM}\nu\,\sigma_{fh}\,\chi^p_{h\to g}\,\phi_{1h}(r,t) + \sum_{n=1}^{NMQ}(2n-1)\,R_n(\underline{\Omega})\,Q_{ng}(r,t) + \sum_{k=1}^{IGD}\lambda_k\,\chi^d_{k,g}\,C_k(r,t),$$

$$g = 1, 2, \ldots, IGM \qquad (12a)$$

and

$$\frac{d\,C_k(r,t)}{dt} = -\lambda_k\,C_k(r,t) + \beta_k\sum_{g=1}^{IGM}\nu\,\sigma_{fg}\,\phi_g(r,t), \qquad k = 1, 2, \ldots, IGD. \qquad (12b)$$

Here, the flux for group g,

$$\psi_g = \int_{\Delta E_g}\psi\,dE \qquad (13)$$

is no longer a distribution in energy, but is the total number of particles in the energy interval. For this reason, when group structures are changed, the effect on the angular flux or its moments must be evaluated by comparing $\psi_g/\Delta E_g$. Because of Eq. (13), energy integrals in TIMEX are evaluated by simple sums.

The cross sections subscripted with g are averages, e.g.,

$$\sigma_g = \int_{\Delta E_g}\sigma\,\psi\,dE \Big/ \int_{\Delta E_g}\psi\,dE, \qquad (14)$$

but, of course, ψ is not known and must be approximated by some means. If in Eq. (14) the angular dependence of ψ is nonseparable, then σ_g will depend on angle. No provision for such dependence is made in TIMEX. Recipes for taking this dependence into account, as well as for improving the averages $\sigma^n_{sh\to g}$ when scattering is severely anisotropic, are given by Bell, Hansen, and Sandmeier.[6]

2. Discretization of the Time Variable

To facilitate the discretization of the time variable, we write Eq. (12a) for a single energy group for isotropic sources and scattering as

$$\frac{1}{v_g}\frac{\partial \psi_g}{\partial t} + \nabla \cdot (\underline{\Omega}\,\psi_g) + \sigma_g\,\psi_g(r,\underline{\Omega},t) = \sum_{h=1}^{IGM}\sigma_{s,h\to g}\,\phi_h(r,t) + (1-\beta)\sum_{h=1}^{IGM}\nu\,\sigma_{sh}\,\chi^p_{h\to g}\,\phi_h(r,t)$$

$$+ Q_g(r,t) + \sum_{k=1}^{IGD}\lambda_k\,\chi^d_{k,g}\,C_k(r,t). \qquad (15)$$

Denoting j as the time step index and Δt as the time step size, we explicitly difference the time variable in Eq. (15) by

$$\frac{1}{v\Delta t}(\psi_g^{j+1} - \psi_g^j) + \nabla \cdot (\underline{\Omega}\,\psi_g^{j+1}) + \sigma_g\,\psi_g^{j+1}(r,\underline{\Omega})$$

$$= \sum_{h=1}^{g-1}\sigma_{s,h\to g}\,\phi_h^{j+1}(r) + \sum_{h=g}^{IGM}\sigma_{s,h\to g}\,\phi_h^j(r)$$

$$+ (1-\beta)\left[\sum_{h=1}^{g-1}\nu\,\sigma_{fh}\,\chi^p_{h\to g}\,\phi_h^{j+1}(r) + \sum_{h=g}^{IGM}\nu\,\sigma_{fh}\,\chi^p_{h\to g}\,\phi_h^j(r)\right] + Q_g^{j+1}(r) + \sum_{k=1}^{IGD}\lambda_k\,\chi^d_{k,g}\,C_k^j(r),$$

$$g = 1, 2, \ldots, IGM, \qquad (16a)$$

where the scattering source is separated into a downscattering and a self-scattering plus upscattering contribution and similarly for the fission source. The precursor equations, Eq. (12b) are differenced by a fully-implicit scheme

$$\frac{1}{\Delta t}(C_k^{j+1} - C_k^j) = -\lambda_k\,C_k^{j+1}(r) + \beta_k\sum_{g=1}^{IGM}\nu\,\sigma_{fg}\,\phi_g^{j+1}(r), \qquad k = 1, 2, \ldots, IGD. \qquad (16b)$$

By rearrangement of terms, Eq. (16a) may be cast into the form (deleting the group subscript)

$$\nabla \cdot (\underline{\Omega}\, \psi^{j+1}) + \tilde{\sigma}\, \psi^{j+1}(r,\underline{\Omega}) = \tilde{S}^{j}(r,\underline{\Omega}), \qquad (17)$$

where the modified cross section is given by

$$\tilde{\sigma} = \sigma + \frac{1}{v\Delta t} \qquad (18)$$

and the modified source term is

$$\tilde{S}^{j}(r,\underline{\Omega}) = \sum_{h=1}^{g-1} \sigma_{s,h\to g}\, \phi_h^{j+1}(r) + \sum_{h=g}^{IGM} \sigma_{s,h\to g}\, \phi_n^{j}(r) + (1-\beta)\left[\sum_{h=1}^{g-1} \nu\sigma_{fh}\, \chi^{p}_{h\to g}\, \phi_h^{j+1}(r) + \sum_{h=g}^{IGM} \nu\sigma_{fh}\, \chi^{p}_{h\to g}\, \phi_h^{j}(r)\right]$$
$$+ Q^{j+1}(r) + \sum_{k=1}^{IGD} \lambda_k\, \chi^{d}_{k,g}\, C_k^{j}(r) + \frac{1}{v\Delta t}\, \psi_g^{j}. \qquad (19)$$

Equation (17) is exactly in the form of the steady-state transport equation (with j corresponding to an inner-iteration index) and thus most of the techniques used in the steady-state code ONETRAN may be applied directly. Note that for very small time steps, $\tilde{\sigma}$ becomes very large so that each mesh cell will appear to be optically thick. In this situation the linear discontinuous finite element treatment of the spatial variable derived in Sec. II.D. is markedly superior to the standard diamond difference scheme. Furthermore, the modified source term depends explicitly upon the angular flux so that, unlike the steady-state code ONETRAN, provision must be made for storage of the angular flux. Equation (17) is written for one energy group. All coupling between the IGM multigroup equations is contained in the known source term on the right-hand side.

3. Discrete Ordinates Equations

The discrete ordinates equation may be derived by differencing the angular variable in Eq. (17). In cylindrical and spherical geometries, the resulting equation will conserve neutrons only in the limit of small angular intervals and may result in complex and unrealistic coupling of the angular variable.[7] The customary procedure is to difference both the angular and spatial variables simultaneously, but due to the finite element approach used on the spatial variable this will not be done. Instead a heuristic derivation of the discrete ordinates equation for each of the three geometries will be given. In the following development we will omit the time step index j and consider Eq. (17) as a steady-state transport problem.

a. Plane Geometry

From Table I, it is observed that no angular derivative appears in the divergence operator so that no angular coupling is present. For the standard geometry, the angular interval of $\mu\varepsilon(-1,+1)$ is discretized into a set of MM quadrature points μ_m and associated quadrature weights w_m ordered, as shown in Fig. 4. The quadrature weights are normalized so that

$$\sum_{m=1}^{MM} w_m = 1,$$

analogous to $d\mu/2$ in Eq. (4). The (angular) cell-centered angular flux is then assumed to be given by

$$\psi_m(r) \approx \psi(r\ \mu_m) \qquad (20)$$

and the angular flux moments of Eq. (4) are approximated by

$$\phi_n(r) \approx \sum_{m=1}^{MM} w_m\, P_n(\mu_m)\, \psi_m(r). \qquad (21)$$

For the two-angle plane geometry option, the angular domain of the complete unit sphere is again discretized into a set of MM quadrature points (μ_m, ϕ_m) and associated quadrature weights w_m. The normalization is again $\sum_{m=1}^{MM} w_m = 1$, analogous to $d\underline{\Omega}/4\pi$ in Eqs. (8) and (9). The ordering of these

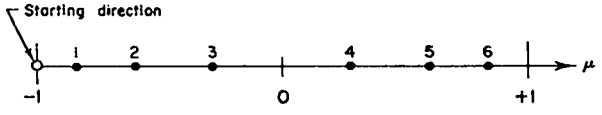

Fig. 4. Ordering of S_6 directions in plane and spherical geometries. The starting direction only applies to spherical geometry.

quadrature points is illustrated in Fig. 6 for an S_4 quadrature. The built-in quadrature set of TIMEX actually chooses μ_m and ξ_m as either the Gauss-Legendre or the double Gauss-Legendre quadrature points. The cell-centered angular flux is again assumed to be given by

$$\psi_m(r) \approx \psi(r, \mu_m, \phi_m) \tag{22}$$

and the angular flux moments of Eqs. (8) and (9) are approximated by

$$\phi_n(r) \approx \sum_{m=1}^{MM} w_m P_n(\mu_m) \psi_m(r) \tag{23}$$

and

$$\phi_n^{\ell}(r) \approx \sqrt{2\frac{(n-\ell)!}{(n+\ell)!}} \sum_{m=1}^{MM} w_m P_n^{\ell}(\mu_m) \begin{Bmatrix} \cos \ell \phi_m \\ \sin \ell \phi_m \end{Bmatrix} \psi_m(r). \tag{24}$$

For both of the plane geometries, the discrete ordinates approximation of the multigroup transport Eq. (17) is

$$\mu_m \frac{\partial \psi_m}{\partial x} + \tilde{\sigma} \psi_m(x) = \tilde{S}_m(x), \tag{25}$$

where $\tilde{S}_m(x)$ is the (known) source evaluated at the m^{th} angular quadrature point.

b. Cylindrical Geometry

From Table I, the multigroup transport Eq. (17) may be written in cylindrical geometry as

$$\mu \frac{\partial(r \psi)}{\partial r} - \frac{\partial(\eta \psi)}{\partial \phi} + r \tilde{\sigma} \psi(r, \underline{\Omega}) = r \tilde{S}(r, \underline{\Omega}). \tag{26}$$

The angular domain of one quadrant of the unit sphere is discretized into a set of MM quadrature points (μ_m, η_m) and associated quadrature weights w_m, normalized so that $\sum_{m=1}^{MM} w_m = 1$. The ordering of these quadrature points is illustrated in Fig. 5 for an S_6 quadrature. The (angular) cell-centered angular flux is assumed to be given by

$$\psi_m(r) \approx \psi(r, \mu_m, \eta_m) \tag{27}$$

and the angular flux moments are approximated by Eqs. (23) and (24). In addition we have the (angular) cell edge fluxes on the same ξ level denoted by $\psi_{m-\frac{1}{2}}(r)$ and $\psi_{m+\frac{1}{2}}(r)$. We then write the discrete ordinates approximation to Eq. (26) as

$$\mu_m \frac{\partial(r \psi_m)}{\partial r} + \frac{\alpha_{m+\frac{1}{2}}}{w_m} \psi_{m+\frac{1}{2}}(r) - \frac{\alpha_{m-\frac{1}{2}}}{w_m} \psi_{m-\frac{1}{2}}(r) + r \tilde{\sigma} \psi_m(r) = r \tilde{S}_m(r). \tag{28}$$

Consider now the case of divergenceless flow in

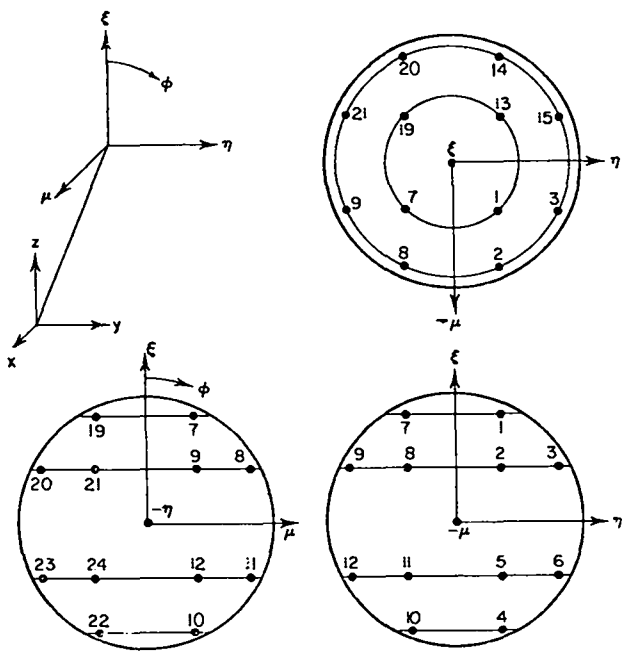

Fig. 6. Ordering of S_4 directions in two-angle plane geometry. The ordinates in the 8^{th} octant are not shown.

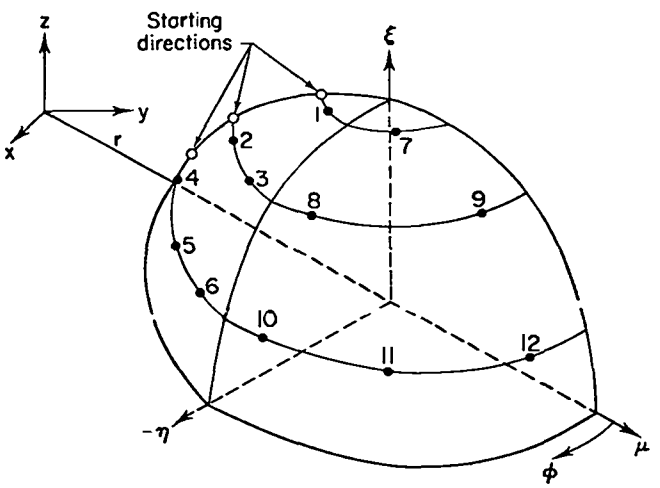

Fig. 5. Ordering of S_6 directions in cylindrical geometry.

which $\psi = S/\sigma$ = constant. Since $\eta = \sqrt{1-\xi^2}\,\sin\phi$ and $\mu = \sqrt{1-\mu^2}\,\cos\phi$, then $\partial\eta/\partial\phi = \mu$ and it is easily shown that the angular coupling coefficient α must satisfy the recursion relation

$$\alpha_{m+\frac{1}{2}} - \alpha_{m-\frac{1}{2}} = - w_m \mu_m, \tag{29}$$

with the requirement from neutron conservation that the first ($\alpha_{\frac{1}{2}}$) and last ($\alpha_{M+\frac{1}{2}}$) coefficients on a ξ level must vanish. It can be shown[8] that Eq. (28) becomes identical to Eq. (26) in the limit of vanishingly small angular intervals.

c. Spherical Geometry

From Table I, the multigroup transport Eq. (17) is written in spherical geometry as

$$\mu \frac{\partial(r^2\psi)}{\partial r} + r \frac{\partial[(1-\mu^2)\psi]}{\partial\mu} + r^2 \tilde{\sigma}\, \psi(r,\mu) = r^2 \tilde{S}(r,\mu). \tag{30}$$

The angular domain of $\mu\varepsilon(-1,+1)$ is discretized into a set of MM quadrature points μ_m and associated quadrature weights w_m, normalized so that $\sum_{m=1}^{MM} w_m = 1$. The ordering of these quadrature points is illustrated in Fig. 4 for an S_6 quadrature. The (angular) cell-centered angular flux is assumed to be given by

$$\psi_m(r) \approx \psi(r, \mu_m) \tag{31}$$

and the angular flux moments approximated by Eq. (21). The (angular) cell edge fluxes are denoted by $\psi_{m-\frac{1}{2}}(r)$ and $\psi_{m+\frac{1}{2}}(r)$. We write the discrete ordinates approximation to Eq. (30) as

$$\mu_m \frac{\partial(r^2\,\psi_m)}{\partial r} + \left[\frac{\beta_{m+\frac{1}{2}}}{w_m}\psi_{m+\frac{1}{2}}(r) - \frac{\beta_{m-\frac{1}{2}}}{w_m}\psi_{m-\frac{1}{2}}(r)\right] r + r^2 \tilde{\sigma}\,\psi_m(r) = r^2 \tilde{S}_m(r). \tag{32}$$

Considering the case of divergenceless flow, we require that the angular coefficients β satisfy the recursion relation

$$\beta_{m+\frac{1}{2}} - \beta_{m-\frac{1}{2}} = - 2\, w_m\, \mu_m, \qquad m = 1, \ldots, MM, \tag{33}$$

with the requirement from neutron conservation that the first ($\beta_{\frac{1}{2}}$) and last ($\beta_{MM+\frac{1}{2}}$) coefficients must vanish. Again it can be shown[8] that Eq. (32) becomes identical to Eq. (30) in the limit of vanishingly small angular intervals.

d. Diamond Difference Assumption and Starting Directions

For the curved geometries discrete ordinates transport equation, Eqs. (28) and (32), there are three unknown functions: the (angular) mesh cell edge fluxes, $\psi_{m+\frac{1}{2}}(r)$ and $\psi_{m-\frac{1}{2}}(r)$, and the cell-centered angular flux, $\psi_m(r)$. The $\psi_{m-\frac{1}{2}}(r)$ edge flux will be assumed known from the previous angular mesh cell computation. The standard diamond difference[9] assumption (in angle only) is made to relate the edge and cell-centered fluxes, viz.,

$$\psi_m(r) = \frac{1}{2}\,[\psi_{m-\frac{1}{2}}(r) + \psi_{m+\frac{1}{2}}(r)]. \tag{34}$$

Thus, in each (angular) mesh cell, we need only solve the transport equation for one function, $\psi_m(r)$.

To initiate the computation in the first angular mesh cell, TIMEX uses special zero-weighted directions to calculate $\psi_{\frac{1}{2}}(r)$. For spherical geometry, this special direction is the straight-inward direction $\mu = -1$, as illustrated in Fig. 4. For cylindrical geometry, these special directions correspond to ordinates directed towards the cylindrical axis, $\eta = 0$, $\phi = 180^\circ$, as illustrated in Fig. 5.

The starting direction calculations are treated separately from the calculations for the other directions and are discussed further in the following section.

C. Discretization of the Spatial Variable

The approximations that have been made thus far are independent of the treatment of the spatial variable and are identical to those used in other one-dimensional discrete ordinate transport codes.[4,10]

In this section, we will depart from the traditional usage of the diamond difference scheme and develop a linear discontinuous finite element scheme for the spatial discretization. Use of the discontinuous scheme is based on the favorable experience of such a method in the two-dimensional, triangular mesh transport code TRIPLET.[11] These discontinuous methods are found to result in a very accurate and stable difference scheme (especially for optically thick mesh cells).

Difference schemes for the transport equation fall into two broad categories: implicit and explicit methods. In an implicit method no attempt is made to solve in the direction in which neutrons are streaming. Instead, variational or weighted residual methods are used to determine a set of linear algebraic equations for all the unknowns. This set of equations is then solved, often by direct methods, to obtain the final solution. An implicit method couples all or some adjacent mesh cells with no regard for the direction of neutron travel. An explicit method, on the other hand, sweeps once through the mesh, solving for the unknowns in the direction in which neutrons are streaming. This is also equivalent to solving a set of linear algebraic equations, but here the matrix to be inverted is triangular. An explicit method couples only the mesh cells visible when looking backward along the direction in which neutrons are traveling. The finite element method developed below, like the diamond difference scheme, is explicit in nature.

Finite element methods for solving differential equations like Eqs. (25), (28), and (32) usually involve the assumption that the unknown function $\psi_m(r)$ can be approximated by some member of a finite-dimensional set of functions. This set of functions is often referred to as the trial space. A particular member of this function space is selected by some procedure like minimizing a functional or requiring the residual to be orthogonal to a set of weighting functions. The selected member is the desired approximate solution to the differential equation.

The finite element method used in TIMEX is dereived using a weight and integrate technique. The trial space consists of functions that are piecewise linear and discontinuous across mesh cell boundaries. More precisely, if $\psi_i(r)$ is our approximation of the exact solution to the discrete ordinates equation in mesh cell i (dropping the discrete ordinate index m), then we assume a linear Lagrangian representation of the form

$$\psi_i(r) \simeq \frac{1}{\Delta r_i}\left[(r_{i+\frac{1}{2}} - r)\,\psi_{i-\frac{1}{2}} + (r - r_{i-\frac{1}{2}})\,\psi_{i+\frac{1}{2}}\right], \tag{35}$$

where $\Delta r_i = r_{i+\frac{1}{2}} - r_{i-\frac{1}{2}}$ and $\psi_{i-\frac{1}{2}}$, $\psi_{i+\frac{1}{2}}$ are the unknown discrete ordinates angular flux on the mesh cell left and right boundaries, respectively. To complete the specification of the trial space, we must assign a unique value to the approximate flux on the mesh cell boundaries. It is essential to the following analysis that the flux on the mesh cell boundary is the limit of the flux as one approaches the boundary in the direction in which neutrons are streaming. This is illustrated in Fig. 7 for the two possible cases, $\mu > 0$ and $\mu < 0$.

For the angular mesh cell, we impose continuity on the mesh cell edges and assume the diamond difference relation, so that the (angle) extrapolated angular flux is

$$\psi_{m+\frac{1}{2}} = 2\left[\tfrac{1}{2}(\psi_{i+\frac{1}{2}} + \psi_{i-\frac{1}{2}})\right] - \psi_{m-\frac{1}{2}}. \tag{36}$$

The arrangement of the angular flux node points in a single space-angle mesh cell is illustrated in Fig. 8.

With the above assumptions inserted therein, the discrete ordinates equations [Eqs. (25), (28), and (32)] in the $(i,m)^{th}$ mesh cell become, respectively,

$$\frac{\mu_m}{\Delta r_i}\frac{d}{dr}\left[(r_{i+\frac{1}{2}} - r)\,\psi_{i-\frac{1}{2}} + (r - r_{i-\frac{1}{2}})\,\psi_{i+\frac{1}{2}}\right]$$
$$+ \frac{\tilde{\sigma}}{\Delta r_i}\left[(r_{i+\frac{1}{2}} - r)\,\psi_{i-\frac{1}{2}} + (r - r_{i-\frac{1}{2}})\,\psi_{i+\frac{1}{2}}\right]$$
$$\simeq \frac{1}{\Delta r_i}\left[(r_{i+\frac{1}{2}} - r)\,\tilde{S}_{i-\frac{1}{2}} + (r - r_{i-\frac{1}{2}})\,\tilde{S}_{i+\frac{1}{2}}\right] \tag{37a}$$

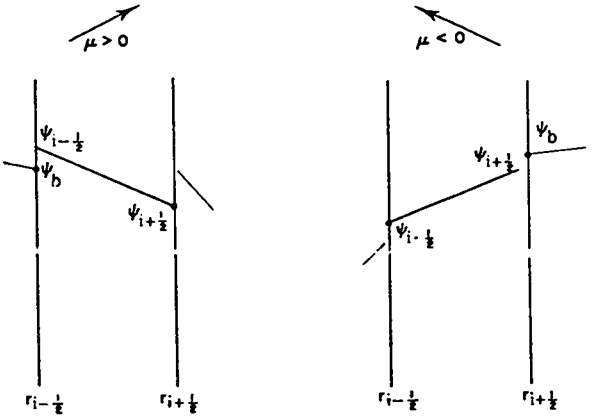

Fig. 7. Linear discontinuous representation of the angular flux in the i^{th} mesh cell. The • indicates the actual value of the angular flux on the mesh cell boundary. The angular flux from the previous mesh-cell boundary is denoted by ψ_b.

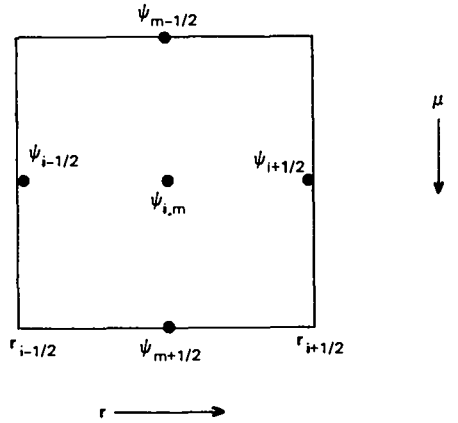

Fig. 8. Angular flux nodal values for the i,m (space, angle) mesh cell.

$$\frac{\mu_m}{\Delta r_i}\frac{d}{dr}\left[r(r_{i+\frac{1}{2}} - r)\,\psi_{i-\frac{1}{2}} + r(r - r_{i-\frac{1}{2}})\,\psi_{i+\frac{1}{2}}\right] + \frac{\alpha_{m+\frac{1}{2}}}{w_m}\left[\psi_{i+\frac{1}{2}} + \psi_{i-\frac{1}{2}} - \psi_{m-\frac{1}{2}}\right] - \frac{\alpha_{m-\frac{1}{2}}}{w_m}\psi_{m-\frac{1}{2}}$$

$$+ \frac{\tilde{\sigma}}{\Delta r_i}\left[r(r_{i+\frac{1}{2}} - r)\,\psi_{i-\frac{1}{2}} + r(r - r_{i-\frac{1}{2}})\,\psi_{i+\frac{1}{2}}\right] \approx \frac{1}{\Delta r_i}\left[r(r_{i+\frac{1}{2}} - r)\,\tilde{S}_{i-\frac{1}{2}} + r(r - r_{i-\frac{1}{2}})\,\tilde{S}_{i+\frac{1}{2}}\right] \tag{37b}$$

and

$$\frac{\mu_m}{\Delta r_i}\frac{d}{dr}\left[r^2(r_{i+\frac{1}{2}} - r)\,\psi_{i-\frac{1}{2}} + r^2(r - r_{i-\frac{1}{2}})\,\psi_{i+\frac{1}{2}}\right] + \frac{\alpha_{m+\frac{1}{2}}}{w_m}\left[\psi_{i+\frac{1}{2}} + \psi_{i-\frac{1}{2}} - \psi_{m-\frac{1}{2}}\right]2r - \frac{\alpha_{m-\frac{1}{2}}}{w_m}\psi_{m-\frac{1}{2}}\,2r$$

$$+ \frac{\tilde{\sigma}}{\Delta r_i}\left[r^2(r_{i+\frac{1}{2}} - r)\,\psi_{i-\frac{1}{2}} + r^2(r - r_{i-\frac{1}{2}})\,\psi_{i+\frac{1}{2}}\right] \simeq \frac{1}{\Delta r_i}\left[r^2(r_{i+\frac{1}{2}} - r)\,\tilde{S}_{i-\frac{1}{2}} + r^2(r - r_{i-\frac{1}{2}})\,\tilde{S}_{i+\frac{1}{2}}\right],$$

for

$$r\varepsilon(r_{i-\frac{1}{2}},\ r_{i+\frac{1}{2}}), \tag{37c}$$

where the sources on the right-hand side have also been approximated by a linear Lagrangian representation analogous to Eq. (35). In the spherical geometry Eq. (37c), the relation

$$\beta_{m\pm\frac{1}{2}} = 2\,\alpha_{m\pm\frac{1}{2}} \tag{38}$$

has been used, where the curvature coefficients α satisfy the recursion relation of Eq. (29).

Since Eq. (37) cannot be satisfied identically for all $r\varepsilon(r_{i-\frac{1}{2}}, r_{i+\frac{1}{2}})$ we require the residual to be orthogonal to certain weight functions. Specifically, we operate on Eq. (37) with $\int_{r_{i-\frac{1}{2}}}^{r_{i+\frac{1}{2}}} dr$ and $\int_{r_{i-\frac{1}{2}}}^{r_{i+\frac{1}{2}}}(r - r_{i-\frac{1}{2}})dr$ for the rightward-directed sweeps ($\mu > 0$), and $\int_{r_{i-\frac{1}{2}}}^{r_{i+\frac{1}{2}}} dr$ and $\int_{r_{i-\frac{1}{2}}}^{r_{i+\frac{1}{2}}}(r_{i+\frac{1}{2}} - r)dr$ for the leftward-directed sweeps ($\mu < 0$). This results in the following system of equations for the mesh cell edge fluxes:

$$\begin{bmatrix} \Delta A_i \dfrac{\alpha_{m+\frac{1}{2}}}{w_m} + \tilde{\sigma} V_{i-\frac{1}{2}} & \mu A_{i+\frac{1}{2}} + \Delta A_i \dfrac{\alpha_{m+\frac{1}{2}}}{w_m} + \tilde{\sigma} V_{i+\frac{1}{2}} \\ \mu z_3 + z_5 \dfrac{\alpha_{m+\frac{1}{2}}}{w_m} + \tilde{\sigma} z_1 & \mu z_4 + z_5 \dfrac{\alpha_{m+\frac{1}{2}}}{w_m} + \tilde{\sigma} z_2 \end{bmatrix} \begin{Bmatrix} \psi_{i-\frac{1}{2}} \\ \psi_{i+\frac{1}{2}} \end{Bmatrix}$$

$$= \begin{Bmatrix} \tilde{S}_{i-\frac{1}{2}} V_{i-\frac{1}{2}} + \tilde{S}_{i+\frac{1}{2}} V_{i+\frac{1}{2}} + \Delta A_i \dfrac{\alpha}{w_m} \psi_{m-\frac{1}{2}} + \mu A_{i-\frac{1}{2}} \psi_b \\ \tilde{S}_{i-\frac{1}{2}} z_1 + \tilde{S}_{i+\frac{1}{2}} z_2 + z_5 \dfrac{\alpha}{w_m} \psi_{m-\frac{1}{2}} \end{Bmatrix}, \qquad \mu > 0, \tag{39a}$$

and

$$\begin{bmatrix} -\mu A_{i-\frac{1}{2}} + \Delta A_i \dfrac{\alpha_{m+\frac{1}{2}}}{w_m} + \tilde{\sigma} V_{i-\frac{1}{2}} & \Delta A_i \dfrac{\alpha_{m+\frac{1}{2}}}{w_m} + \tilde{\sigma} V_{i+\frac{1}{2}} \\ \mu z_8 + z_{10} \dfrac{\alpha_{m+\frac{1}{2}}}{w_m} + \tilde{\sigma} z_6 & \mu z_9 + z_{10} \dfrac{\alpha_{m+\frac{1}{2}}}{w_m} + \tilde{\sigma} z_7 \end{bmatrix} \begin{Bmatrix} \psi_{i-\frac{1}{2}} \\ \psi_{i+\frac{1}{2}} \end{Bmatrix}$$

$$= \begin{Bmatrix} \tilde{S}_{i-\frac{1}{2}} V_{i-\frac{1}{2}} + \tilde{S}_{i+\frac{1}{2}} V_{i+\frac{1}{2}} + \Delta A_i \dfrac{\alpha}{w_m} \psi_{m-\frac{1}{2}} - \mu A_{i+\frac{1}{2}} \psi_b \\ \tilde{S}_{i-\frac{1}{2}} z_6 + \tilde{S}_{i+\frac{1}{2}} z_7 + z_{10} \dfrac{\alpha}{w_m} \psi_{m-\frac{1}{2}} \end{Bmatrix}, \qquad \mu < 0. \tag{39b}$$

Here, $\alpha = \alpha_{m-\frac{1}{2}} + \alpha_{m+\frac{1}{2}}$, ψ_b is the angular flux on the boundary of the previous mesh cell as indicated in Fig. 7, and the remaining symbols are defined in Table V.

For the starting direction sweeps in cylindrical and spherical geometry there is no angular redistribution so that

$$\psi_{m+\frac{1}{2}} = \psi_{m-\frac{1}{2}} = \tfrac{1}{2}(\psi_{i-\frac{1}{2}} + \psi_{i+\frac{1}{2}}), \tag{40}$$

for m = starting direction. Since $\alpha_{m-\frac{1}{2}} = 0$, so that

$$\frac{\alpha_{m+\frac{1}{2}}}{w_m} - 0 = -\mu_m \tag{41}$$

for m = starting direction from Eq. (29), then

$$\frac{\alpha_{m+\frac{1}{2}}}{w_m} \psi_{m+\frac{1}{2}} = -\frac{1}{2} \mu_m (\psi_{i-\frac{1}{2}} + \psi_{i+\frac{1}{2}}) \tag{42}$$

for m = starting direction.

The relationship of Eq. (42) replaces the curvature terms in Eq. (37). We again operate with $\int_{r_{i-\frac{1}{2}}}^{r_{i+\frac{1}{2}}} dr$ and $\int_{r_{i-\frac{1}{2}}}^{r_{i+\frac{1}{2}}} (r_{i+\frac{1}{2}} - r)dr$. This results in the following system of equations for the mesh cell edge fluxes:

$$\begin{bmatrix} -\frac{1}{2}\mu(A_{i-\frac{1}{2}}+A_{i+\frac{1}{2}}) + \tilde{\sigma} V_{i-\frac{1}{2}} & -\frac{1}{2}\mu \Delta A_i + \tilde{\sigma} V_{i+\frac{1}{2}} \\ \mu(z_8 - \frac{1}{2} z_{10}) + \tilde{\sigma} z_6 & \mu(z_9 - \frac{1}{2} z_{10}) + \tilde{\sigma} z_7 \end{bmatrix} \begin{Bmatrix} \psi_{i-\frac{1}{2}} \\ \psi_{i+\frac{1}{2}} \end{Bmatrix}$$

$$= \begin{Bmatrix} \tilde{S}_{i-\frac{1}{2}} V_{i-\frac{1}{2}} + \tilde{S}_{i+\frac{1}{2}} V_{i+\frac{1}{2}} - \mu A_{i+\frac{1}{2}} \psi_b \\ \tilde{S}_{i-\frac{1}{2}} z_6 + \tilde{S}_{i+\frac{1}{2}} z_7 \end{Bmatrix}, \tag{39c}$$

for μ = starting directions. It should be noted that by imposing continuity on the mesh-cell boundary for the second equation in Eq. (39) ($\psi_{i-\frac{1}{2}} = \psi_b$ for $\mu > 0$ and $\psi_{i+\frac{1}{2}} = \psi_b$ for $\mu < 0$, the diamond difference equations are obtained. For curved geometries, these are a weighted diamond difference slightly different from that of Reed and Lathrop.[12]

For the diamond difference case in a source-free plane geometry mesh cell (S = 0), the solution of Eq. (39a) is easily shown to be $\psi_{i+\frac{1}{2}} = -\psi_b$ as the optical thickness of a mesh cell becomes infinitely large ($\tilde{\sigma}\Delta r/\mu \to \infty$). Thus, negative fluxes are a problem for such mesh cells. For the discontinuous case, it is easily shown the $\psi_{i-\frac{1}{2}} = \psi_{i+\frac{1}{2}} \to 0$ for mesh cells with an infinite optical thickness. Negative fluxes may still appear for the discontinuous case, but the worst possible situation occurs for $\tilde{\sigma}\Delta r/\mu = 8.196$ at

TABLE V

TABLE OF GEOMETRIC FUNCTIONS

Notation: $r_+ = r_{i+\frac{1}{2}}$, $r_- = r_{i-\frac{1}{2}}$

Quantity	Plane Geometry	Cylindrical Geometry	Spherical Geometry
Δr	$r_+ - r_-$	$r_+ - r_-$	$r_+ - r_-$
A_-	1	$2\pi r_-$	$4\pi r_-^2$
A_+	1	$2\pi r_+$	$4\pi r_+^2$
ΔA	0	$A_+ - A_-$	$A_+ - A_-$
V_-	$\frac{1}{2}\Delta r$	$\frac{\pi}{3}\Delta r(r_+ + 2r_-)$	$\frac{\pi}{3}\Delta r(r_+^2 + 2r_+r_- + 3r_-^2)$
V_+	$\frac{1}{2}\Delta r$	$\frac{\pi}{3}\Delta r(2r_+ + r_-)$	$\frac{\pi}{3}\Delta r(3r_+^2 + 2r_+r_- + r_-^2)$
z_1	$10\Delta r$	$5(r_+ + r_-)\Delta r$	$(3r_+^2 + 4r_+r_- + 3r_-^2)\Delta r$
z_2	$20\Delta r$	$5(3r_+ + r_-)\Delta r$	$(12r_+^2 + 6r_+r_- + 2r_-^2)\Delta r$
z_3	-30	$-10(r_+ + 2r_-)$	$-5(r_+^2 + 2r_+r_- + 3r_-^2)$
z_4	$+30$	$10(4r_+ - r_-)$	$5(9r_+^2 - 2r_+r_- - r_-^2)$
z_5	0	$30\Delta r$	$20(2r_+ + r_-)\Delta r$
z_6	$20\Delta r$	$5(r_+ + 3r_-)\Delta r$	$(2r_+^2 + 6r_+r_- + 12r_-^2)\Delta r$
z_7	$10\Delta r$	$5(r_+ + r_-)\Delta r$	$(3r_+^2 + 4r_+r_- + 3r_-^2)\Delta r$
z_8	-30	$10(r_+ - 4r_-)$	$5(r_+^2 + 2r_+r_- - 9r_-^2)$
z_9	$+30$	$10(2r_+ + r_-)$	$5(3r_+^2 + 2r_+r_- + r_-^2)$
z_{10}	0	$30\Delta r$	$20(r_+ + 2r_-)\Delta r$

which $\psi_{i-\frac{1}{2}} = + 0.366\ \psi_b$ and $\psi_{i+\frac{1}{2}} = - 0.0981\ \psi_b$. Thus, negative fluxes are much less in magnitude with the discontinuous scheme than for the diamond difference solution.

There are two important disadvantages to the linear discontinuous finite element scheme: computational times and core storage requirements. Although an explicit solution of Eq. (39) may be expressed, it is much more complicated than the corresponding diamond difference solution, requiring approximately twice as many operations (other than divides). Thus the computation costs will be greater than for other transport codes based on the diamond difference. Since the mesh cell edge values for the fluxes and sources are required (as compared to only the cell-centered quantities for a diamond difference code), the core storage for these quantities is doubled. In addition, all the finite element arrays for quantities in Table V must be stored on the fine mesh. It is possible that a choice of different weight functions in the derivation of Eq. (39) could result in a system both simpler to solve and requiring less core storage, but this has not been investigated.

On the other hand, it is found that a coarser spatial mesh is usually sufficient to give an accuracy equivalent to that obtained by a diamond difference solution.

D. Solution Algorithms

The basic algebraic equation that is actually solved at each time step by TIMEX is Eq. (39) for each space-angle mesh cell. In this section we detail the algorithms used to implement the solution of Eq. (39) in the TIMEX code.

1. Boundary Conditions

Information about the right and left boundary flux values may be specified by the TIMEX user designating one of the following boundary conditions:

- Vaccuum boundary condition -- the angular flux on the boundary is set to zero for all incoming directions: $\psi_{\text{incoming}}(\mu_m) = 0$.

- Reflective boundary condition -- the incoming angular flux on the boundary is set equal to the outgoing angular flux on that boundary in the direction corresponding to specular reflection: $\psi_{incoming}(\mu_m) = \psi_{outgoing}(-\mu_m)$.

- Periodic boundary condition -- the incoming angular flux on the boundary is set equal to the outgoing angular flux in the same direction on the opposite boundary:

$$\psi_{incoming}(r = r_{left}, \mu_m) = \psi_{outgoing}(r = r_{right}, \mu_m) \text{ and}$$

$$\psi_{incoming}(r = r_{right}, \mu_m) = \psi_{outgoing}(r = r_{left}, \mu_m).$$

- White boundary condition -- the incoming angular flux on the boundary is set equal to a single value such that the net flow through the boundary is zero, viz.,

$$\psi_{incoming}(\mu_m) = \frac{\sum_m w_m \mu_m \psi_{outgoing}(\mu_m)}{\sum_m w_m \mu_m}$$

where the sums range over all outgoing directions. This condition is used primarily for cell calculations in cylindrical and spherical geometry where it is applied to the outer radial boundary.

- Albedo boundary condition -- the incoming angular flux on the boundary is set equal a user-supplied albedo times the outgoing angular flux on that boundary in the direction corresponding to specular reflection:

$$\psi_{incoming}(\mu_m) = \alpha \, \psi_{outgoing}(-\mu_m).$$

The albedo factor α is an energy group-dependent quantity. The reflective boundary condition corresponds to $\alpha = 1$.

- Inhomogeneous source boundary condition -- the incoming angular flux on the boundary is set equal to a user-supplied source:

$$\psi_{incoming}(\mu_m) = Q_m.$$

The inhomogeneous boundary source is both group- and angle-dependent.

Use of the reflective or albedo boundary condition requires the S_N quadrature ordinates to be symmetric about $\mu = 0$.

At the start of each sweep of the spatial mesh (for a given discrete ordinate direction), the subroutine SETBC is called which returns the value of the boundary angular flux for that direction, namely ψ_b. This is the boundary flux, ψ_b, of the adjacent mesh cell as used in Eq. (39). Thus the equalities indicated above for the boundary conditions will not actually be true due to the discontinuity of the angular flux at the mesh cell boundary. Furthermore, for the reflecting boundary condition at the origin in cylindrical or spherical geometry, this reflecting boundary makes no contributions to the source term in Eq. (39) since $A_{i-\frac{1}{2}} = 0$.

2. Sweep of the Space-Angle Mesh

The unknown angular fluxes are ordered so that the difference scheme is stable and so that the coefficient matrix is lower triangular. Physically, this corresponds to proceeding in the direction of particle flow.

The angular mesh is swept in the same sequence in which the quadrature directions are ordered as indicated in Figs. 4, 5, and 6. For a particular quadrature direction, the spatial mesh is then swept either from left to right ($\mu > 0$) or from right to left ($\mu < 0$). For curved geometries, there are NLEV starting directions (ISN/2 for cylindrical, 1 for spherical). The angular flux, $\psi_{m-\frac{1}{2}}$, is generated on the fine mesh for all NLEV starting directions (stored in the array AFE). The angular mesh is then swept for all inward directions ($\mu < 0$). For each direction, the spatial mesh is swept from right to left, generating the mesh cell edge fluxes $\psi_{i-\frac{1}{2}}$, $\psi_{i+\frac{1}{2}}$ (stored in the array AFC). In each spatial mesh cell, the angular extrapolation is made by Eq. (32) (overstored in array AFE). The angular mesh is then swept for all outward directions ($\mu > 0$), with the spatial mesh now swept from left to right. This sweeping of the space-angle mesh is performed in subroutine SWEEP.

3. Negative Flux Fixup

As briefly mentioned in Sec. II.C., it is possible for the mesh cell edge angular fluxes in

Eq. (39) to be negative, primarily in optically-thick mesh cells with no sources present. In such cases the offending angular fluxes are usually small in magnitude, are rapidly damped in space, and have little effect on integral quantities. Nonetheless, many transport code users become alarmed by the presence of these negative fluxes. Consequently, a negative flux fixup has been incorporated into TIMEX which results in an increase in computation time of typically 3% or more. This is the cost of the test for negative fluxes only, and does not include the expense of computing the fixed-up flux.

The flux fixup algorithm proceeds as follows: (for rightward sweeps):

(a) After the mesh cell edge fluxes are computed, the far or extrapolated angular flux, $\psi_{i+\frac{1}{2}}$, is checked for positivity. (The near angular flux, $\psi_{i-\frac{1}{2}}$, will always be positive for positive sources.) If it is positive, the computation proceeds normally. If the total source in the mesh cell is negative, the flux fixup is bypassed.

(b) If $\psi_{i+\frac{1}{2}}$ is negative, the second equation of Eq. (39) is replaced with the requirement that this flux vanish, $\psi_{i+\frac{1}{2}} = 0$, and the first (conservation) equation of Eq. (39) is solved for the near angular flux, $\psi_{i-\frac{1}{2}}$.

If the computation time for a problem is significant and negative fluxes are not a serious problem, the negative flux fixup algorithm (in subroutine SWEEP) may easily be deleted.

It is also possible to generate negative fluxes with the angular diamond difference extrapolation of Eq. (36). This is not normally encountered and a fixup test and correction is not made.

4. Adjoint Problems

The TIMEX program solves the adjoint transport equation by transposing the scattering and fission matrices and inverting the group order of the problem. Transposition of the scattering matrix converts the normal, predominantly downscattering problem to an upscattering problem while the group order inversion restores this downscattering dominance and eliminates unnecessary upscattering iteration. The solution of the resulting problem in the direction $\underline{\Omega}$ is then identified with the adjoint solution in the direction $-\underline{\Omega}$.[16]

5. Acceleration Methods

Two acceleration devices to improve the accuracy of the numerical solution, rebalance, and exponential extrapolation, are available at the option of the TIMEX user. An acceleration device in time-dependent calculations here refers to a scheme that improves the accuracy of the result for a given time-step size. Each method is designed to work properly in most situations, although there are occasions in which the use of one or the other of these techniques is specifically recommended. Both methods are usually stable, but there are certain circumstances discussed later in this section under which the use of fine-mesh rebalance can lead to an unstable algorithm.

a. Exponential Extrapolation

To derive the exponential extrapolation method,[13] we write the multigroup transport equations, Eq. (12a), as

$$V^{-1}\frac{d\psi}{dt} + L\,\psi = (S + F)\psi + Q \tag{43}$$

where V^{-1} is a diagonal matrix of the inverse group speeds, L is the diagonal leakage operator $\nabla\cdot(\underline{\Omega}\,)+\sigma$ or its discretized analog, S and F are nondiagonal scattering and fission matrices, and ψ and Q are vectors containing the group angular fluxes and other sources (inhomogeneous plus delayed neutrons). We then assume the angular flux can be written as

$$\psi(t) = e^{\omega t}\,\hat{\psi}(t) \tag{44}$$

where ω is a diagonal matrix and the function $\hat{\psi}$ represents a small modulation of the assumed exponential behavior. When Eq. (44) is inserted into Eq. (43) $\hat{\psi}(t)$ satisfies the equation

$$V^{-1}\frac{d\hat{\psi}}{dt} + L\,\hat{\psi} = e^{-\omega t}\,(S+F)e^{\omega t}\,\hat{\psi} + e^{-\omega t}\,Q - V^{-1}\,\omega\,\hat{\psi}. \tag{45}$$

Equation (45) may be solved more accurately numerically than Eq. (43) if $\hat{\psi}$ is slowly varying with time. This will occur if the frequencies ω are properly chosen as discussed below.

The explicit time-differencing scheme in Sec. II.B.2. applied to Eq. (43) is

$$V^{-1}\frac{1}{\Delta t}(\psi^{j+1} - \psi^{j}) + L\,\psi^{j+1} = (S+F)\psi^{j} + Q \tag{46}$$

or after rearrangement

$$(L + \frac{1}{\Delta t}V^{-1})\psi^{j+1} = (S+F + \frac{1}{\Delta t}V^{-1})\psi^{j} + Q. \tag{47}$$

In Eq. (46), the scattering and fission source from higher groups is shown incorrectly to be calculated from fluxes at the previous time step in order to simplify the notation.

If we apply the same explicit time-differencing scheme to Eq. (42), we have

$$V^{-1}\frac{1}{\Delta t}(\hat{\psi}^{j+1}-\hat{\psi}^{j})+(L+V^{-1}\omega_{+})\hat{\psi}^{j+1}=e^{-\omega\Delta t}(S+F)e^{\omega\Delta t}\hat{\psi}^{j}-V^{-1}\omega_{-}\hat{\psi}^{j}+e^{-\omega\Delta t}Q, \tag{48a}$$

or after rearrangement

$$(L+V^{-1}\frac{1}{\Delta t}+V^{-1}\omega_{+})\hat{\psi}^{j+1}=e^{-\omega\Delta t}(S+F)e^{\omega\Delta t}\hat{\psi}^{j}-V^{-1}\frac{1}{\Delta t}\hat{\psi}^{j}-V^{-1}\omega_{-}\hat{\psi}^{j}+e^{-\omega\Delta t}Q \tag{48b}$$

where the factor $e^{\omega t}$ has been approximated by the values at the start of the time step. The matrix $\omega=\omega_{+}+\omega_{-}$ has been split into its positive components, ω_{+}, and its negative components, ω_{-}. This splitting is made so they will always appear as positive contributions in the relevant equations. Were the negative components kept on the left-hand side of Eq. (48), they could become larger in magnitude than the cross sections and result in unstable equations after the spatial differencing.

When Eq. (48) is multiplied by $e^{\omega t}$ and the fact that $\psi^{j+1}=e^{\omega\Delta t}\hat{\psi}^{j+1}$ and $\psi^{j}=\hat{\psi}^{j}$ if $t=0$ at the start of the time step is used, Eq. (48) becomes

$$(L+V^{-1}\frac{1}{\Delta t}+V^{-1}\omega_{+})\psi^{j+1}=(S+F+V^{-1}\frac{1}{\Delta t}-V^{-1}\omega_{-})e^{\omega\Delta t}\psi^{j}+Q. \tag{49}$$

Equation (49) is now in the form of the modified steady-state transport equation, Eq. (17), with the modified cross section of Eq. (18) given by

$$\tilde{\sigma}=\sigma+\frac{1}{v\Delta t}+\frac{\omega_{+}}{v} \tag{50}$$

and the modified source term of Eq. (19) given by

$$\tilde{S}^{j}(r,\underline{\Omega})=S^{j}(r,\underline{\Omega})+(\frac{1}{v\Delta t}-\frac{\omega_{-}}{v})e^{\omega\Delta t}\psi^{j}+\sum_{k=1}^{IGD}\lambda_{k}\chi^{d}_{k,g}C^{j}_{k}(r), \tag{51}$$

with the exception that the flux moments must be scaled by $e^{\omega\Delta t}$ before the scattering and fission contributions to the source term $S^{j}(r,\underline{\Omega})$ are computed. Thus the exponential extrapolation may be easily incorporated into the algorithms used to solve the steady-state equation.

The frequencies are altered after each time step to obtain the best accuracy. On the basis of numerical experiments, a practical choice for these frequencies is given by

$$\omega_{j}=\frac{1}{\Delta t}\ln\psi^{j}/\psi^{j+1}. \tag{52}$$

These frequencies ω_{j} are then used in the modified steady-state transport equation, Eq. (49), for the solution of the angular flux ψ^{j+1}. If some of the fluxes in Eq. (52) are zero, the frequencies are set to zero at those points.

The frequencies of Eq. (52) depend on angle, energy, and space. To allow an angular dependence would be expensive in core storage with only a marginal increase in accuracy. Thus, TIMEX allows only energy- and space-dependent frequencies.

The extrapolation derived above is a special kind of predictor-corrector method and is especially efficacious in situations where the time variation of the flux is smooth and nearly exponential. This condition is always true at long times following some initial transient if the system properties remain constant with time. Thus the exponential extrapolation is most advantageous in diffusion situations and is not usually recommended when wave fronts are propagating through the system. At long times following a perturbation in the system, the above frequencies converge to a single

number approximating the inverse asymptotic period of the system or the time-absorption eigenvalue (alpha) calculated for the same system by the steady-state code ONETRAN.[1]

The exponential extrapolation could also be applied to the delayed neutron precursors, using a different set of frequency factors. However, since the precursors are usually slowly varying in time, minimal improvement in accuracy would be obtained.

b. Within-group Fine-Mesh Rebalance

The rebalance acceleration available in the TIMEX code is more advantageous than exponential extrapolation in situations in which the flux is rapidly changing, such as wave front propagation problems. The explicit difference scheme used to obtain Eq. (46) is inaccurate due to the splitting of the L and S+F operators, such that the loss mechanisms are taken as proportional to the flux at the new time and the source mechanisms to the fluxes at the old time. The resulting imbalance between sources and losses prevents the computed flux from following transients as rapidly as it should. The difference equation that we would really like to solve is the fully implicit scheme

$$V^{-1}\frac{1}{\Delta t}(\psi^{j+1}-\psi^{j})+L\,\psi^{j+1}=(S+F)\psi^{j+1}+Q. \quad (53)$$

Unfortunately, to solve this equation at each time step would require the inversion of the full S+F-L operator, necessitating the inner iteration process of a steady-state calculation. This iteration may be slowly convergent so that an inordinate amount of computational effort is expended at each time step. It is our purpose here to adapt the well-known coarse-mesh rebalance[14] technique to the solution of Eq. (46).

The TIMEX rebalance acceleration enforces particle balance on each fine-mesh interval for each energy group in Eq. (53). That is, we multiply the angular flux in Eq. (53) by an unknown rebalance factor, f_i, and integrate over all angles and the i^{th} fine-mesh interval. This results in a tridiagonal system of equations for the rebalance factors for each group

$$f_i(FL_{i-\frac{1}{2}}^{j+1}+FR_{i-\frac{1}{2}}^{j+1}+AB_i^{j+1})=QQ_i^{j}+f_{i-1}\,FR_{i-\frac{1}{2}}^{j+1}+f_{i+1}\,FL_{i+\frac{1}{2}}^{j+1}, \qquad i=1,2,\ldots,IT. \quad (54)$$

For the i^{th} fine-mesh interval (deleting the j+1 superscript) the leftward and rightward flows are

$$FL_{i-\frac{1}{2}}=\sum_{\mu_m<0} w_m|\mu_m|\,A_{i-\frac{1}{2}}\,\psi_{i-\frac{1}{2}}, \quad (55a)$$

$$FR_{i+\frac{1}{2}}=\sum_{\mu_m>0} w_m\,\mu_m\,A_{i+\frac{1}{2}}\,\psi_{i+\frac{1}{2}}, \quad (55b)$$

the effective absorption is

$$AB_i=(\sigma_t+\frac{1}{v\Delta t}-\sigma^{o}_{s,g\to g}-\chi^{p}_{g\to g}\,\nu\,\sigma_{fg})^{*}\sum_{m=1}^{MM} w_m(V_{i-\frac{1}{2}}\,\psi_{i-\frac{1}{2}}+V_{i+\frac{1}{2}}\,\psi_{i+\frac{1}{2}}), \quad (55c)$$

and the rebalance source is

$$QQ_i=\sum_{m=1}^{MM} w_m(V_{i-\frac{1}{2}}\,S_{i-\frac{1}{2}}+V_{i+\frac{1}{2}}\,S_{i+\frac{1}{2}})+\frac{1}{v\Delta t}\sum_{m=1}^{MM} w_m(V_{i-\frac{1}{2}}\,\psi_{i-\frac{1}{2}}+V_{i+\frac{1}{2}}\,\psi_{i+\frac{1}{2}}) \quad (55d)$$

where $S_{i\pm\frac{1}{2}}$ contains all sources to the group (inhomogeneous + fission + scattering + delayed neutrons) but no within-group scatter or fission. Equation (54) may be rapidly solved by forward elimination-backward substitution for the rebalance factors.

The fine-mesh rebalance acceleration may also be applied in conjunction with the exponential extrapolation with slight modifications. The fully-implicit scheme for Eq. (48a) that we would really like to solve, analogous to Eq. (53), is

$$\frac{1}{v\Delta t}(\hat{\psi}^{j+1}-\hat{\psi}^{j})+(L+V^{-1}\omega_{+})\,\hat{\psi}^{j+1}=e^{-\omega\Delta t}(S+F)e^{\omega\Delta t}\,\hat{\psi}^{j+1}-V^{-1}\omega_{-}\,\hat{\psi}^{j}+e^{-\omega\Delta t}\,Q, \quad (56)$$

but again an undesired iteration would be required to invert S+F-L. The fine-mesh rebalance technique developed above can again be applied to Eq. (56) to yield the same Eq. (54) for the rebalance factors, provided the effective absorption is defined

$$AB_i = (\sigma_t + \frac{1}{v\Delta t} + \frac{\omega_+}{v} - \sigma^o_{s,g\to g} - \chi^p_{g\to g}\ \nu\ \sigma_{fg}) \sum_{m=1}^{MM} w_m(V_{i-\frac{1}{2}}\ \psi_{i-\frac{1}{2}} + V_{i+\frac{1}{2}}\ \psi_{i+\frac{1}{2}}) \tag{57a}$$

and the rebalance source

$$QQ_i = \sum_{m=1}^{MM} w_m(V_{i-\frac{1}{2}}\ S_{i-\frac{1}{2}} + V_{i+\frac{1}{2}}\ S_{i+\frac{1}{2}}) + (\frac{1}{v\Delta t} - \frac{\omega_-}{v})e^{\omega\Delta t} \sum_{m=1}^{MM} w_m(V_{i-\frac{1}{2}}\ \psi_{i-\frac{1}{2}} + V_{i+\frac{1}{2}}\ \psi_{i+\frac{1}{2}}). \tag{57b}$$

It has been observed[14] in steady-state calculations that fine-mesh rebalance may have a destabilizing effect on convergence of the inner iterations, although this is much less likely with a discontinuous spatial difference scheme. It is possible that this destabilizing effect would also appear in the time-dependent calculation by TIMEX, although this has not been observed in test calculations.

c. Outer Rebalance

In the within-group fine-mesh rebalance of the preceding section, the flows (FL and FR) and the absorption (AB) are computed with fluxes at the $j + 1^{st}$ time step. However, for the sources (QQ), the in-scattering source and fission source to group g from groups h > g are computed with fluxes from the j^{th} time step as indicated by Eq. (19). A more accurate procedure would be to recompute the fine-mesh rebalance factors for each group at the end of the group sweep when the fluxes for all groups at the $j + 1^{st}$ time point have been computed. This would require recomputing the flows, sources, and absorptions on the fine mesh for each group. A far easier procedure, less accurate, is to compute a single system rebalance factor for all groups. The single equation for this outer rebalance factor is obtained from multiplying the fluxes in Eq. (16a) by the rebalance factor and summing over all groups and integrating over the spatial and angular variables. The outer rebalance factor is then given by

$$ORFACT = \frac{ORSOR}{ORLEAK + ORABS}\ . \tag{58}$$

The outer rebalance source is

$$ORSOR = \sum_i \sum_g \left[(\frac{1}{v\Delta t} - \frac{\omega_-}{v})\phi^j_{ig}\ V_i + Q^{j+1}_{ig}\ V_i\right] + \sum_k \sum_i \lambda_k\ C^j_k\ V_i, \tag{59a}$$

where ϕ^j_{ig} is the scalar flux in the i^{th} mesh cell for group g at the j^{th} time step, V_i the i^{th} mesh-cell volume and Q^{j+1}_{ig} the inhomogeneous distributed source. The outer rebalance leakage is the total leakage for all groups from the system, given by

$$ORLEAK = \sum_g \sum_{\mu_m<0} w_m|\mu_m|(A_{1\frac{1}{2}}\ \psi_{1\frac{1}{2}} - A_{IT+\frac{1}{2}}\ \psi_{IT+\frac{1}{2}}) + \sum_g \sum_{\mu_m>0} w_m\ \mu_m(A_{IT+\frac{1}{2}}\ \psi_{IT+\frac{1}{2}} - A_{1\frac{1}{2}}\ \psi_{1\frac{1}{2}}). \tag{59b}$$

The outer rebalance absorption is given by

$$ORABS = \sum_g \sum_i \left[\frac{1}{v\Delta t} + \frac{\omega_+}{v} + \sigma_a - (1-\beta)\nu\ \sigma_f\right]\phi^{j+1}_{ig}\ V_i, \tag{59c}$$

where σ_a is the effective absorption for group g

$$\sigma_a = \sigma_t - \sum_h \sigma^o_{s,g\to h} + \text{Buckling absorption.}$$

For the case in which the exponential extrapolation is not applied, the appropriate terms of Eq. (59) are obtained by setting $\omega_\pm = 0$.

6. First-Collision Source

In some transport problems the exact flux at an instant of time involves Dirac delta functions. For example, such functions are obtained for an instantaneous point burst of neutrons at time zero. The accurate prediction of such irregular functions is quite difficult with standard finite difference methods, so that exceedingly fine meshes are required. To circumvent this difficulty, a first-collision source option is provided in the TIMEX code. This option is restricted to the treatment of instantaneous sources located at the origin of the coordinate system, that is, point sources in spherical geometry, line sources in cylindrical geometry, and plane sources in slab geometry. The angular dependence of the source neutrons is assumed to be given by $\delta(\mu-1)$ in all three geometries, so that in each case the neutrons are assumed to stream directly away from the origin.

If the first-collision source option is specified, the neutron flux is considered as the sum of two terms, the flux due to neutrons that have suffered no collisions (the uncollided flux) and the flux due to neutrons that have suffered one or more collisions (the collided flux). We define the two functions ψ_u and ψ_c to be the uncollided and collided fluxes, respectively, so that the total flux ψ is given by $\psi = \psi_u + \psi_c$. These two functions are assumed to obey the two equations

$$\frac{1}{v}\frac{\partial \psi_u}{\partial t} + L\,\psi_u = Q_u \qquad (60a)$$

and

$$\frac{1}{v}\frac{\partial \psi_c}{\partial t} + L\,\psi_c = (S+F)(\psi_u + \psi_c), \qquad (60b)$$

where $Q_u(r,\underline{\Omega},t)$ is the delta function inhomogeneous source at the origin. Equation (60) is easy to solve analytically for ψ_u because there are no scattering sources. When ψ_u has been obtained, Eq. (60) can be solved with the difference methods derived in Sec. II.C. We note that the sum of Eqs. (60a) and (60b) gives the full transport equation for the complete angular flux.

The rationale for splitting the angular flux into collided and uncollided components is that the function ψ_c is smoother than ψ_u. Because we are solving Eq. (60a) by analytic methods, a nonsmooth solution does not cause concern. All errors in the calculation are introduced in the solution of Eq. (60b) for the collided flux. Because ψ_c is smooth, these errors will be smaller than those involved in the direct solution of the full transport equation by difference methods.

The analytic uncollided fluxes due to the sources mentioned above are presented in Table VI for a single group of neutrons with speed v. In the following we deal exclusively with a single energy group; all groups are treated in the same manner.

The quantities N_o shown in Table VI for slabs, cylinders, and spheres are the total number of source neutrons emitted per unit area, the total number of neutrons per unit length, and the total number of neutrons, respectively.

To calculate the source in Eq. (60b) due to the uncollided flux, we need the spherical harmonic moments of the uncollided flux. In slab and spherical geometry these moments are given by

$$\phi_\ell(r,t) = \int_{-1}^{+1} \frac{d\mu}{2}\, P_\ell(\mu)\, \psi_u(\mu,r,t) .$$

Because ψ_u involves the delta function $\delta(1-\mu)$, and because $P_\ell(1) = 1.0$ for all the Legendre polynomials, all of the above moments are identical. In cylindrical geometry, the angular contribution of the uncollided source, $\delta(1-\mu)$, is written as $\delta(\phi)\delta(\xi)$ in the coordinates of Fig. 2. From Eqs. (8) and (9), the moments of the uncollided flux are

$$\phi_{u,n}(r,t) = P_n(0)\,\psi_u(r,t) \qquad (61a)$$

and

$$\phi^{\ell}_{u,n}(r,t) = \sqrt{2\frac{(n-\ell)!}{(n+\ell)!}}\; P^{\ell}_n(0)\,\psi_u(r,t), \qquad (61b)$$

where $\psi_u(r,t)$ is the spatial and time-dependent fraction of the uncollided flux in Table VI. These coefficients of the uncollided flux moments may easily be computed using the relation

$$P^m_m(0) = \frac{(2m)!}{2^m\, m!}$$

and the recursion

TABLE VI

ANALYTIC UNCOLLIDED FLUX

Geometry	Source: $Q_n(r,\underline{\Omega},t)$	Uncollided Flux: $\psi_n(r,t)\delta(1-\mu)$
Plane	$N_o\delta(r)\delta(1-\mu)\delta(t)$	$N_o e^{-\int_o^r \sigma(r')dr'} \delta(t-\frac{r}{v})\delta(1-\mu)$
Cylindrical	$\frac{N_o\delta(r)\delta(1-\mu)\delta(t)}{2\pi r}$	$\frac{N_o e^{-\int_o^r \sigma(r')dr'} \delta(t-\frac{r}{v})\delta(1-\mu)}{2\pi r}$
Spherical	$\frac{N_o\delta(r)\delta(t)\delta(1-\mu)}{4\pi r^2}$	$\frac{N_o e^{-\int_o^r \sigma(r')dr'} \delta(t-\frac{r}{v})\delta(1-\mu)}{4\pi r^2}$

(σ = total cross section)

$$P_{n+1}^m(0) = -\frac{(n+m)}{(n-m+1)} P_{n-1}^m(0).$$

For the two-angle plane geometry option of TIMEX, the problem is identical to the standard plane geometry due to the azimuthal symmetry of the uncollided source. In all geometries, only the spatial and time-dependent fraction (average) is computed (in subroutine UNCOLL) and added to all the moments of the flux, weighting by the coefficients of Eq. (61) in cylindrical geometry.

The uncollided flux is a delta function moving through the system and may not be simply added to the collided flux in the discretized space. Instead, the uncollided flux is smeared out over the discretized space by taking a space-time average. For the i^{th} mesh cell and the j^{th} time interval, we utilize the averaged uncollided flux

$$\bar{\phi}_{u,i}^j = \frac{1}{V_i\Delta t}\int_{\Delta V_i} dV \int_{t_j}^{t_j+\Delta t} dt\ \phi_u(r,t). \qquad (62)$$

Inserting the expression for $\phi_u(r,t)$ for the appropriate geometry into Eq. (62), we obtain

$$\bar{\phi}_{u,i}^j = \frac{N_o}{V_i\Delta t}\int_{r_{i-\frac{1}{2}}}^{r_{i+\frac{1}{2}}} dr \int_{t_j}^{t_j+\Delta t} dt\ e^{-\int_o^r \sigma(r')dr'} \delta(t-\frac{r}{v}) = \frac{N_o}{V_i\Delta t}\int_{r_{i-\frac{1}{2}}}^{r_{i+\frac{1}{2}}} dr\ e^{-\int_o^r \sigma(r')dr'} \left[U(r-vt_j) - U(r-vt_j-v\Delta t)\right] \qquad (63)$$

where U(x) is the step function defined by

$$U(x) = \begin{cases} 0 & x < 0 \\ 1 & x \geq 0 \end{cases}.$$

When the integration over this square wave function is performed in Eq. (63), the average uncollided flux becomes

$$\bar{\phi}_{u,i}^j = \frac{N_o}{V_i\Delta t\sigma(r_i)}\ e^{-\int_o^{a_j}\sigma(r')dr'}\left[1 - e^{-\sigma(r_i)(b_j-a_j)}\right] \qquad (64a)$$

for $\sigma(r_i) \neq 0$, or for the case of a void

$$\bar{\phi}_{u,i}^j = \frac{N_o}{V_i\Delta t}(b_j - a_j). \qquad (64b)$$

The integration limits in Eq. (64) are given by

$$a_j = \max(r_{i-\frac{1}{2}},\ vt_j)$$

and

$$b_j = \min(r_{i+\frac{1}{2}},\ v\,t_j + v\Delta t),$$

provided the intervals $(vt_j, vt_j + v\Delta t)$ and $(r_{i-\frac{1}{2}}, r_{i+\frac{1}{2}})$ are not disjoint. If these intervals are disjoint, then the uncollided flux is zero in the i^{th} mesh cell during the j^{th} time step so that $\bar{\phi}^j_{u,i} = 0$.

The averaged uncollided flux is computed in TIMEX from Eq. (64) for each energy group. There is no coupling between energy groups since there are no scattering terms on Eq. (60a) for the uncollided flux. These averaged uncollided fluxes are then added to all moments of the collided fluxes. This total flux is then used in the algorithms to generate the scattering and fission sources in Eq. (60b).

The TIMEX user is allowed to print and perform activity edits at the end of the j^{th} time step. The uncollided flux $\phi^{j+1}_{u,i}$ to be added to the collided flux is obtained by taking the limit of Eq. (64) as $\Delta t \to 0$ to obtain

$$\phi^{j+1}_{u,i} = \frac{N_o\, v}{V_i}\, e^{-\int_o^{v\, t_{j+1}} \sigma(r')dr'} . \qquad (65)$$

This uncollided flux is added only in the spatial mesh cell containing the radial point $r = v\, t_{j+1}$.

7. Moving Boundaries

The TIMEX user is permitted to enter new system properties (cross sections, coarse-mesh boundaries, densities, etc.) at the beginning of each time zone. Most of these options present no special difficulty for the code. However, if the user wishes to move the coarse-mesh boundaries at the start of a time zone, then the TIMEX code must interpolate the old fluxes onto the new mesh. There are a variety of ways to perform this interpolation. TIMEX uses the simplest method possible that guarantees conservation of neutrons.

If the moving boundary option is used, the coarse-mesh boundaries are assumed to move instantaneously from their previous positions to the new positions. The code requires that the outer (right-hand) boundary remain fixed throughout the computation (the left-hand boundary is always fixed at 0.0). This eliminates the necessity of an extrapolation onto the new mesh at the outer boundary. This restriction may be easily circumvented by placing a large fictitious vacuous region as the outermost coarse-mesh zone. For the interpolation algorithm, the angular flux in each fine-mesh cell is assumed to be represented by a single value, the cell-centered value. The new angular flux in the i^{th} mesh cell in the m^{th} direction is computed from

$$\psi^{new}_{i\pm\frac{1}{2},m} = \frac{1}{V^{new}_i} \int_{r^{new}_{i-\frac{1}{2}}}^{r^{new}_{i+\frac{1}{2}}} \psi^{old}_m(r)\, dV. \qquad (66)$$

The integral is a volume integral and the old angular flux, $\psi^{old}_m(r)$, is construed as a series of step functions for each of the old fine-mesh cells. Note that this interpolation procedure destroys the slope (or tilt) of the angular flux in each mesh cell.

III. A GUIDE TO USER APPLICATION

In this section we provide information needed by the user to understand TIMEX options and to prepare input for the code.

A. Overall Program Flow

A schematic flow chart for TIMEX is given in Fig. 9. The subroutine names in which that computation is performed are indicated beside each block.

B. Details of Program Options

1. Cross Sections

a. Input Formats

The TIMEX program accepts cross sections either from the standard file ISOTXS,[3] in FIDO format,[4] or in the standard Los Alamos format as described in this section. In upscattering problems, the program does not need the special σ^{up} cross section which is required in earlier Los Alamos programs.[10] In TIMEX, it is assumed that σ^{up} is NOT present, but σ^{up} is automatically removed from the card input cross-section sets if the user tags the input number IHS with a minus sign. Note that this is the opposite procedure for removal of σ^{up} from that used in other LASL transport codes.[11,15] Cross sections read with the FIDO format may not contain σ^{up}.

The Los Alamos cross-section format assumes that each nuclide is described by a block of cross sections of IHM rows for IGM group columns. The row position of cross sections is specified relative to the total cross section, σ_t (row IHT), and within-group scattering cross section, $\sigma_{s,g\to g'}$ (row IHS). It is assumed that the row order of the cross sections is as follows:

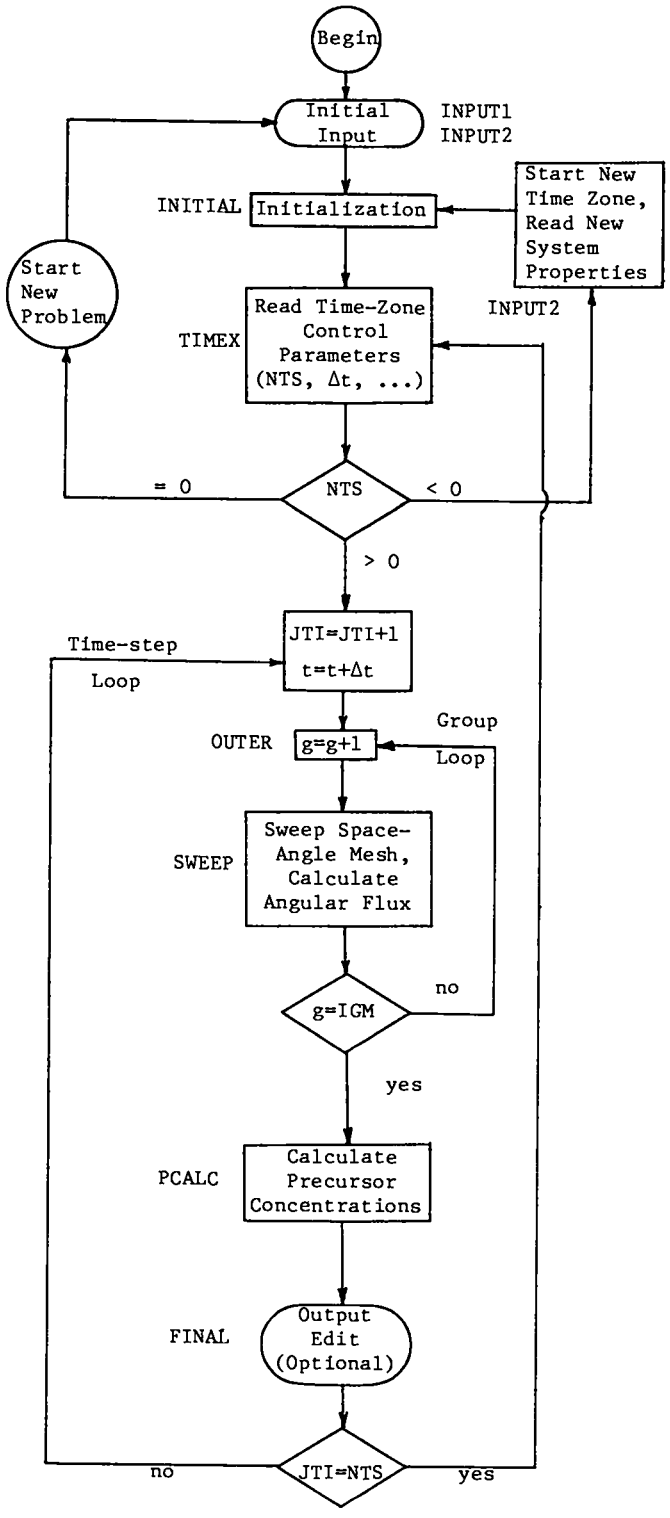

Fig. 9. Simplified logical flow diagram for TIMEX.

Row	Cross Section Type Group g
.	
.	
.	
IHT-4	$\sigma_{n,2n}$
IHT-3	σ_{tr}
IHT-2	σ_{a}
IHT-1	$\nu\sigma_{f}$
IHT	σ_{t}
IHT+1	$\sigma_{s,g+N\rightarrow g}$
IHM .	
.	
.	
IHS-2	$\sigma_{s,g+2\rightarrow g}$
IHS-1	$\sigma_{s,g+1\rightarrow g}$
IHS	$\sigma_{s,g\rightarrow g}$
IHS+1	$\sigma_{s,g-1\rightarrow g}$
IHS+2	$\sigma_{s,g-2\rightarrow g}$
.	
.	
.	
IHS+M	$\sigma_{s,g-M\rightarrow g}$

In this format, group g+1 corresponds to a group of lower energy than group g. The symbol $\sigma_{s,g-2\rightarrow g}$ denotes the scattering transfer probability from group g-2 to group g. The format allows N groups of upscatter and M groups of downscatter; i.e., the scattering matrix need not be square. However, all cross-section blocks must have the same values of IHM, IHS, and IHT. The fission cross section, σ_f, times the mean number of neutrons per fission, ν, must be located in row IHT-1, and the absorption cross section σ_a must be entered in row IHT-2. The transport cross section, σ_{tr}, must be entered in position IHT-3 if the transverse buckling correction is to be made using σ_{tr} rather than σ_t as detailed in Sec. III.B.2.c. The (n,2n) scattering cross section, $\sigma_{n,2n}$, must be entered in position IHT-4 if the scattering matrix is used to represent (n,2n) reactions, as detailed in Sec. III.B.1.g. The user is free to enter additional cross sections at the top of the format. These extra cross sections are not used in the calculation, but

are used for reaction-rate computations in the flux edits.

b. Cross-Section Mixing

The user is free in TIMEX to enter macroscopic cross sections and bypass the mixing algorithms; specification of the input value MS = 0 is all that is required for this. If MS ≠ 0, the user must provide three sets of MS numbers which are stored in the vectors MIXNUM, MIXCOM, and MIXDEN. These numbers are used in the following algorithm to manipulate cross-sections blocks:

```
      DO     315     M = 1, MS
      N = MIXNUM(M)
      L = MIXCOM(M)
      AD = MIXDEN(M)
      DO     315     I = 1, IHM
      IF(L.EQ.0) GO TO 310
      C(I,N) = C(I,N) + AD*C(I,L)
      GO TO 315
  310 C(I,N) = AD*C(I,N)
  315 CONTINUE
```

In this algorithm, cross-section block N is created or altered by adding multiples of block L or by multiplying the block N by a factor. Let us consider some examples.

Suppose we have entered 45 cross-section blocks as input. Then any mixtures that are made must be given block numbers higher* than 45. Suppose we enter:

MIXNUM (N)	MIXCOM (L)	MIXDEN (AD)
46	0	0.0
46	1	0.0478
46	20	0.0333
47	0	0.0
47	2	0.75
47	3	0.25
47	0	0.1179
48	0	0.0
48	15	0.0049
48	14	0.0078

*To preserve the input values. If these need not be saved, mixtures can be created in lower block numbers.

For this example we have MS = 10 instructions. In the first three instructions, block 46 is cleared (set to zero) and then made up of 0.0478 parts of block 1 and 0.0333 parts of block 20. If blocks 1 and 20 are microscopic cross sections in barns, then 0.0333 and 0.478 times 10^{24} are the atomic densities. In the second set of instructions, block 47 is cleared and then made up of 0.1179 times the result of adding three-fourths of block 2 to one-fourth of block 3. In the next set of instructions, block 48 is cleared and made up of portions of blocks 15 and 14. It should be clear that there are many possibilities not covered in this example, but by examining the FORTRAN instructions above the user should be able to prepare his own set of mixture instructions.

c. Anisotropic Cross Sections

In the TIMEX program it is assumed that the scattering transfer probability can be represented by a finite Legendre polynomial expansion; i.e.,

$$\sigma_s(E' \to E,\mu_o) = \sum_{n=0}^{ISCT} \frac{2n+1}{4\pi} P_n(\mu_o)\sigma_s^n(E' \to E), \quad (67)$$

where ISCT is an input control integer. Thus if ISCT > 0, additional blocks of scattering transfer cross sections must be entered for those nuclides for which anisotropic scattering sources are to be computed. Note that the anisotropic scattering blocks do NOT contain the (2n+1) factor as in some transport codes.[4] Should the cross-section blocks contain this factor, they may easily be removed via the mixing tables. In these blocks, the rows 1 through IHT are zero, and $\sigma^n_{s,g\to h}$ (the energy average of $\sigma^n_s(E' \to E)$ in groups g and h is entered as for the isotropic component of the cross section. It is assumed in TIMEX that blocks of anisotropic cross sections which are used in the calculation have block numbers in ascending sequence, starting with the isotropic cross-section block. For example, suppose that block 50 is the isotropic cross-section block for hydrogen and that ISCT = 3. Then, block 51 must be σ^1_s for hydrogen, block 52 must be σ^2_s, and block 53 must be σ^3_s. If a material is made by mixing two anisotropic scatterers, then the anisotropic blocks must also be mixed with the same densities to form anisotropic blocks for the material. In each zone in which anisotropic scattering sources are

computed the number of anisotropic scattering blocks must be the same, namely ISCT.

d. Adjoint Cross Sections

In adjoint calculations, cross sections are entered just as for a direct calculation. The program then transposes the scattering matrices and, because this usually changes a downscattering problem to an upscattering problem, reverses the group order of the blocks. Further, the effective absorption in an adjoint calculation is not simply related to σ_a. That is, the effective absorption is normally

$$(\sigma_a)_{eff} = \sigma_t - \sum_{\text{all } h} \sigma^0_{s,g\to h}. \qquad (68a)$$

But when the scattering matrix has been transposed, the effective absorption is

$$(\sigma_a)_{eff} = \sigma_t - \sum_{\text{all } h} \sigma^0_{s,h\to g}. \qquad (68b)$$

e. Cross-Section Checking

As input cross sections are processed in subroutine CSPREP, the effective absorption of Eq. (68a) is computed and compared to the input value of σ_a. If the relative difference between the input total cross section and the computed total cross section exceeds 10^{-4} an error message is printed. However, the computation will proceed normally using the input absorption cross section with no attempt being made to correct this inconsistency.

f. Fission Fractions

The TIMEX user may specify the prompt fission fractions as either a spectrum (χ_g: the probability of a fission in any group releasing a neutron in group g) or a matrix ($\chi_{h\to g}$: the probability of a fission in group h releasing a prompt neutron in group g). These fission fractions may also be coarse-mesh-dependent. The fission fractions must be normalized to $\sum_g \chi_g = 1$ or $\sum_g \chi_{h\to g} = 1$. This normalization is not checked by TIMEX and any lack of normalization will be reflected proportionally in the k_{eff} of the system.

The fission fractions are specified by the input parameter IFISS:

IFISS	Option
1	A single fission spectrum for the entire system
2	A fission spectrum for each of the IM coarse-mesh regions
3	A single fission matrix for the entire system
4	A fission matrix for each of the IM coarse-mesh regions.

For coarse-mesh-dependent fission spectra (IFISS=2), the fission fractions are ordered as:

$$[\chi_1 \cdots \chi_{IGM}]_{i=1} \cdots\cdots\cdots [\chi_1 \cdots \chi_{IGM}]_{i=IM},$$

and loaded as a single block. For coarse-mesh-dependent fission matrices (IFISS=4), the fission fractions are ordered as:

$$\begin{bmatrix} [\chi_{1\to1}\cdots\chi_{IGM\to1}]_{i=1}\cdots[\chi_{1\to1}\cdots\chi_{IGM\to1}]_{i=IM} \\ [\chi_{1\to IGM}\cdots\chi_{IGM\to IGM}]_{i=1}\cdots[\chi_{1\to IGM}\cdots\chi_{IGM\to IGM}]_{i=IM} \end{bmatrix}$$

and each row is loaded as a single block.

g. (n,2n) Reactions

The TIMEX user may utilize the scattering matrices to represent (n2,n) reactions by flagging the input parameter IHT negative. If $\sigma_{(n,2n)h\to g}$ is the reaction cross section for a neutron in group h releasing two neutrons in group g, then $2 * \sigma_{(n,2n)h\to g}$ must be entered as the scattering transfer matrix, $\sigma_{s,h\to g}$, in order to obtain the proper neutron multiplication in the scattering computation by TIMEX. The total (n,2n) reaction cross section

$$\sigma_{n,2n} = \sum_g \sigma_{(n,2n)h\to g},$$

must then be entered in cross section position IHNN = IHT - 4. This cross section is then used to correct the group sum of the outscatter term in the system balance tables.

If IHT is not flagged negative, TIMEX assumes no (n,2n) reactions are present and cross section position IHNN may be used for any other cross section to be used in the reaction-rate computations in the flux edits.

h. Fine-Mesh Density Factors

The TIMEX user has the option of specifying fine-mesh density factors to describe a pointwise

spatial variation of the macroscopic cross sections. Thus, the macroscopic cross section is multiplied by DEN(I) whenever the cross section is required in mesh cell I. These density factors are very useful in problems such as air transport calculations where a single material is present but with a continuously varying spatial density.

i. Delayed Neutron Parameters

If the delayed neutron option is selected (IGD>0), the TIMEX code requires the parameters:

- β_k - the delayed neutron fraction (the fraction of the fission neutrons appearing from decay of the k^{th} delayed neutron precursor)
- λ_k - the decay constant (usually in dimensions of sec^{-1}) for the k^{th} delayed neutron precursor group
- $\chi^d_{k,g}$ - the delayed neutron fission spectra (the probability of a decay in the k^{th} precursor group releasing a neutron in the g^{th} energy group).

The user may also enter the initial delayed neutron precursor concentrations as described in Sec. III. B.6. TIMEX calculates the total delayed neutron fraction $\beta = \sum_k \beta_k$ and requires normalization of the delayed fission spectra to

$$\sum_g \chi^d_{k,g} = 1.$$

The above delayed parameters are coarse-mesh-dependent if the prompt fission fractions are coarse-mesh-dependent (IFISS=2 or 4 so that KM=IM, the number of coarse-mesh intervals). The decay constants and delay fractions are each loaded as a single block in the order:

$$[\lambda_1 \cdots \lambda_{IM}]_{k=1} \cdots [\lambda_1 \cdots \lambda_{IM}]_{k=IGD}$$

and

$$[\beta_1 \cdots \beta_{IM}]_{k=1} \cdots [\beta_1 \cdots \beta_{IM}]_{k=IGD} .$$

The delayed neutron fission spectra are loaded as a single block in the order:

$$[(\chi^d_{1,1}), \cdots (\chi^d_{1,1})_{IM}] \cdots [(\chi^d_{IGD,1}), \cdots (\chi^d_{IGD,1})_{IM}] \cdots$$
$$[(\chi^d_{1,2}), \cdots (\chi^d_{1,2})_{IM}] \cdots [(\chi^d_{IGD,2}), \cdots (\chi^d_{IGD,2})_{IM}] \cdots$$
$$\vdots$$
$$[(\chi^d_{1,IGM}), \cdots (\chi^d_{1,IGM})_{IM}] \cdots [\chi^d_{IGD,IGM}), \cdots (\chi^d_{IGD,IGM})_{IM}] .$$

For the case in which the prompt fission fractions are not coarse-mesh-dependent (IFISS=1 or 3 so that KM=1), the IM entries in the above brackets, [], reduce to one entry.

2. Geometry and Boundary Condition Specifications

a. Spatial Mesh

To specify the spatial domain of the problem, the user supplies IM+1 coarse-mesh boundaries (defining IM intervals). Except for the first radius in cylindrical or spherical geometries, this set need not begin at 0.0, but must form a monotone increasing sequence. The user also supplies IM integers which indicate how many fine-mesh intervals are in each coarse-mesh interval. The fine-mesh spacing is uniform between the coarse-mesh boundaries. This results in a total of IT fine-mesh intervals, indexed from left to right. Finally, the user specifies the boundary condition on the left and right boundaries.

The coarse-mesh boundaries define IM zones. The user must supply a number for each of these zones (IDC array) to designate which cross-section block belongs in the zone. That is, the material mesh is identical to the coarse mesh. If anisotropic scattering is desired in any zone, the block number for that zone is flagged negative, otherwise the scattering is computed as isotropic. This indicates that the next ISCT blocks in numerical sequence contain the anisotropic scattering cross sections for this zone. The scattering will be computed as isotropic if ISCT > 0 and IDC is not flagged negative or if ISCT = 0 (regardless of the sign on IDC).

All of the above information is converted by subroutine MAPPER into a pictorial description of the system.

b. Boundary Conditions

The TIMEX user must select one of the following five boundary conditions for each of the system boundaries:

- Vacuum boundary condition -- the angular flux on the boundary is set to zero for all incoming directions.

- Reflective boundary condition -- the incoming angular flux on the boundary is set equal to the outgoing flux in the direction corresponding to specular reflection.

- Periodic boundary condition -- the incoming angular flux on the boundary is set equal to outgoing flux in the same direction on the opposite boundary.

- White boundary condition -- the incoming angular flux on the boundary is set equal to the single value such that the net flow through the boundary is zero, namely:

$$\psi_{\text{incoming}}(\mu_{m'}) = \frac{\sum_m w_m \mu_m \psi(\mu_m)_{\text{outgoing}}}{\sum_m w_m \mu_m} ,$$

where the sums range over all outgoing directions. This condition is used primarily for cell calculations in cylindrical and spherical geometry where it is applied to the outer radial boundary.

- Albedo boundary condition -- the incoming angular flux on the boundary is set equal to a user-supplied albedo times the outgoing flux in the direction corresponding to specular reflection.

Use of reflective or albedo boundary conditions requires the S_N quadrature set to be symmetric about $\mu = 0$.

c. Buckling Absorption

Leakage from the transverse dimensions of a multidimensional system may be simulated by a user-specified buckling height and width (for plane geometry only). These buckling dimensions must be in units consistent with the cross sections (in cm if cross sections are in cm^{-1}). If diffusion theory is assumed adequate then the flux shape in the transverse direction z is of the form $\cos \pi z/\tilde{h}$, so that the flux vanishes at the extrapolated half-heights $\pm \tilde{h}/2$. If this assumption is substituted into the multidimensional form of the transport equation, Eq. (1), then the transverse leakage appears as a buckling absorption cross section of the form

$$\sigma_{a,BHT} = \frac{\sigma}{3} \left(\frac{\pi}{\sigma * BHT + 1.4209}\right)^2 ,$$

where σ is the total cross section, BHT is the actual buckling transverse dimension (height or width), and $1.4209/\sigma$ is twice the Milne problem extrapolation distance. If the input buckling height (BHGT) is flagged negative, then the transport cross section, σ_{tr}, is assumed to be in cross section position IHTR = IHT - 3. The extrapolation distance of $1.4209/\sigma_{tr}$ is then used so that the buckling absorption is

$$\sigma_{a,BHT} = \frac{\sigma}{3} \left(\frac{\pi}{\sigma * BHT + 1.4209\ \sigma/\sigma_{tr}}\right)^2 .$$

The buckling absorption is added to both the total cross section (CT) and absorption cross section (CA) arrays in subroutine INITAL. Consequently, the absorption in the output coarse-mesh balance table also contains this buckling absorption. The activities computed in the flux edits do not contain this buckling absorption.

If BHGT is not flagged negative, then σ_{tr} is assumed to not be present and cross section position IHTR may be used for any other cross section to be used in reaction-rate computations in the flux edits.

3. Angular Quadrature Coefficient Specifications

The TIMEX user has the option of obtaining the angular quadrature coefficients from interface file ISNCON,[3] one of two built-in sets of subroutine SNCON, or from card input. The input parameter IQUAD specifies the source of these coefficients. The number of quadrature coefficients (MM) is determined from the input S_N order parameter ISN and the geometry type specification (IGEOM) as

$$MM = \begin{cases} \text{ISN for plane and spherical geometry} \\ \text{ISN*(ISN+2)/4 for cylindrical geometry (IGEOM=2), or} \\ \text{ISN*(ISN+2) for two-angle plane geometry (IGEOM=4).} \end{cases}$$

The built-in constants are either the P_N (Gaussian) quadrature constants for: S_2, S_4, S_6, S_8, S_{12}, S_{16}, S_{20}, S_{32}, or S_{48}; or the DP_N (double Gaussian) quadrature constants for: S_4, S_8, S_{12}, S_{16}, S_{24}, S_{32}, S_{40}, S_{48}, S_{64}, or S_{96}. For most problems, the P_N set is the recommended set. However, for thin-slab problems in which the angular representation of the leakage flux is important, use of the DP_N quadrature set is recommended.

For problems with anisotropic scattering, it is important that the S_N order be chosen sufficiently large such that the spherical harmonic polynomials are correctly integrated. Otherwise, the numerical quadrature error may introduce a nonphysical contribution to the neutron balance.

For user input S_N constants, it is necessary that they be correctly ordered as illustrated in Sec. II.B.3. In addition, if the sums $1 - \sum_m w_m$, and $\sum_m \mu_m$, and $\sum_m w_m \mu_m$ are greater than 10^{-5}, an error message is printed.

4. Source Options

The TIMEX user may specify an anisotropic distributed source and the boundary flux at either boundary of the system. The inhomogeneous distributed source must be represented by a finite spherical harmonic expansion of the form

$$Q(r,\underline{\Omega}) = \sum_{n=1}^{NMQ} (2n-1)\, R_n(\underline{\Omega})\, Q_n(r), \qquad (69)$$

where the energy group index has been omitted. For standard plane or spherical geometry, the moments of the source are

$$Q_n(r) = \frac{1}{2}\int_{-1}^{1} d\mu\, P_n(\mu)\, Q(r,\mu), \qquad (70)$$

and for cylindrical and two-angle plane geometry

$$Q_n(r) = \frac{1}{4\pi}\int_{-1}^{1} d\xi \int_{0}^{2\pi} d\phi\, P_n(\xi)\, Q(r,\xi,\phi) \qquad (71)$$

and

$$Q_n^{\ell}(r) = \frac{1}{4\pi}\sqrt{2\frac{(n-\ell)!}{(n+\ell)!}} \int_{-1}^{1} d\xi \int_{0}^{2\pi} d\phi\, P_n^{\ell}(\xi) \begin{Bmatrix} \cos & \ell & \phi \\ \sin & \ell & \phi \end{Bmatrix} Q(r,\xi,\phi), \qquad (72)$$

as defined in a similar fashion for the flux moments in Sec. II.A.2. The anisotropic source components are entered in the order indicated in Tables III and IV.

When the anisotropic distributed source option is used, the order of anisotropic scattering, ISCT, must be at least as large as IQAN so that the requisite number of spherical harmonics, $R_n(\underline{\Omega})$, is computed.

The TIMEX user is also allowed to specify the incoming flux on either boundary. This boundary source is specified for the MM/2 incoming directions in the same order as the S_N quadrature ordinates as illustrated in Sec. II.B.3.

5. Source Input Options

If a distributed source of anisotropy IQAN is designated, then

$$NMQ = \begin{cases} IQAN+1 \text{ for plane and spherical geometry, or} \\ (IQAN+2)^2/4 \text{ for cylindrical geometry, or} \\ (IQAN+1)^2 \text{ for two-angle plane geometry} \end{cases}$$

components (spherical harmonic moments) of the source must be entered for each group in the order listed in Tables III and IV. The complete dimensions of the inhomogeneous distributed source for a single group are Q(NMQ,2,IT). Appropriate choice of the source input parameter IQOPT will reduce the amount of input required as specified below.

Boundary sources may also be specified by setting the input boundary source triggers IQL=1 and/or IQR=1 for the left and/or right boundary sources, respectively. This requires the input of the boundary sources for all MM/2 incoming directions and for each group. For IQOPT positive or zero, the complete boundary sources at each direction for each group are required input. For IQOPT negative, the energy spectra of the boundary sources are assumed isotropic in angle.

The ordering of the source input is:

1. Distributed sources (if any); for all groups of an anisotropic order; for all orders of source anisotropy, then
2. Left boundary sources (if any), right boundary sources (if any); for all groups.

One can imagine the sources to be read by the following FORTRAN statements:

```
      DO   10    N=1,NMQ
      DO   10    G=1,IGM
10    READ       ((Q_G(N,K,I),K=1,2),I=1,IT)
      DO   12    G=1,IGM
      READ       (QL_G(M),M=1,MM/2)
12    READ       (QR_G(M),M=1,MM/2).
```

The IQOPT parameters available to the user are:

IQOPT	Option
0	Zero distributed source (no input).
± 1	Energy spectrum for the distributed source: EQ(IGM). One spectrum for each NMQ components.
± 2	Flat distributed source on the fine mesh: Q(IT). One distribution for each group and each NMQ components.
± 3	Linear distributed source on the fine mesh: Q(2,IT). The first subscript is the left edge and the right edge sources, respectively. One distribution for each group and for each NMQ components.
± 4	A single energy spectrum for the distributed source: EQ(IGM), followed by a single linear distributed source on the fine mesh: Q(2,IT). The distributed source is formed by the product of the energy spectrum and the fine-mesh spatial distribution. One spectrum and one spatial distribution for each NMQ components.
5	Input of both distributed and boundary sources from standard interface file FIXSRC mounted on unit IFIXSR.

6. Initial Condition Specification

The initial conditions for a TIMEX problem that must be specified are the angular flux $\psi(r,E,\underline{\Omega},t=0)$ and the precursor concentrations $C_k(r,t=0)$, k = 1, 2, ..., IGD. The reading of these distributions from card input is performed in subroutine READF.

The source and form of the initial angular flux are determined by the input integer ISTART. The ISTART options available to the TIMEX user are:

ISTART	Option
0	Zero initial flux, no input required.
1	Cell-centered isotropic angular flux on the fine mesh: F(IT). One distribution is entered from cards for each of IGM energy groups.
2	Complete angular flux on the fine mesh: F(2,IT). One distribution is entered from cards for each of MM angles. A set of MM distributions is entered for each of IGM energy groups.
± 3	A problem restart dump is read from unit NDMP1. See Sec. III.B.7.
4	The initial angular flux is read from standard interface file RAFLUX or AAFLUX mounted on unit IAFLUX.
5	Energy spectrum for the first collision source: UFS(IGM). The first collision source is computed as described in Sec. II.D.6. The initial angular flux is assumed zero throughout the system.
6	The initial angular flux is read from the special NTIMEX file created by the ONETRAN code.

The source of the initial precursor concentration distributions is determined by the input integer IPCOPT. The IPCOPT options available to the TIMEX user are:

IPCOPT	Option
0	Zero initial concentration, no input required.
1	Equilibrium initial concentration, no input required.
2	Card input of initial concentrations on the fine mesh: PC(2,IT). A distribution is entered for each of IGD delayed neutron groups.

7. Flux Dumps and Restart Procedures

If the problem being run requires a considerable amount of computer time, it is advisable to dump core occasionally onto an external file so that the problem may be restarted at a selected time step. This option has been included in the TIMEX code. The reading and writing of the dump files are performed in subroutine DUMPER.

There are two types of dumps written by TIMEX: periodic dumps and time-limit dumps. The user may request a periodic dump at regular intervals in each time zone by appropriate specification of the input parameter NSPD (number of time steps per dump). TIMEX will then take a dump at every NSPD time steps. In addition, a periodic dump is taken every DUMPT seconds where DUMPT (currently 15 min) is a program variable set in the main program segment to meet particular computing installation requirements. A time-limit dump is taken after a user input-specified time limit (ITLIM). An output print is made identifying each time-step index at which a dump was taken. The dump for each time step is written successively on the dump file. At the end of each problem execution, an end-of-file is written on the dump file and a rewind performed. Thus if several problems are stacked together in the input stream, only the dumps for the last problem will remain on the dump file.

The TIMEX problem may be restarted at any of the time steps for which a dump was taken by

specifying the input parameter ISTART=± 3 and the desired time-step index ITN. In addition, the input parameter IACC may be changed at restart.

When a restart from dump is requested, the dumps for previous time steps are skipped until the dump for time step ITN is reached. The small and large cores are then restored to their contents at that time step. All further dumps taken are then written in succession on the same file following the restart data for the ITN time step. Old data following this time step will be obliterated by the new data. If it is suspected that the restart file is approaching capacity, then flagging ISTART=-3 will cause this file to be rewound after the ITNth time-step core contents are restored and before new dumps are taken so that all of the old dump data are obliterated.

To restart a problem, the first card (only) of the input control integers is read (following the job title cards) containing the following control parameters:

ITN:	time-step index at which problem is restarted,
IACC:	changed value of the time-step acceleration option, and
ISTART:	=±3, trigger to indicate problem restart.

This first integer control card is read on a (2I6, 36X,I6) format. No other control integer cards or additional problem specification arrays are read. The large and small core contents are restored, new time-zone control input is read from the input stream, and problem execution resumed.

8. Adjoint Computations

The TIMEX program solves the adjoint transport equation by transposing the matrices of scattering coefficients and inverting the group order of the problem. The solution of the resulting problem in direction Ω is then identified with the solution of the adjoint equation in direction $-\Omega$.[16]

The inversion of the group order is made because the transposition of the scattering matrices usually converts a downscattering problem to an upscattering problem. Because of the inversion, the user must:

(a) Enter any inhomogeneous sources, including boundary fluxes, in inverse group order,

(b) Enter initial flux in inverse group order, and

(c) Remember that any output is in inverse group order, i.e., that groups labeled 1, 2, ..., are really groups IGM, IGM -1, etc. Similarly, the output flux from an adjoint problem must be inverted before insertion into a direct problem. On the other hand, an output flux from one adjoint problem is in the proper group order for use in another adjoint problem.

The group order of the group speeds and the fission spectrum is inverted by the program.

Finally, the direct transport equation is an initial value problem starting at t=0 and proceeding forward in time to some final time, t_f. The adjoint transport equation is a final value problem starting at a final time, t_f, and proceeding backwards in time to t=0.[17] The TIMEX code does not automatically perform this reversal of the time variable. Thus the user must remember that

$$t_{true} = t_f - t_{output}$$

for adjoint problems.

9. Edit Options

The TIMEX user may perform the edit processing at selected times throughout the calculation by appropriate choice of the NSPP (number of time steps per printout) parameter as described in Sec. III.B.10. At each edit, various arrays may be printed, a zone-edit performed, a film plot made, and the scalar and angular flux standard interface files written. The printing of the arrays at each edit is determined by the following print triggers:

Print Trigger	Quantity Printed
KP1	Delayed neutron precursor concentrations
KP2	Zone edit
KP3	Angular flux
KP4	Exponential extrapolation factors ω_i
KP5	Scalar flux and flux moments.

If the print trigger is set to zero, the corresponding quantity will not be printed.

The zone edits, defined below, are used to compute various activities over the system. If zone edits are to be made, the initial input KP2 must be set to unity. The zone-edit input will then be read with the initial input and copied to

the scratch unit NEDIT for repeated use throughout the computation.

An edit zone is a collection of fine-mesh intervals which have the same zone number. The user defines a zone by entering a set of IT numbers (NEDZ array) which associate with each interval on the fine mesh a zone identification number (zone i.d.). The intervals of an edit zone need not be contiguous. For each group and zone, a table containing the macroscopic activities (for cross section positions 1 through IHT) is given. The macroscopic activity $A_k(g,IPOS)$ in zone k and group g for cross section position IPOS is defined by

$$A_k(g,IPOS) = \sum_i C(g,IPOS,m_i)\phi_i V_i \text{ for } i \in \text{zone } k, \tag{73}$$

where m_i is the material i.d. (cross-section block identification number) for mesh cell i, $C(g,IPOS,m_i)$ is the cross section for group g in position IPOS for material m_i, V_i is the mesh cell volume, and ϕ_i is the average flux in mesh cell i. Thus A_k is the activity computed with the macroscopic cross section actually used in the problem, summed over all mesh cells in zone k.

For each zone edit, the TIMEX user is provided the option of calculating constituent activities and microscopic activities for any material desired. The constituent activity $A_k^j(g,IPOS)$ for material j in zone k is defined by

$$A_k^j(g,IPOS) = \sum_i C(g,IPOS,m_i)\phi_i V_i \delta_{jm_i} \text{ for } i \in \text{zone } k. \tag{74}$$

Here δ_{jm_i} equals unity if material j equals material m_i, the mixture table density (MIXDEN) if material j is a "constituent" of material m_j, and is zero otherwise. A "constituent" means that material j appears as an entry in the MIXNUM array with density MIXDEN (see Sec. III.B.1.b.) that is used to form material m_i. Thus, if material j is used to form a material j', which is used to form material m_i, then material j is not a "constituent" of material m_i within this definition.

The microscopic activity for material j in zone k is defined by

$$A_k^j(g,IPOS) = \sum_i C(g,IPOS,j)\phi_i V_i \text{ for } i \in \text{zone } k. \tag{75}$$

Thus A_k^j would be the activity obtained in zone k if material j were uniformly distributed throughout the system, even though material j may not actually have appeared in the problem cross sections.

The edit input parameters NCA and NMA specify the number of constituent activities and number of microscopic activities to be calculated. The user must then enter NCA material i.d.'s for the constituent activities and NMA material i.d.'s for the microscopic activities.

To edit a material which is not actually a part of the problem, the TIMEX user may add a mixture instruction to the mixture tables; or, if interested in only a few cross sections, he may add these cross sections to other blocks in rows IHT-5, IHT-6, etc.

Finally, following any constituent activities or microscopic activities, the zone edit provides the zone relative power density (group sum of the zone volume integral of $\nu \times$ fission rate divided by the zone volume), normalized to that of a user-designated zone. The zone relative power density (unnormalized) is defined by

$$PD_k = \frac{\sum_g \sum_i C(g,IHT-1,m_i)\phi_i V_i}{\sum_i V_i} \text{ for } i \in \text{zone } k. \tag{76}$$

If the user selects zone zero (NORMZ=0), the normalization is to the whole system power density. The normalized zone power densities are all computed relative to time t=0.

10. Time-Zone Control Parameters

TIMEX assumes that the time axis is divided into a series of time zones, not necessarily of equal length. Within each time zone all physical parameters (cross sections, inhomogeneous sources, dimensions, etc.) of the system are assumed to be constant. By specification of the appropriate triggers (variables ITXS through ITDELY of Sec. III. D.2.) in the initial input, the TIMEX user must input new arrays describing the system properties at each time zone. At the beginning of each time zone, the user must enter the time-zone control parameters described in Table VII.

TABLE VII

TIME-ZONE CONTROL PARAMETERS

Input Parameter	Remarks
NTS	Number of time steps for the time zone. For NTS=-1, TIMEX returns to the input processing routine to read the required new arrays describing the system properties (cross sections, inhomogeneous sources, coarse-mesh boundaries, etc.). For NTS=0, the problem is terminated and processing of the input data for the next problem (if any) is begun.
NSPP	Number of time steps per printout.
NSPD	Number of time steps per restart dump. For NSPD=0, no restart dumps are taken in the time zone.
IFREQ	Exponential extrapolation trigger. For IFREQ=1, the exponential extrapolation acceleration of Sec. II.D. 5.a. is used throughout the time zone. For IFREQ=0, no exponential extrapolation acceleration is used.
INDTS	Group-dependent time-step trigger. For INDTS=1, the group-dependent time steps are used and specification of the group-dependent time-step scale factor array, $IGTSF_g$, is required. For INDTS=0, no group-dependent time steps are used.
KP1 KP2 KP3 KP4 KP5	Print triggers described in Sec. III.B.9.
DELTAT	Time-step size for the time zone.

Each time zone is divided into one or more time steps of equal size, the Δt of Sec. II.B.2. For problems in which the group speeds differ greatly in magnitude, TIMEX permits the use of group-dependent time-step scale factor, $IGTSF_g$. The group-dependent time step, $(\Delta t)_g$, is related to the time-zone step size by

$$(\Delta t)_g = \Delta t / IGTSF_g .$$

When the group-dependent time-step option is used, the scattering and fission source from other groups [see Eq. (19)] is not recomputed at each group-dependent time step, $(\Delta t)_g$.

11. Movie Option

The TIMEX code contains a subroutine PLOTTR, which plots the scalar flux on a film file NFILM. Subroutine PLOTTR calls 15 LASL film plotting subroutines. Numerous comment cards describing these system-dependent routines are placed in the subroutine to facilitate the user's conversion of PLOTTR to the plotting software of his installation.

The TIMEX user may specify (with the IPLOT parameter) the plots to be on either a semi-log or a linear scale. Furthermore, the plot may be made at each edit processing or at specified time steps. When the plots are made during the edit processing (IPLOT=1 or 2), PLOTTR automatically chooses the abscissa range based on the maximum and minimum values of the scalar flux at that point in time. Thus, the abscissa range will vary from one edit plot to the next.

TIMEX may be utilized to generate a movie film of the scalar flux as a function of time by requiring the plots to be made at specified time steps (IPLOT=3 or 4). If this movie option is selected, the user must enter the number of time steps per movie plot (NSPMP) and the minimum and maximum values of the scalar flux over the complete time range. This implies that the user has previously run the problem at the desired time-step size and ascertained the maximum and minimum scalar flux values by scanning the edit output.

C. Data Input Rules

Except for the control parameters, cross sections, and edit parameters, all floating-point numbers and integers are read into TIMEX in special formats by the LOAD subroutine. These formats are [6(I1,I2,E9.4)] for reading floating-point numbers and [6(I1,I2,I9)] for integers. In each word of both of these formats, the first integer field, I1, designates the options listed below. The second integer field, I2, controls the execution of the option, and the remainder of the field, I9 or E9.4, is for the input data. All data blocks read with these formats must be ended with a 3 in the I1 field after the last word of the block. The available options are given in Table VIII. Five illustrations of the use of the special formats are given below. These illustrate:

1 - Zero is repeated 47 times,

2 - Zero is repeated 470 times,

3 - Four interpolants are inserted between 0.0 and 5.0 giving six data numbers: 0.0, 1.0, 2.0, 3.0, 4.0, 5.0,

4 - Four interpolants are inserted between 0.0 and 5.0, two between 5.0 and 7.0, and 7.0 is repeated 10 times, and

TABLE VIII

OPTIONS FOR SPECIAL READ FORMATS IN LOAD

Value of I1	Nature of Option
0 or blank	No action.
1	Repeat data word in 9 field number of times indicated in I2 field.
2	Place number of linear interpolants indicated in I2 field between data word in 9 field and data word in next 9 field. Not allowed for integers.
3	Terminate reading of data block. A 3 must follow last data word of all blocks.
4	Fill remainder of block with data word in 9 field. This operation must be followed by a terminate (3).
5	Repeat data word in 9 field 10 times the value of the I2 fields.
9	Skip to the next data card.

5 - After reading 0 and 4 we skip to the next card and read 7.

A special routine, WRITE, is used to print some of the two- and three-dimensional arrays that occur in the program. This routine can be used for one-, two-, or three-dimensional arrays and has an option for printing a portion of an array, e.g., the mixed cross-section blocks, if any.

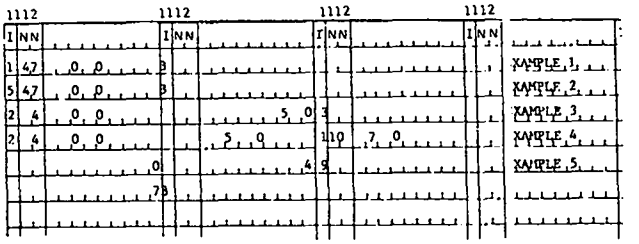

D. Description of Input Data

On the following pages the input data for TIMEX are listed in exactly the order in which they are entered on the code. The data are divided into five categories: (1) job title cards, (2) control integers on cards 1 through 4 and control floating-point numbers on cards 5 and 6, (3) problem-dependent data on subsequent cards, (4) edit input, and (5) time-zone control input.

1. Job Title Cards

The user begins by indicating on a card in an I6 format the number of title or job description cards he wants to use. He then enters the descriptive material on these cards which are read with an 18A4 format.

2. Input of Control Numbers

On cards 1 through 3, the user enters the following control integers which are read in a 12I6 format and on cards 4 and 5 the following control floating-point numbers in a 6E12.4 format:

Number of Word on Card	Name of Variable	Comments
CONTROL INTEGERS (12I6)----------		CARD 1
1	ITH	0/1 (direct/adjoint) type of calculation performed.
2	ISCT	0/N (isotropic/N^{th} order anisotropic) order of scattering calculation. NM spherical harmonics flux components are computed.
3	ISN	S_N angular quadrature order. Must be an even number.
4	IGM	Number of energy groups.
5	IM	Number of coarse-mesh intervals.
6	IBL	0/1/2/3/4 (vacuum/reflective/periodic/white/albedo) left boundary condition.
7	IBR	0/1/2/3/4 right boundary condition.
8	IGD	Number of delayed neutron groups.
9	ISTART	0/1/2/±3/4/5/6 angular flux initial condition. See Sec. III.B.6.
10	IQOPT	0/±1/±2/±3/±4/5 inhomogeneous source input option. See Sec. III.B.5.
11	IGEOM	1/2/3/4 (plane/cylindrical/spherical/two-angle plane) geometry option.
12	IQUAD	1/2/±3 (built-in P_n/built-in DP_n/+: card input, -: interface file) source of S_N quadrature constants w and μ.

CONTROL INTEGERS (12I6)----------CARD 2

1	MT	Total number of materials (cross-section blocks including anisotropic cross sections) in the problem.
2	MTP	Number of input material sets from interface file ISOTXS. CAUTION: Each material set from this field yields ISCT+1 materials. See LMTP below.
3	MCR	Number of input materials from the code-dependent input file. If MCR is negative, each MCR material is read as a single block on the FIDO format, terminated by the FIDO terminator: T.
4	MS	Number of mixture instructions. See Sec. III.B.1.6 and items MIXNUM, MIXCOM, MIXDEN below.
5	IHT	Row of total cross section in the cross-section format. If IHT is flagged negative, then n,2n scattering is present in the scattering matrices and cross section position IHT-4.
6	IHS	Row of within-group scattering cross section in the cross-section format. For problems with upscattering (IHS>IHT+1), IHS must be flagged negative if σ^{up} is present in the cross-section table, and to be removed. Not applicable for FIDO format input.
7	IHM	Total number of rows in the cross-section format.
8	IDEN	0/1 (no/yes) space-dependent density factors.
9	IQAN	0/N (isotropic/N^{th}-order anisotropic) order of source anisotropy. NMQ spherical harmonics source components are required input. CAUTION: ISCT≥IQAN is required.
10	IQL	0/1 (no/yes) left boundary source.
11	IQR	0/1 (no/yes) right boundary source.
12	IACC	0/1/2 (no/within-group/within-group plus outer) rebalance option.

CONTROL INTEGERS(I6,1X,5I1,I6,6I1,3I6)----------CARD 3

1	IFISS	1/2/3/4 (fission spectrum/zone-dependent fission spectrum/fission matrix/zone-dependent fission matrix) type of fission fractions.
2	KP1	0/1 (no/yes) delayed neutron precursor print trigger.
	KP2	0/1 (no/yes) zone edit option print triggers.
	KP3	0/1 (no/yes) angular flux print trigger.
	KP4	0/1 (no/yes) exponential extrapolation factor print trigger.
	KP5	0/1 (no/yes) flux components print trigger.
3	IPLOT	0/1/2/3/4 (no/semi-log/linear/semi-log movie/linear movie) scalar flux plotting option.
4	I1	0/1 (no/yes) initial flux print suppression trigger.
	I2	0/1/2 (all/isotropic/none) time zone flux print trigger.
	I3	0/1/2 (all/mixed/none) cross-section print trigger.
	I4	0/1 (no/yes) time zone fission print trigger.
	I5	0/1/2/3 (all/unnormalized/normalized/none) source print trigger.
	I6	0/1 (no/yes) fine-mesh geometry table print suppression trigger.
5	ITLIM	0/N (none/N second) time limit.
6	IFO	0/1 (no/yes) interface file output trigger.
7	IPCOPT	0/1/2 (zero/equilibrium/card input) initial precursor concentration option.

CONTROL INTEGERS(12I6)----------CARD 4

1	ITXS	0/1 (no/yes) load new cross-section blocks at each time zone.
2	ITQ	0/1 (no/yes) load new inhomogeneous sources at each time zone.
3	ITB	0/1 (no/yes) load new coarse-mesh boundaries at each time zone.
4	ITIDXS	0/1 (no/yes) load new cross-section identification array at each time zone.
5	ITFISS	0/1 (no/yes) load new fission fractions at each time zone.
6	ITVEL	0/1 (no/yes) load new group speeds at each time zone.

7	ITMIX	0/1 (no/yes) load new mixture tables at each time zone.
8	ITDEN	0/1 (no/yes) load new fine-mesh density factors at each time zone.
9	ITLBDO	0/1 (no/yes) load new left boundary group-albedos at each time zone.
10	ITRBDO	0/1 (no/yes) load new right boundary group-albedos at each time zone.
11	ITDELY	0/1 (no/yes) load new delayed neutron parameters at each time zone.

CONTROL FLOATING POINT DATA(6E12.6)----------CARD 5

1	NORM	Normalization factor. If NORM≠0, the total number of source particles (if inhomogeneous sources are present) or the total number of prompt fission particles (if inhomogeneous sources are not present) is normalized to this number. No normalizations are performed if NORM=0.0.
2	BHGT	Buckling height (in cm if cross sections are in cm^{-1}). If BHGT is flagged negative, the transport cross section in position IHT-3 is used for calculation of the buckling absorption.
3	BWTH	Buckling width (plane geometry only).

MOVIE CONTROL DATA(I6,2E12.6)----------CARD 6

Enter only for movie plots (IPLOT>2)

1	NSPMP	Number of time steps per movie plot.
2	FMIN	Minimum value of scalar flux over complete time range.
3	FMAX	Maximum value of scalar flux over complete time range.

3. Problem-Dependent Data

In the input data listed below, all the items are dimensionless except for the source, flux, velocities, mesh specifications, cross sections, bucklings, and mixture densities. The dimensions of these quantites are arbitrary in the following sense. Macroscopic cross sections define a unit of inverse length (usually cm^{-1} but occasionally km^{-1}) in which the mesh boundary values are measured. For source problems, the flux will have the dimensions of source/cross section where cross section is the quantity used in the calculation. Normally, distributed sources are in units of particles/ $length^3$/solid angle/s (the energy-dependence is removed by the multigroup approximation, i.e., $\int Q d\dot{E}$ is used, see Sec. II.B.1.), microscopic cross sections are in units of barns x $length^2/cm^2$, nuclide number densities in units of 10^{24} x number/ $length^3$, and velocities in length/s, although Los Alamos velocities are habitually measured in units of length/10^{-8} s.

With the exception of the cross sections from the code-dependent input file, all the following data are loaded by the LASL block loader using the special formats described in Sec. III.C. We denote these formats by S(I) for integers and S(E) for floating point numbers.

Block Name and Dimension	Format	Number of Entries	Comments
IHR(IM)	S(I)	IM	Number of fine mesh intervals in each coarse mesh.
WGT(MM)	S(E)	MM	S_N quadrature weights. Enter only if IQUAD=+3.
U(MM)	S(E)	MM	S_N quadrature μ cosines. Enter only if IQUAD=+3.
C(IHM,IGM,MIN)	-	-	Cross-section blocks. MIN=MCR+MTP*(ISCT+1). Three options are available for reading cross sections. The LASL input format may not be mixed with the FIDO format. 1. LASL Input. If MCR>0, MCR blocks of IHM*IGM numbers are read in a 6E12.5 format. Each block is preceeded by an identification card read in a 18A4 format. 2. FIDO Input. If MCR<0, MCR blocks of data are created from FIDO input. The 14* card must not preceed the FIDO input data.

3. Interface File ISOTXS. When MTP≠0, MTP material sets are read from standard interface file ISOTXS. On this file each material set consists of ISCT+1 cross-section blocks for the isotropic and ISCT anisotropic cross sections. The first (isotropic) component of the first material is stored in cross-section block MCR+1, the first component of the second material is stored in cross-section block MCR+ISCT+2, etc. Should the ISOTXS file not contain ISCT anisotropic components, zeroes are supplied for the components not present. If the ISOTXS file contains more components than needed, only the first ISCT+1 components are read. The maximum number of upscatter groups and downscatter groups (MAXUP,MAXDN) in the ISOTXS file must be consistent with the choice of IHT, IHS, and IHM. If they are not consistent, this will be flagged as an error.

LMTP(MTP)	S(I)	MTP	Position numbers of material sets to be read from ISOTXS. Do not enter unless MTP>0. The material sets are loaded into the C block in the order they appear on the ISOTXS file, and not in the order they appear in the LMTP array.
Initial angular flux AF(2,IT)	S(E)	-	Number of entries depends on option. See Sec. III.B.6.

ISTART	Number of entries
0	None.
1	IT, one distribution for each group.
2	MM sets of 2*IT, MM sets for each group.
±3	Problem restart dump from unit NDMP1.
4	Angular flux from standard interface file on unit IAFLUX.
5	IGM
6	ONETRAN angular flux file on unit NTIMEX.

Initial precursor concentrations PC(2,IT)	S(E)	2*IT	Initial precursor concentrations. IGD blocks of length 2*IT. Enter only if IPCOPT=2.
Input sources Q(NMQ,2,IT) QL(MM/2) QR(MM/2)	S(E)	-	Number of entries depends on option. See Sec. III.B.5. The sources are loaded as: (a) distributed source (if any) for each group; for each anisotropic component; (b) left boundary source (if any) and right boundary source (if any); for each group. For IQOPT flagged negative, an energy spectrum is input for each (assumed isotropic) boundary source. For IQOPT positive or zero, the complete angular distribution of the boundary sources is input, a distribution for each group.

IQOPT	Number of entries for distributed source
0	None.
±1	IGM; one for each NMQ components.
±2	IT; one for each group; for each NMQ components.
±3	2*IT; one for each group; for each NMQ components.
±4	IGM and 2*IT; both for each NMQ components.

RAD(IM+1)	S(E)	IM+1	Coarse-mesh radii.
IDC(IM)	S(I)	IM	Cross-section material identification numbers. These numbers assign a cross-section block to each coarse-mesh interval. These numbers must be flagged negative for an anisotropic source to be calculated in that coarse-mesh interval.
CHI(IGM,IM)	S(E)	-	Prompt fission fractions. Fraction of fission yield emerging in each group. May be either a spectrum (χ_g) or a matrix ($\chi_{g'\to g}$) and may be coarse-mesh zone-dependent. See Sec. III.B.1.f.

IFISS	Number of entries
1	IGM; single fission spectrum.
2	IGM*IM; IM sets of spectra loaded as a single block.
3	IGM sets of length IGM; single fission matrix, loaded by rows in blocks of IGM length.
4	IGM sets of length IGM*IM; IM sets of matrices, loaded by rows in blocks of IGM*IM length.

VEL(IGM)	S(E)	IGM	Group speeds.
MIXNUM(MS)	S(I)	MS	Numbers of identifying cross-section block being mixed. See Sec. III.B.1.b. Do not enter if MS=0.
MIXCOM(MS)	S(I)	MS	Numbers controlling cross-section mixture process. See Sec. III.B.1.b. Do not enter if MS=0.
MIXDEN(MS)	S(E)	MS	Mixture densities. See Sec. III.B.1.b. Do not enter if MS=0.
DEN(IT)	S(E)	IT	Fine-mesh density factors. Enter only if IDEN=1.
LB(IGM)	S(E)	IGM	Left boundary group-albedos. Enter only if IBL=4.
RB(IGM)	S(E)	IGM	Right boundary group-albedos. Enter only if IBR=4.
LAM(KM,IGD)	S(E)	KM*IGD	Delayed neutron decay constants. Enter only if IGD>0. See Sec. III.B.1.i. KM=1 for IFISS=1 or 3. KM=IM (coarse-mesh-dependent) for IFISS=2 or 4.
BETA(KM,IGD)	S(E)	KM*IGD	Delayed neutron fractions. Enter only if IGD>0. See Sec. III.B.1.i.
PS(KM,IGD,IGM)	S(E)	KM*IGD*IGM	Delayed neutron spectrum. Enter only if IGD>0. See Sec. III.B.1.i.

4. Zone-Edit Input

The zone-edit input, entered only if KP2=1, consists of control integers entered on cards indicated by EDIT1 and 2; and the remaining edit input entered in the special format discussed above in Sec. III.C. The zone-edit control integers and the zone-edit arrays are read for all NZEDS edits with the initial problem and written onto a scratch file (NEDIT) for use during edits as required.

EDIT CONTROL INTEGERS(I6)----------EDIT 1

1	NZEDS	Number of zone edits.

ZONE EDIT CONTROL INTEGERS(4 I6)----------EDIT 2

1	NZ	Total number of zones.
2	NCA	Number of constituent activities calculated.
3	NMA	Number of microscopic activities calculated.
4	NORMZ	Zone identification number for normalization of power density. If NORMZ=0, whole-system normalization is performed.

ZONE EDIT ARRAYS THROUGH LOAD----------

IDCA(NCA)	S(I)	NCA	Cross-section material identification numbers for constituent activities. Enter only if NCA>0.
IDMA(NMA)	S(I)	NMA	Cross-section material identification numbers for microscopic activities. Enter only if NMA>0.
NEDZ(IT)	S(I)	IT	Zone identification numbers. These numbers assign a zone number to each fine-mesh interval.

5. Time-Zone Control Input

The time-zone control input consists of the time-zone control parameters entered on TZCARD1 and an optional array through the LASL LOAD routine. As many time-zone control variables cards as desired may be read in each time zone.

Setting the variable NTS=-1 indicates the beginning of a new time zone. The program then returns to processing the input of the new problem-dependent arrays of Sec. III.D.3. Only those arrays specified by the triggers ITXS through ITDELY of CARD 4 are required to be input, in the same order as they appear in Sec. III.D.3. Once the new arrays have been read, the time-zone control parameters for the new time zone are read and the time-integration resumed.

Setting the variable NTS=0 indicates the termination of the problem. The program then begins processing the input of a new problem, starting with the job title card of Sec. III.B.1. As many problems as desired may be stacked on the input file. Execution of TIMEX is normally terminated with a detection of an end-of-file on the input stream.

TIME-ZONE CONTROL VARIABLES(5I6,1X,5I1,E12.6)----------TZCARD 1

1	NTS	Number of time steps. For NTS=0, the problem is terminated. For NTS=-1, all other variables on TZCARD 1 are ignored and the new problem-dependent data of Sec. III.D.3. are entered as specified by the triggers on CARD 4 of Sec. III.D.2.
2	NSPP	Number of time steps per printout.
3	NSPD	Number of time steps per restart dump. NSPD=0 specifies no restart dump.
4	IFREQ	0/1 (no/yes) frequency extrapolation.
5	INDTS	0/1 (no/yes) group-dependent time step sizes.
6	KP1	0/1 (no/yes) delayed neutron precursor print trigger.
	KP2	0/1 (no/yes) zone-edit print trigger.
	KP3	0/1 (no/yes) angular flux print trigger.
	KP4	0/1 (no/yes) exponential extrapolation factor print trigger.
	KP5	0/1 (no/yes) flux components print trigger.
7	DELTAT	Time step size.

TIME ZONE ARRAY THROUGH LOAD----------

IGTSF(IGM)	S(I)	IGM	Time step scale factors. Enter only if INDTS>0.

E. Output Description for a Test Problem

The TIMEX program comes with a set of five test problems plus an example problem designed to illustrate many of the TIMEX options whose output is presented on the following pages. Each page of this output is numbered, and we refer to these numbers in the text below.

The problem is a three-group, three-region, cylindrical geometry reactor kinetics problem. Zone 1 contains a fissile plus scattering material, Zone 2 constains a strong absorber, and Zone 3 a weakly fissile plus scattering material. As seen from the first output page (1), the problem is run with S_4 angular quadrature and within-group fine-mesh rebalance. The fission fractions and delayed neutron parameters are zone-dependent spectra. The mixture instructions and the fine-mesh density factors may be changed at each time zone.

All integer and floating-point input control data are printed on page (1). The S_N angular quadrature coefficients are the built-in S_4 Gaussian quadrature set and are printed on page (2). The LI, XI, and PHI columns refer to the ξ level index, ξ angle cosine, and ϕ angle of Fig. 5. The remaining problem input is printed on output pages (2) and (3). It is noted that the initial condition is a flat, isotropic angular flux for group 1 in Zone 2 and zero elsewhere.

The coarse-mesh and material map is printed on page (3). The mixture table printed on pages (3) and (4) shows the input microscopic cross sections converted to macroscopic cross sections and then

the scattering material (material block 4) added to the two fissile materials (material blocks 1 and 3). The coarse-mesh and fine-mesh geometry tables, the zone-dependent delayed neutron spectra, the zone-dependent total delayed neutron fractions, the group velocities, and the zone-dependent prompt fission fractions are printed on pages (4) and (5). On output pages (6) and (7), the output edit is given for the initial conditions. The flux components are the two cell-edge fluxes, $\phi_{i\pm\frac{1}{2}}$, on the fine mesh. Zone edit 1 gives the activities for the entire system and zone edit 2 the activities for each of the three coarse-mesh zones.

The first time-zone control parameters are printed on output page (8) followed by the output edit at 100 time steps after the initial flux has been redistributed into the two fissile zones. Since a wave front was propagated through the system as the initial flux redistributed, the exponential extrapolation was not attempted.

For the next time zone starting on output page (10), the exponential extrapolation is switched on and the frequencies, ω_i, are printed after another 100 time steps. On page (12), the new mixture instructions and fine-mesh density factors are read at the start of the third time zone. The mixture instructions subtract out the scattering material in the fissile zones 1 and 3. The density of the fissile zones is reduced and the density of the absorber zone increased. From the output edit prints on pages (13) through (17), the flux is observed to decay very rapidly at first and later at a much slower rate as the decay is limited by the delayed neutrons.

```
 THIS TIMEX PROBLEM RUN ON  11/06/75 WITH VERSION      7/1/75
TIMEX EXAMPLE PROBLEM

        0  ITH      0/1  DIRECT/ADJOINT
        0  ISCT     0/N  ISOTROPIC/NTH ORDER ANISOTROPIC
        4  ISN      SN ORDER
        3  IGM      NUMBER OF GROUPS
        3  IM       NUMBER OF COARSE MESH INTERVALS
        1  IBL      LEFT/RIGHT BOUNDARY CONDITION=0/1/2/3/4
        0  IBR       VACUUM/REFLECTIVE/PERIODIC/WHITE/ALBEDO
        2  IGO      NUMBER OF DELAYED NEUTRON GROUPS
        1  ISTART   0 THRU 6 STARTING OPTIONS (SEE MANUAL)
        0  IQOPT    0 THRU 5 SOURCE INPUT OPTIONS (SEE MANUAL)
        2  IGEOM    1/2/3/4 PLANE/CYLINDER/SPHERE/TWO-ANGLE PLANE
        1  IQUAD    1=PN W AND MU,2=DPN W AND MU,+3=CARD INPUT W AND MU
                   -3=INTERFACE INPUT W AND MU


        4  MT       TOTAL NUMBER OF MATERIALS
        0  MTP      NUMBER OF MATERIALS FROM LIBRARY
        4  MCR      NUMBER OF MATERIALS FROM CARDS (= FOR FIDO FORMAT)
        6  MS       NUMBER OF MIXTURE INSTRUCTIONS
        3  IHT      ROW OF TOTAL CROSS SECTION (= FOR N,2N REACTION PRESENT)
        4  IHS      ROW OF SELF SCATTER CROSS SECTION  (- INDICATES SIGMA-UP PRESENT)
        6  IHM      LAST ROW OF CROSS SECTION TABLE
        1  IDEN     0/1 NO/YES SPACE DEPENDENT MATERIAL DENSITY
        0  IQAN     0/N ISOTROPIC/NTH ORDER ANISOTROPIC SOURCE
        0  IQL      0/1 NO/YES LEFT BOUNDARY SOURCE
        0  IQR      0/1 NO/YES RIGHT BOUNDARY SOURCE
        0  IACC     0/1/2 NO/WITHIN-GROUP/WITHIN-GROUP + OUTER   REBALANCE OPTION


        2  IFISS    1/2/3/4 FISSION FRACTIONS/ZONE FISSION FRACTIONS/FISSION MATRIX/ZONE FISSION MATRIX
    11011  KP1=5    0/1 NO/YES  (PRECURSOR,ZONE EDIT,ANGULAR FLUX,FREQUENCY,FLUX COMPONENTS) PRINT TRIGGERS
        0  IPLOT    0/1/2 NO/SEMI-LOG/LINEAR PLOTTING OPTION
        0  I1       0/1 NO/YES SUPPRESS INPUT FLUX PRINT
        0  I2       0/1/2 ALL/ISOTROPIC/NONE FINAL FLUX PRINT
        2  I3       0/1/2 ALL/MIXED/NONE CROSS SECTION PRINT
        0  I4       0/1 NO/YES FISSION RATE PRINT
        0  I5       0/1/2/3 ALL/UNNORMALIZED/NORMALIZED/NONE SOURCE PRINT
        0  I6       0/1 YES/NO PRINT F.M. GEOMETRY TABLE
        0  ITLIM    0/N NO/N-SECOND TIME LIMIT
        0  IFO      0/1 NO/YES INTERFACE FILE OUTPUT
        1  IPCOPT   0/1/2  ZERO/EQUILIBRIUM/INPUT  INITIAL PRECURSOR CONCENTRATIONS
        0  ITN      RESTART TIME STEP NUMBER

    ONE OR MORE OF THE FOLLOWING CONDITIONAL ARRAYS MAY BE LOADED AT EACH TIME ZONE.
        0  ITXS     0/1 NO/YES  CROSS SECTIONS
        0  ITQ      0/1 NO/YES  SOURCES
        0  ITB      0/1 NO/YES  COARSE MESH BOUNDARIES
        0  ITIDXS   0/1 NO/YES  CROSS SECTION IDENTIFICATION
        0  ITFISS   0/1 NO/YES  FISSION FRACTIONS
        0  ITVEL    0/1 NO/YES  VELOCITIES
        1  ITMIX    0/1 NO/YES  MIXTURE INSTRUCTIONS
        1  ITDEN    0/1 NO/YES  FINE MESH DENSITIES
        0  ITLBOO   0/1 NO/YES  LEFT ALBEDO FACTORS
        0  ITRBOO   0/1 NO/YES  RIGHT ALBEDO FACTORS
        0  ITDELY   0/1 NO/YES DELAY NEUTRON PARAMETERS


  0.       NORM    NORMALIZATION AMPLITUDE
 -0.       BHGT    BUCKLING HEIGHT (= FOR TRANSPORT CROSS SECTION IN CORRECTION)
 -0.       BWTH    BUCKLING WIDTH
```

```
INPUT FINE R MESH      3
ALL ENTRIES =          10


STORAGE    REQUIRED ALLOWED
SMALL CORE    1493   24000
LARGE CORE    2605  375000


LEVEL  LEVEL WEIGHT  LEVEL COSINE  STARTING COSINE
   1   1.739274E-01 -8.611363E-01 -5.083741E-01
   2   3.260726E-01 -3.399810E-01 -9.404323E-01
   3   3.260726E-01  3.399810E-01  0.
   4   1.739274E-01  8.611363E-01  0.

  M   REFL M   LI   POINT WEIGHT   MU COSINE       WGT*MU      BETA PLUS     BETA MINUS          XI          PHI(DEG)
  1      4     1   1.630363E-01 -3.399810E-01 -5.542925E-02 3.399810E-01  0.              .86113631    131.9715
  2      6     2   1.739274E-01 -8.611363E-01 -1.497752E-01 8.611363E-01  0.              .33998104    156.3027
  3      5     2   1.630363E-01 -3.399810E-01 -5.542925E-02 1.258643E+00  9.186619E-01    .33998104    111.1933
  4      1     1   1.630363E-01  3.399810E-01  5.542925E-02 0.             3.399810E-01    .86113631     48.0285
  5      3     2   1.630363E-01  3.399810E-01  5.542925E-02 9.186619E-01  1.258643E+00    .33998104     68.8067
  6      2     2   1.739274E-01  8.611363E-01  1.497752E-01 0.             8.611363E-01    .33998104     23.6973


**********INPUT CROSS SECTIONS**********
     1                    LOADED FROM CARDS MATERIAL ONE
     2                    LOADED FROM CARDS MATERIAL TWO
     3                    LOADED FROM CARDS MATERIAL THREE
     4                    LOADED FROM CARDS MATERIAL FOUR

INITIAL FLUX FOR GROUP   1

INPUT INITAL FLUX     30
  0.          0.          0.          0.          0.          0.          0.          0.          0.          0.
  1.0000E+00  1.0000E+00  1.0000E+00  1.0000E+00  1.0000E+00  1.0000E+00  1.0000E+00  1.0000E+00  1.0000E+00  1.0000E+00
  0.          0.          0.          0.          0.          0.          0.          0.          0.          0.

INITIAL FLUX FOR GROUP   2

INPUT INITAL FLUX     30
ALL ENTRIES =   0.

INITIAL FLUX FOR GROUP   3

INPUT INITAL FLUX     30
ALL ENTRIES =   0.

INPUT COARSE MESH      4
  0.          1.1000E+00  2.0000E+00  2.5000E+00
```

```
INPUT CROSS SEC ID      3
          1             2             3

INPUT FISS SPECTRA      9
  7.0000E-01  2.0000E-01  1.0000E-01  0.          0.          0.          2.0000E-01  4.0000E-01  4.0000E-01

INPUT VELOCITIES        3
  2.5000E+07  1.0000E+07  2.0000E+06

INPUT MIX NUMBERS       6
          1             2             3             4             1             4

INPUT MIX COMMANDS      6
          0             0             0             0             4             4

INPUT MIX DENSITY       6
  9.2000E-01  1.0500E-01  5.2000E-02  6.3000E-02  2.5000E-01  2.5000E-01

INPUT R DENSITY        30
ALL ENTRIES =   1.0000E+00

INPUT LAMBDAS           6
  1.5200E-01  1.0000E+00  3.0000E-01  3.2600E+00  1.0000E+00  5.2400E+00

INPUT BETAS             6
  2.0000E-03  0.          1.0000E-03  4.0000E-03  0.          2.0000E-03

INPUT PS ARRAY         18
  7.0000E-01  2.0000E-01  1.0000E-01  0.          0.          0.          8.0000E-01  1.0000E-01  1.0000E-01  2.0000E-01
  2.0000E-01  6.0000E-01  0.          0.          0.          1.5000E-01  5.0000E-02  8.0000E-01

INPUT NEOZ ARRAY       30
ALL ENTRIES =           1

INPUT NEOZ ARRAY       30
          1             1             1             1             1             1             1             1             1
          2             2             2             2             2             2             2             2             2
          3             3             3             3             3             3             3             3             3


STORAGE    REQUIRED ALLOWED
SMALL CORE     1544   24000
LARGE CORE     2605  375000


                                        M IS NUMBER OF FINE INTERVALS IN EACH COARSE INTERVAL

          1111111111111111111
          1       *       *       0
          1   1   *   2   *   3   0
          1       *       *       0
          1111111111111111111
    R     0.      1.      2.      2.
          0    1000       0    5000

    M        10      10      10
 COLUMN       1       2       3


MIXTURE NUMBER MIXTURE COMMAND  MATERIAL ATOMIC DENSITY
          1               0          9.2000000E-01
```

2	0	1.0500000E-01	2
3	0	5.2000000E-02	3
4	0	6.3000000E-02	4
1	4	2.5000000E-01	5
3	4	2.5000000E-01	6

COARSE MESH GEOMETRY

	NO. OF INTERVALS	WIDTH	FINE MESH SIZE	LEFT BOUNDARY
1	10	.11000000E+01	.11000000E+00	0.
2	10	.90000000E+00	.90000000E-01	.11000000E+01
3	10	.50000000E+00	.50000000E-01	.20000000E+01
4	0	0.	0.	.25000000E+01

FINE MESH GEOMETRY

	COARSE MESH	LEFT BOUNDARY	AVERAGE RADIUS	VOL-1	VOL-2	LEFT AREA
1	1	0.	.55000000E-01	.12471000E-01	.25342181E-01	0.
2	1	.11000000E+00	.16500000E+00	.58484361E-01	.63355452E-01	.69115038E+00
3	1	.22000000E+00	.27500000E+00	.88497493E-01	.10134872E+00	.13823008E+01
4	1	.33000000E+00	.38500000E+00	.12471000E+00	.13938199E+00	.20734512E+01
5	1	.44000000E+00	.49500000E+00	.16473417E+00	.17739527E+00	.27646015E+01
6	1	.55000000E+00	.60500000E+00	.20373745E+00	.21540854E+00	.34557519E+01
7	1	.66000000E+00	.71500000E+00	.24275072E+00	.25342181E+00	.41469023E+01
8	1	.77000000E+00	.82500000E+00	.28176399E+00	.29143508E+00	.48380527E+01
9	1	.88000000E+00	.93500000E+00	.32077726E+00	.32944835E+00	.55292031E+01
10	1	.99000000E+00	.10450000E+01	.35979053E+00	.36746162E+00	.62203535E+01
11	2	.11000000E+01	.11450000E+01	.39880380E+00	.32798727E+00	.69115038E+01
12	2	.11900000E+01	.12350000E+01	.34434647E+00	.35342917E+00	.74769005E+01
13	2	.12800000E+01	.13250000E+01	.37239377E+00	.37887107E+00	.80424772E+01
14	2	.13700000E+01	.14150000E+01	.39994047E+00	.40432297E+00	.86079439E+01
15	2	.14600000E+01	.15050000E+01	.42798777E+00	.42976988E+00	.91734505E+01
16	2	.15500000E+01	.15950000E+01	.44473448E+00	.45521478E+00	.97389172E+01
17	2	.16400000E+01	.16850000E+01	.47218178E+00	.48066168E+00	.10304424E+02
18	2	.17300000E+01	.17750000E+01	.49962898E+00	.50611058E+00	.10869911E+02
19	2	.18200000E+01	.18650000E+01	.52707618E+00	.53155748E+00	.11435397E+02
20	2	.19100000E+01	.19550000E+01	.54952208E+00	.55700438E+00	.12000884E+02
21	3	.20000000E+01	.20250000E+01	.31477726E+00	.31939525E+00	.12566371E+02
22	3	.20500000E+01	.20750000E+01	.32443134E+00	.32724023E+00	.12880530E+02
23	3	.21000000E+01	.21250000E+01	.33408542E+00	.33510322E+00	.13194689E+02
24	3	.21500000E+01	.21750000E+01	.34373950E+00	.34295720E+00	.13508848E+02
25	3	.22000000E+01	.22250000E+01	.35339358E+00	.35081118E+00	.13823008E+02
26	3	.22500000E+01	.22750000E+01	.36304767E+00	.35866516E+00	.14137167E+02
27	3	.23000000E+01	.23250000E+01	.37270175E+00	.36651914E+00	.14451326E+02
28	3	.23500000E+01	.23750000E+01	.38175513E+00	.37437312E+00	.14765485E+02
29	3	.24000000E+01	.24250000E+01	.39040911E+00	.38222711E+00	.15079645E+02
30	3	.24500000E+01	.24750000E+01	.39906309E+00	.39008109E+00	.15393804E+02
31	4	.25000000E+01	.12500000E+01	0.	0.	.15707963E+02

DELAYED NEUTRON FISSION SPECTRA (CHI-D) BY ZONE

FROM DELAY GROUP	TO ENERGY GROUP	1	2	3
1	1	.70000E+00	.20000E+00	.10000E+00
1	2	.80000E+00	.10000E+00	.10000E+00
1	3	0.	0.	0.
2	1	0.	0.	0.

2	2	.20000E+00	.20000E+00	.40000E+00
2	3	.15000E+00	.50000E-01	.80000E+00

TOTAL DELAYED NEUTRON FRACTIONS .006000 0.000000 .007000

GROUP VELOCITIES

	SPEEDS
1	.25000000E+08
2	.10000000E+08
3	.20000000E+07

FISS FRAC BY GROUP 1

	ZONE 1	ZONE 2	ZONE 3
1	.700000E+00	0.	.200000E+00
2	.200000E+00	0.	.400000E+00
3	.100000E+00	0.	.400000E+00

TIME STEP NUMBER 0 REAL TIME= 0. TIME STEP SIZE= 0.

GROUP 1 FLUX COMPONENTS(ISOTROPIC)

1	0.	0.	9	0.	0.	17	1.00000E+00	1.00000E+00	24	0.	0.
2	0.	0.	10	0.	0.	18	1.00000E+00	1.00000E+00	25	0.	0.
3	0.	0.	11	1.00000E+00	1.00000E+00	19	1.00000E+00	1.00000E+00	26	0.	0.
4	0.	0.	12	1.00000E+00	1.00000E+00	20	1.00000E+00	1.00000E+00	27	0.	0.
5	0.	0.	13	1.00000E+00	1.00000E+00	21	0.	0.	28	0.	0.
6	0.	0.	14	1.00000E+00	1.00000E+00	22	0.	0.	29	0.	0.
7	0.	0.	15	1.00000E+00	1.00000E+00	23	0.	0.	30	0.	0.
8	0.	0.	16	1.00000E+00	1.00000E+00						

GROUP 2 FLUX COMPONENTS(ISOTROPIC)

ALL ENTRIES= 0.

GROUP 3 FLUX COMPONENTS(ISOTROPIC)

ALL ENTRIES= 0.

GROUP 1 PRECURSOR CONCENTRATION

ALL ENTRIES= 0.

GROUP 2 PRECURSOR CONCENTRATION

ALL ENTRIES= 0.

********** ZONE EDIT 1 **********

GROUP	ZONE	ACTIVITY FOR CROSS SECTION POSITIONS 1 THRU THT		
1	1	2.3008239E+00	0.	4.6016478E+00
2	1	0.	0.	0.
3	1	0.	0.	0.
4	1	2.3008239E+00	0.	4.6016478E+00

ZONE	RELATIVE POWER DENSITY
1	0.

********** ZONE EDIT 2 **********

GROUP	ZONE	ACTIVITY FOR CROSS SECTION POSITIONS 1 THRU THT		
1	1	0.	0.	0.
1	2	2.3008239E+00	0.	4.6016478E+00
1	3	0.	0.	0.
2	1	0.	0.	0.
2	2	0.	0.	0.
2	3	0.	0.	0.
3	1	0.	0.	0.
3	2	0.	0.	0.
3	3	0.	0.	0.
4	1	0.	0.	0.
4	2	2.3008239E+00	0.	4.6016478E+00
4	3	0.	0.	0.

ZONE	RELATIVE POWER DENSITY

```
1    0.
2    0.
3    0.
```

TIME ZONE PARAMETERS
NUMBER OF TIME STEPS = 100
NUMBER OF STEPS/PRINT = 100
NUMBER OF STEPS/DUMP = 101
FREQUENCY INDICATOR = 0
VARIABLE TIME STEP INDICATOR = 0
PRINT TRIGGERS KPT_5 = 11011
TIME STEP SIZE = 1.000000E-07

TIME STEP NUMBER 100 REAL TIME= 1.000000E-05 TIME STEP SIZE= 1.000000E-07

GROUP 1 FLUX COMPONENTS(ISOTROPIC)

1	7.83126E-01	7.83344E-01	9	3.93093E-01	3.93345E-01	17	8.31617E-02	7.36876E-02	24	4.56885E-02	4.39315E-02
2	7.79229E-01	7.58516E-01	10	3.04063E-01	2.85443E-01	18	7.35147E-02	6.53241E-02	25	4.39192E-02	4.22431E-02
3	7.57156E-01	7.23050E-01	11	2.05518E-01	1.71048E-01	19	6.51797E-02	5.80234E-02	26	4.22316E-02	4.06293E-02
4	7.22422E-01	6.75579E-01	12	1.70253E-01	1.44854E-01	20	5.79013E-02	5.15834E-02	27	4.06186E-02	3.90835E-02
5	6.75402E-01	6.17540E-01	13	1.44289E-01	1.24547E-01	21	5.15739E-02	4.95216E-02	28	3.90735E-02	3.75997E-02
6	6.17663E-01	5.50184E-01	14	1.24124E-01	1.08208E-01	22	4.95061E-02	4.75621E-02	29	3.75903E-02	3.61724E-02
7	5.50530E-01	4.74810E-01	15	1.07882E-01	9.47191E-02	23	4.75478E-02	4.57018E-02	30	3.61635E-02	3.47962E-02
8	4.75321E-01	3.92473E-01	16	9.44598E-02	8.33718E-02						

GROUP 2 FLUX COMPONENTS(ISOTROPIC)

1	1.92800E-01	1.91161E-01	9	9.36512E-02	7.04477E-02	17	2.24745E-02	2.06342E-02	24	1.51225E-02	1.46747E-02
2	1.90786E-01	1.85379E-01	10	7.05865E-02	4.34930E-02	18	2.06164E-02	1.90069E-02	25	1.46760E-02	1.42158E-02
3	1.85189E-01	1.76618E-01	11	4.34239E-02	3.78209E-02	19	1.89922E-02	1.75882E-02	26	1.42170E-02	1.37451E-02
4	1.76514E-01	1.64853E-01	12	3.77487E-02	3.34836E-02	20	1.75762E-02	1.63626E-02	27	1.37461E-02	1.32629E-02
5	1.64809E-01	1.50391E-01	13	3.34313E-02	3.00014E-02	21	1.63693E-02	1.59694E-02	28	1.32637E-02	1.27692E-02
6	1.50384E-01	1.33517E-01	14	2.99613E-02	2.71022E-02	22	1.59715E-02	1.55532E-02	29	1.27699E-02	1.22637E-02
7	1.33535E-01	1.14525E-01	15	2.70704E-02	2.44318E-02	23	1.55550E-02	1.51210E-02	30	1.22642E-02	1.17456E-02
8	1.14557E-01	9.36253E-02	16	2.46059E-02	2.24958E-02						

GROUP 3 FLUX COMPONENTS(ISOTROPIC)

1	1.36815E-01	1.35366E-01	9	6.61707E-02	5.00400E-02	17	2.20613E-02	2.08229E-02	24	1.57538E-02	1.51638E-02
2	1.35220E-01	1.31348E-01	10	5.00560E-02	3.20153E-02	18	2.08263E-02	1.96632E-02	25	1.51631E-02	1.45750E-02
3	1.31248E-01	1.25145E-01	11	3.20553E-02	2.99441E-02	19	1.96656E-02	1.85713E-02	26	1.45744E-02	1.39870E-02
4	1.25087E-01	1.16801E-01	12	2.98721E-02	2.79746E-02	20	1.85729E-02	1.75428E-02	27	1.39863E-02	1.33981E-02
5	1.16776E-01	1.06525E-01	13	2.79953E-02	2.61077E-02	21	1.75479E-02	1.69458E-02	28	1.33974E-02	1.28070E-02
6	1.06518E-01	9.45179E-02	14	2.63207E-02	2.47833E-02	22	1.69452E-02	1.63480E-02	29	1.28063E-02	1.22120E-02
7	9.45244E-02	8.09959E-02	15	2.47925E-02	2.33725E-02	23	1.63474E-02	1.57544E-02	30	1.22113E-02	1.16112E-02
8	8.10117E-02	6.61481E-02	16	2.33792E-02	2.20565E-02						

GROUP 1 PRECURSOR CONCENTRATION

1	1.59676E-08	1.59042E-08	9	8.08074E-09	6.24988E-09	17	0.	0.	24	3.56263E-11	3.42632E-11
2	1.58485E-08	1.54268E-08	10	6.25178E-09	4.19703E-09	18	0.	0.	25	3.42565E-11	3.29422E-11
3	1.54057E-08	1.47233E-08	11	0.	0.	19	0.	0.	26	3.29360E-11	3.14649E-11
4	1.47128E-08	1.37788E-08	12	0.	0.	20	0.	0.	27	3.16591E-11	3.04259E-11
5	1.37750E-08	1.26189E-08	13	0.	0.	21	4.01006E-11	3.85489E-11	28	3.04204E-11	2.92202E-11
6	1.26195E-08	1.12664E-08	14	0.	0.	22	3.85405E-11	3.70596E-11	29	2.92151E-11	2.80435E-11
7	1.12702E-08	9.74504E-09	15	0.	0.	23	3.70519E-11	3.56335E-11	30	2.80386E-11	2.68912E-11
8	9.75114E-09	8.07340E-09	16	0.	0.						

GROUP 2 PRECURSOR CONCENTRATION

1	3.19348E-08	3.18082E-08	9	1.61613E-08	1.24996E-08	17	0.	0.	24	7.12511E-11	6.85249E-11
2	3.16967E-08	3.08532E-08	10	1.25034E-08	8.39397E-09	18	0.	0.	25	6.85116E-11	6.58831E-11
3	3.08110E-08	2.94463E-08	11	0.	0.	19	0.	0.	26	6.58707E-11	6.33285E-11
4	2.94252E-08	2.75573E-08	12	0.	0.	20	0.	0.	27	6.33169E-11	6.08505E-11

5	2.75498E-08	2.52375E-08	13	0.	0.
6	2.52388E-08	2.25326E-08	14	0.	0.
7	2.25402E-08	1.94899E-08	15	0.	0.
8	1.95021E-08	1.61466E-08	16	0.	0.

21	8.01995E-11	7.70963E-11	28	6.08396E-11	5.84393E-11
22	7.70794E-11	7.41177E-11	29	5.84290E-11	5.60858E-11
23	7.41022E-11	7.12655E-11	30	5.60761E-11	5.37813E-11

********** ZONE EDIT 1 **********

GROUP	ZONE	ACTIVITY FOR CROSS SECTION POSITIONS 1 THRU THT		
1	1	1.9275031E+00	2.5397060E+00	3.6641373E+00
2	1	8.6788917E-01	1.0128800E+00	1.6600621E+00
3	1	8.5975289E-01	1.0002945E+00	1.4868746E+00
4	1	3.6551452E+00	4.5528804E+00	6.8110740E+00

ZONE	RELATIVE POWER DENSITY
1	4.956484E-01

********** ZONE EDIT 2 **********

GROUP	ZONE	ACTIVITY FOR CROSS SECTION POSITIONS 1 THRU THT		
1	1	1.6703610E+00	2.5055416E+00	3.1494291E+00
1	2	2.2608353E-01	0.	4.5214707E-01
1	3	3.1058545E-02	3.4164400E-02	4.2341071E-02
2	1	8.0202463E-01	1.0025308E+00	1.5513074E+00
2	2	5.7585191E-02	0.	9.2134305E-02
2	3	8.2793525E-03	1.0349191E-02	1.6618412E-02
3	1	8.5283728E-01	9.9497682E-01	1.4505959E+00
3	2	2.1297242E-03	0.	2.1297242E-02
3	3	4.7858920E-03	5.3176578E-03	7.4981478E-02
4	1	3.3252229E+00	4.5030492E+00	6.1515324E+00
4	2	2.8579845E-01	0.	6.6560041E-01
4	3	4.4123790E-02	4.9831248E-02	6.3969940E-02

ZONE	RELATIVE POWER DENSITY
1	4.932080E-01
2	0.
3	2.440309E-03

EXECUTION TIME IN SECONDS = 4.289

•• TIME ZONE PARAMETERS ••

NUMBER OF TIME STEPS = 100
NUMBER OF STEPS/PRINT = 100
NUMBER OF STEPS/DUMP = 101
FREQUENCY INDICATOR = 1
VARIABLE TIME STEP INDICATOR = 0
PRINT TRIGGERS KPI-5 = 01010
TIME STEP SIZE = 1.000000E-07

• •

TIME STEP NUMBER 200 REAL TIME= 2.000000E-05 TIME STEP SIZE= 1.000000E-07

GROUP 1 FREQUENCIES

1	6.76863E+05	6	6.76863E+05	11	6.76863E+05	15	6.76863E+05	19	6.76863E+05	23	6.76863E+05	27	6.76863E+05
2	6.76863E+05	7	6.76863E+05	12	6.76863E+05	16	6.76863E+05	20	6.76863E+05	24	6.76863E+05	28	6.76863E+05
3	6.76863E+05	8	6.76863E+05	13	6.76863E+05	17	6.76863E+05	21	6.76863E+05	25	6.76863E+05	29	6.76863E+05
4	6.76863E+05	9	6.76863E+05	14	6.76863E+05	18	6.76863E+05	22	6.76863E+05	26	6.76863E+05	30	6.76863E+05
5	6.76863E+05	10	6.76863E+05										

GROUP 2 FREQUENCIES

1	6.76863E+05	6	6.76863E+05	11	6.76863E+05	15	6.76863E+05	19	6.76863E+05	23	6.76863E+05	27	6.76863E+05
2	6.76863E+05	7	6.76863E+05	12	6.76863E+05	16	6.76863E+05	20	6.76863E+05	24	6.76863E+05	28	6.76863E+05
3	6.76863E+05	8	6.76863E+05	13	6.76863E+05	17	6.76863E+05	21	6.76863E+05	25	6.76863E+05	29	6.76863E+05
4	6.76863E+05	9	6.76863E+05	14	6.76863E+05	18	6.76863E+05	22	6.76863E+05	26	6.76863E+05	30	6.76863E+05
5	6.76863E+05	10	6.76863E+05										

GROUP 3 FREQUENCIES

1	6.76863E+05	6	6.76863E+05	11	6.76863E+05	15	6.76863E+05	19	6.76863E+05	23	6.76863E+05	27	6.76863E+05
2	6.76863E+05	7	6.76863E+05	12	6.76863E+05	16	6.76863E+05	20	6.76863E+05	24	6.76863E+05	28	6.76863E+05
3	6.76863E+05	8	6.76863E+05	13	6.76863E+05	17	6.76863E+05	21	6.76863E+05	25	6.76863E+05	29	6.76863E+05
4	6.76863E+05	9	6.76863E+05	14	6.76863E+05	18	6.76863E+05	22	6.76863E+05	26	6.76863E+05	30	6.76863E+05
5	6.76863E+05	10	6.76863E+05										

•••••••••• ZONE EDIT 1 ••••••••••

GROUP	ZONE	ACTIVITY FOR CROSS SECTION POSITIONS 1 THRU IHT		
1	1	1.5145644E+03	1.9999093E+03	2.8787478E+03
2	1	6.7134199E+02	7.8580445E+02	1.2844937E+03
3	1	6.2908434E+02	7.3231574E+02	1.0839849E+03
4	1	2.8149908E+03	3.5180295E+03	5.2474244E+03

ZONE	RELATIVE POWER DENSITY
1	3.758631E+02

•••••••••• ZONE EDIT 2 ••••••••••

GROUP	ZONE	ACTIVITY FOR CROSS SECTION POSITIONS 1 THRU IHT		
1	1	1.3159815E+03	1.9739722E+03	2.4814118E+03
1	2	1.7500379E+02	0.	3.5000757E+02
1	3	2.3579175E+01	2.5937092E+01	4.7328392E+01
2	1	6.2276135E+02	7.7845169E+02	1.2045494E+03
2	2	4.2698427E+01	0.	6.8317484E+01
2	3	5.8822094E+00	7.3527617E+00	1.1808838E+01
3	1	6.2541894E+02	7.2965543E+02	1.0637787E+03
3	2	1.2711246E+00	0.	1.2711246E+01

3	3	2.3942798E+00	2.6603108E+00	7.4949142E+00
4	1	2.5641618E+03	3.4820794E+03	4.7497599E+03
4	2	2.1897334E+02	0.	4.3103690E+02
4	3	3.1855664E+01	3.5950165E+01	4.6630145E+01

ZONE	RELATIVE POWER DENSITY
1	3.741381E+02
2	0.
3	1.724979E+00

EXECUTION TIME IN SECONDS = 9.242

```
THE FOLLOWING INPUT WAS READ AT THE END OF TIME STEP     200


INPUT MIX NUMBERS       6
          1             3             1             1             1             1

INPUT MIX COMMANDS      6
          4             4             1             1             1             1

INPUT MIX DENSITY       6
 -2.5000E-01 -2.5000E-01  0.            0.            0.            0.

INPUT R DENSITY        30
  5.0000E-01  5.0000E-01  5.0000E-01  5.0000E-01  5.0000E-01  5.0000E-01  5.0000E-01  5.0000E-01  5.0000E-01  5.0000E-01
  1.5000E+00  1.5000E+00  1.5000E+00  1.5000E+00  1.5000E+00  1.5000E+00  1.5000E+00  1.5000E+00  1.5000E+00  1.5000E+00
  5.0000E-01  5.0000E-01  5.0000E-01  5.0000E-01  5.0000E-01  5.0000E-01  5.0000E-01  5.0000E-01  5.0000E-01  5.0000E-01

MIXTURE NUMBER MIXTURE COMMAND  MATERIAL ATOMIC DENSITY
          1                4          -2.5000000E-01                1
          3                4          -2.5000000E-01                2
          1                1           0.                           3
          1                1           0.                           4
          1                1           0.                           5
          1                1           0.                           6
```

●●●●●●●●●● TIME ZONE PARAMETERS ●●●●●●●●●●

NUMBER OF TIME STEPS = 200
NUMBER OF STEPS/PRINT = 100
NUMBER OF STEPS/DUMP = 201
FREQUENCY INDICATOR = 1
VARIABLE TIME STEP INDICATOR = 0
PRINT TRIGGERS KPI-5 = 01010
TIME STEP SIZE = 1.000000E-07

● ●

TIME STEP NUMBER 300 REAL TIME= 3.000000E-05 TIME STEP SIZE= 1.000000E-07

GROUP 1 FREQUENCIES

1 -1.15651E+06	6 -1.16803E+06	11 -1.19015E+06	15 -1.19619E+06	19 -1.20273E+06	23 -1.20877E+06	27 -1.21296E+06
2 -1.15742E+06	7 -1.17244E+06	12 -1.19158E+06	16 -1.19775E+06	20 -1.20472E+06	24 -1.20988E+06	28 -1.21389E+06
3 -1.15907E+06	8 -1.17752E+06	13 -1.19309E+06	17 -1.19933E+06	21 -1.20644E+06	25 -1.21095E+06	29 -1.21477E+06
4 -1.16136E+06	9 -1.18293E+06	14 -1.19463E+06	18 -1.20097E+06	22 -1.20762E+06	26 -1.21198E+06	30 -1.21559E+06
5 -1.16434E+06	10 -1.18759E+06					

GROUP 2 FREQUENCIES

1 -1.04290E+06	6 -1.06326E+06	11 -1.12440E+06	15 -1.15503E+06	19 -1.17812E+06	23 -1.19401E+06	27 -1.20490E+06
2 -1.04442E+06	7 -1.07181E+06	12 -1.13352E+06	16 -1.16111E+06	20 -1.18382E+06	24 -1.19683E+06	28 -1.20745E+06
3 -1.04716E+06	8 -1.08234E+06	13 -1.14144E+06	17 -1.16690E+06	21 -1.18824E+06	25 -1.19958E+06	29 -1.20990E+06
4 -1.05112E+06	9 -1.09514E+06	14 -1.14853E+06	18 -1.17253E+06	22 -1.19115E+06	26 -1.20228E+06	30 -1.21225E+06
5 -1.05644E+06	10 -1.11041E+06					

GROUP 3 FREQUENCIES

1 -1.15571E+06	6 -1.18466E+06	11 -1.31209E+06	15 -1.35466E+06	19 -1.38793E+06	23 -1.40828E+06	27 -1.42088E+06
2 -1.15771E+06	7 -1.19885E+06	12 -1.32446E+06	16 -1.36356E+06	20 -1.39529E+06	24 -1.41171E+06	28 -1.42358E+06
3 -1.16128E+06	8 -1.21836E+06	13 -1.33532E+06	17 -1.37207E+06	21 -1.40081E+06	25 -1.41495E+06	29 -1.42612E+06
4 -1.16666E+06	9 -1.24551E+06	14 -1.34529E+06	18 -1.38019E+06	22 -1.40464E+06	26 -1.41801E+06	30 -1.42849E+06
5 -1.17425E+06	10 -1.28342E+06					

●●●●●●●●●● ZONE EDIT 1 ●●●●●●●●●●

GROUP	ZONE	ACTIVITY FOR CROSS SECTION POSITIONS 1 THRU IHT		
1	1	2.5359283E-04	2.5441944E-04	4.7116507E-04
2	1	1.2513784E-04	1.2063183E-04	2.2829200E-04
3	1	1.8996310E-04	2.1567194E-04	3.5050809E-04
4	1	5.6869377E-04	5.9072321E-04	1.0499652E-03

ZONE	RELATIVE POWER DENSITY
1	1.894192E-04

●●●●●●●●●● ZONE EDIT 2 ●●●●●●●●●●

GROUP	ZONE	ACTIVITY FOR CROSS SECTION POSITIONS 1 THRU IHT		
1	1	1.6706292E-04	2.5059438E-04	3.0071325E-04
1	2	8.3052579E-05	0.	1.6610516E-04
1	3	3.4773298E-06	3.8250627E-06	4.3466622E-06
2	1	9.5151337E-05	1.1893917E-04	1.8078754E-04
2	2	2.8632373E-05	0.	4.5811797E-05
2	3	1.3541300E-06	1.6926625E-06	1.6926625E-06
3	1	1.7625259E-04	2.0562802E-04	2.9375431E-04
3	2	4.6709860E-06	0.	4.6709860E-05

3	3	9.0395255E-06	1.0043917E-05	1.0043917E-05
4	1	4.3846684E-04	5.7514157E-04	7.7525511E-04
4	2	1.1635594E-04	0.	2.5862882E-04
4	3	1.3870985E-05	1.5561642E-05	1.6083242E-05

ZONE	RELATIVE POWER DENSITY
1	1.869995E-04
2	0.
3	2.419643E-06

TIME STEP NUMBER 400 REAL TIME= 4.000000E-05 TIME STEP SIZE= 1.000000E-07

GROUP 1 FREQUENCIES

1	-5.55850E+00	6	-5.70743E+00	11	-6.02604E+00	15	-6.10584E+00	19	-6.21141E+00	23	-6.32474E+00	27	-6.4044AE+00
2	-5.56972E+00	7	-5.76815E+00	12	-6.04206E+00	16	-6.12918E+00	20	-6.24845E+00	24	-6.34569E+00	28	-6.4223AE+00
3	-5.59029E+00	8	-5.84042E+00	13	-6.06247E+00	17	-6.15390E+00	21	-6.28121E+00	25	-6.36602E+00	29	-6.43920E+00
4	-5.61947E+00	9	-5.92037E+00	14	-6.08359E+00	18	-6.18096E+00	22	-6.30324E+00	26	-6.38565E+00	30	-6.45475E+00
5	-5.65820E+00	10	-5.99046E+00										

GROUP 2 FREQUENCIES

1	-4.73001E+00	6	-4.86954E+00	11	-5.38580E+00	15	-5.72A9AE+00	19	-6.089A5E+00	23	-6.41585E+00	27	-6.6299AE+00
2	-4.73982E+00	7	-4.93278E+00	12	-5.47694E+00	16	-5.8A097E+00	20	-6.20646E+00	24	-6.47141E+00	28	-6.67959E+00
3	-4.75788E+00	8	-5.01474E+00	13	-5.56244E+00	17	-5.9A41AE+00	21	-6.30101E+00	25	-6.52570E+00	29	-6.72713E+00
4	-4.78448E+00	9	-5.12049E+00	14	-5.64511E+00	18	-5.9AA22E+00	22	-6.35906E+00	26	-6.57861E+00	30	-6.77222E+00
5	-4.82106E+00	10	-5.25487E+00										

GROUP 3 FREQUENCIES

1	-5.87235E+00	6	-6.30730E+00	11	-1.04651E+01	15	-1.42458E+01	19	-2.10978E+01	23	-3.06554E+01	27	-4.27507E+01
2	-5.89891E+00	7	-6.56084E+00	12	-1.12701E+01	16	-1.55442E+01	20	-2.37583E+01	24	-3.32171E+01	28	-4.66812E+01
3	-5.94812E+00	8	-6.96258E+00	13	-1.21526E+01	17	-1.70000E+01	21	-2.62506E+01	25	-3.60622E+01	29	-5.10711E+01
4	-6.02495E+00	9	-7.65220E+00	14	-1.31270E+01	18	-1.89056E+01	22	-2.83455E+01	26	-3.92265E+01	30	-5.59813E+01
5	-6.13912E+00	10	-8.99272E+00										

•••••••••• ZONE EDIT 1 ••••••••••

GROUP	ZONE	ACTIVITY FOR CROSS SECTION POSITIONS 1 THRU 1HT		
1	1	5.3030068E-05	5.4643741E-05	6.8384295E-05
2	1	3.3720067E-05	3.4096939E-05	4.1968A16E-05
3	1	3.2272395E-05	3.7276111E-05	5.6240A53E-05
4	1	1.1902253E-04	1.2601679E-04	2.1659376E-04

ZONE	RELATIVE POWER DENSITY
1	2.703977E-05

•••••••••• ZONE EDIT 2 ••••••••••

GROUP	ZONE	ACTIVITY FOR CROSS SECTION POSITIONS 1 THRU 1HT		
1	1	3.5955116E-05	5.3932675E-05	6.4719209E-05
1	2	1.6428528E-05	0.	3.2857055E-05
1	3	6.4642425E-07	7.1104667E-07	8.0A03031E-07
2	1	2.7021002E-05	3.3776252E-05	5.1339904E-05
2	2	6.4425157E-06	0.	1.030A025E-05
2	3	2.5654945E-07	3.2068681E-07	3.206AA31E-07
3	1	3.1725792E-05	3.7013424E-05	5.2876320E-05

3	2	3.1018457E-07	0.	3.1018457E-06
3	3	2.3641836E-07	2.6268707E-07	2.6268707E-07
4	1	9.4701910E-05	1.2472235E-04	1.6893543E-04
4	2	2.3181228E-05	0.	4.6264926E-05
4	3	1.1393921E-06	1.2944406E-06	1.3914042E-06

ZONE	RELATIVE POWER DENSITY
1	2.691078E-05
2	0.
3	1.289880E-07

EXECUTION TIME IN SECONDS = 19.230

TIME ZONE PARAMETERS

NUMBER OF TIME STEPS = 200
NUMBER OF STEPS/POINT = 200
NUMBER OF STEPS/DUMP = 201
FREQUENCY INDICATOR = 1
VARIABLE TIME STEP INDICATOR = 0
PRINT TRIGGERS KPI-5 = 01011
TIME STEP SIZE = 1.000000E-06

TIME STEP NUMBER 600 REAL TIME= 2.400000E-04 TIME STEP SIZE= 1.000000E-06

GROUP 1 FLUX COMPONENTS(ISOTROPIC)

1	3.01701E-05	3.06767E-05	9	1.77791E-05	1.47570E-05	17	3.79496E-06	3.25702E-06	24	1.86162E-06	1.80801E-06
2	3.03700E-05	2.98112E-05	10	1.47944E-05	1.18711E-05	18	3.24582E-06	2.79094E-06	25	1.80764E-06	1.75669E-06
3	2.97365E-05	2.86688E-05	11	1.14339E-05	9.22350E-06	19	2.78175E-06	2.39142E-06	26	1.75635E-06	1.70780E-06
4	2.86374E-05	2.71146E-05	12	9.16426E-06	7.55404E-06	20	2.38373E-06	2.04300E-06	27	1.70749E-06	1.66112E-06
5	2.71066E-05	2.52055E-05	13	7.51366E-06	6.28134E-06	21	2.04283E-06	1.97930E-06	28	1.66083E-06	1.61645E-06
6	2.52127E-05	2.29842E-05	14	6.25161E-06	5.27915E-06	22	1.97884E-06	1.91899E-06	29	1.61618E-06	1.57362E-06
7	2.30026E-05	2.04890E-05	15	5.25658E-06	4.47147E-06	23	1.91857E-06	1.86201E-06	30	1.57336E-06	1.53244E-06
8	2.05156E-05	1.77464E-05	16	4.45394E-06	3.80886E-06						

GROUP 1 FREQUENCIES

1	-2.94577E+00	6 -2.94650E+00	11 -2.94797E+00	16 -2.94777E+00	19 -2.94792E+00	23 -2.94827E+00	27 -2.94837E+00		
2	-2.94581E+00	7 -2.94682E+00	12 -2.94787E+00	14 -2.94777E+00	20 -2.94806E+00	24 -2.94831E+00	28 -2.94838E+00		
3	-2.94591E+00	8 -2.94720E+00	13 -2.94781E+00	17 -2.94780E+00	21 -2.94817E+00	25 -2.94834E+00	29 -2.94837E+00		
4	-2.94605E+00	9 -2.94763E+00	14 -2.94778E+00	18 -2.94784E+00	22 -2.94822E+00	26 -2.94836E+00	30 -2.94836E+00		
5	-2.94624E+00	10 -2.94795E+00							

GROUP 2 FLUX COMPONENTS(ISOTROPIC)

1	1.20517E-05	1.20684E-05	9	6.52975E-06	5.22150E-06	17	1.60248E-06	1.42115E-06	24	9.20983E-07	8.97767E-07
2	1.20059E-05	1.17208E-05	10	5.22642E-06	3.78185E-06	18	1.41876E-06	1.26033E-06	25	8.97727E-07	8.74864E-07
3	1.17002E-05	1.12246E-05	11	3.74656E-06	3.14977E-06	19	1.25830E-06	1.11874E-06	26	8.74832E-07	8.52274E-07
4	1.12147E-05	1.05575E-05	12	3.14051E-06	2.72034E-06	20	1.11701E-06	9.93128E-07	27	8.52242E-07	8.29939E-07
5	1.05540E-05	9.73870E-06	13	2.71412E-06	2.34255E-06	21	9.93462E-07	9.68841E-07	28	8.29907E-07	8.07804E-07
6	9.73922E-06	8.78411E-06	14	2.35729E-06	2.04708E-06	22	9.68793E-07	9.44698E-07	29	8.07775E-07	7.85820E-07
7	8.78749E-06	7.70913E-06	15	2.06289E-06	1.81819E-06	23	9.44653E-07	9.21025E-07	30	7.85793E-07	7.63934E-07
8	7.71438E-06	6.52376E-06	16	1.81477E-06	1.60532E-06						

GROUP 2 FREQUENCIES

1	-2.97937E+00	6 -2.97942E+00	11 -2.98314E+00	16 -2.99467E+00	19 -3.03259E+00	23 -3.08251E+00	27 -3.09513E+00		
2	-2.97935E+00	7 -2.97954E+00	12 -2.98481E+00	14 -3.00023E+00	20 -3.05287E+00	24 -3.08726E+00	28 -3.09573E+00		
3	-2.97934E+00	8 -2.97979E+00	13 -2.98715E+00	17 -3.00784E+00	21 -3.06942E+00	25 -3.09091E+00	29 -3.09535E+00		
4	-2.97934E+00	9 -2.98030E+00	14 -2.99033E+00	18 -3.01822E+00	22 -3.07640E+00	26 -3.09352E+00	30 -3.09395E+00		
5	-2.97936E+00	10 -2.98147E+00							

GROUP 3 FLUX COMPONENTS(ISOTROPIC)

1	9.40157E-06	9.37423E-06	9	5.10934E-06	4.14243E-06	17	2.14476E-06	2.01085E-06	24	1.50782E-06	1.46813E-06
2	9.34038E-06	9.11013E-06	10	4.14972E-06	3.11627E-06	18	2.01142E-06	1.88282E-06	25	1.46799E-06	1.42981E-06
3	9.09736E-06	8.72358E-06	11	3.13099E-06	2.92844E-06	19	1.88324E-06	1.75894E-06	26	1.42968E-06	1.39280E-06
4	8.71723E-06	8.20494E-06	12	2.93254E-06	2.74999E-06	20	1.75926E-06	1.63825E-06	27	1.39268E-06	1.35693E-06
5	8.20269E-06	7.56924E-06	13	2.75278E-06	2.58444E-06	21	1.63890E-06	1.52316E-06	28	1.35683E-06	1.32205E-06
6	7.56966E-06	6.83027E-06	14	2.58661E-06	2.42946E-06	22	1.52298E-06	1.54956E-06	29	1.32196E-06	1.28802E-06
7	6.83272E-06	6.00338E-06	15	2.43109E-06	2.28323E-06	23	1.54939E-06	1.50797E-06	30	1.28794E-06	1.25472E-06
8	6.00750E-06	5.10369E-06	16	2.28427E-06	2.14399E-06						

GROUP 3 FREQUENCIES

1 -3.06499E+00	6 -3.06364E+00	11 -3.06404E+00	15 -3.07444E+00	19 -3.10260E+00	23 -3.13350E+00	27 -3.14317E+00
2 -3.06487E+00	7 -3.06319E+00	12 -3.06400E+00	16 -3.07056E+00	20 -3.11405E+00	24 -3.13713E+00	28 -3.14363E+00
3 -3.06467E+00	8 -3.06278E+00	13 -3.06717E+00	17 -3.08678E+00	21 -3.12351E+00	25 -3.13994E+00	29 -3.14332E+00
4 -3.06439E+00	9 -3.06259E+00	14 -3.07036E+00	18 -3.09334E+00	22 -3.12898E+00	26 -3.14194E+00	30 -3.14224E+00
5 -3.06405E+00	10 -3.06312E+00					

********** ZONE EDIT 1 **********

GROUP	ZONE	ACTIVITY FOR CROSS SECTION POSITIONS 1 THRU THT		
1	1	5.2998858E-05	5.4611589E-05	9.8326392E-05
2	1	3.3699988E-05	3.4076665E-05	6.1931726E-05
3	1	3.2252626E-05	3.7253281E-05	6.6206383E-05
4	1	1.1895147E-04	1.2594153E-04	2.1446450E-04

ZONE	RELATIVE POWER DENSITY
1	2.702359E-05

********** ZONE EDIT 2 **********

GROUP	ZONE	ACTIVITY FOR CROSS SECTION POSITIONS 1 THRU THT		
1	1	3.5933961E-05	5.3900941E-05	8.4681130E-05
1	2	1.6418854E-05	0.	3.2837708E-05
1	3	6.4604345E-07	7.1064780E-07	8.0756432E-07
2	1	2.7004941E-05	3.3756176E-05	5.1309387E-05
2	2	6.4386557E-06	0.	1.0301849E-05
2	3	2.5639119E-07	3.2048898E-07	3.2048898E-07
3	1	3.1706369E-05	3.6990764E-05	5.2843948E-05
3	2	3.0999178E-07	0.	3.0999178E-06
3	3	2.3626522E-07	2.6251691E-07	2.6251691E-07
4	1	9.4645271E-05	1.2464788E-04	1.6883447E-04
4	2	2.3167502E-05	0.	4.6239475E-05
4	3	1.1386999E-06	1.2936537E-06	1.3905602E-06

ZONE	RELATIVE POWER DENSITY
1	2.689468E-05
2	0.
3	1.289095E-07

EXECUTION TIME IN SECONDS = 29.170

IV. PROGRAMMING INFORMATION

In this section we give some of the details of the TIMEX program. The material contained in this section is designed to help in the local modification of the program. Much supplementary information is provided by the program comment cards.

A. Program Structure

1. Role and Function of Subprograms

We describe in Table IX the function of all the subprograms in TIMEX.

2. Relation of Problem Variables and Program Mnemonics

In much of the material in this manual we have used variables actually appearing in the FORTRAN of the program. A list of the relations between problem variable symbols and program variable names is given in Table X.

3. Definition of Variables in Common Blocks

Tables XI and XII define the variables stored in blank common block IA and the named common block of ONETRAN. The container array, A, for problem data is also in blank common. Block IA contains problem input parameters, first word addresses of data stored in the A array, and data generated by the program.

TABLE IX

FUNCTION OF TIMEX SUBROUTINES

Subroutine	Function
TIMEX	Main driver of program. Initializes program parameters; calls input, initialization, computation, and output routines; performs time-step incrementing.
	Input Functions
INPUT1	Reads header and control integer and floating point variables, performs some checking of input data.
INPUT2	Calculates commonly used integers, large and small core storage pointers; calls various input subroutines; reads problem-dependent input arrays; performs more checking of input data; reads new problem-dependent input arrays at beginning of each time zone as required.
SNCON	Reads or generates S_N quadrature constants; calculates some indexing arrays and spherical harmonic polynomials.
IFINSN	Reads S_N constants from interface file ISNCON.
FACT	Calculates factorial function for use in SNCON.
CSPREP	Reads cross sections in standard LASL format, FIDO format, or from interface file by calling IFINXS. Prints cross sections, performs adjoint transpositions and reversals of cross sections, checks cross sections for consistency, and stores cross sections in LCM.
IFINXS	Interface input of cross sections from standard interface file ISOTXS.
READF	Reads angular flux initial condition and precursor concentration initial condition.
IFINF	Reads angular flux initial condition from standard interface file IAFLUX.
READQ	Reads distributed and boundary sources from cards or standard interface file by calling IFINQ.
IFINQ	Reads distributed and boundary sources from standard interface file FIXSRC.
	Initialization Functions
INITAL	Performs mixing of cross sections, calculates geometric functions by call to GEOFUN, initializes inhomogeneous sources by call to INITQ and fission arrays by call to INITF, calculates macroscopic cross-section arrays.
GEOFUN	Calculates various geometric functions on the coarse and fine mesh.
REBOUND	Interpolates the scalar and angular fluxes onto the new mesh in a manner that conserves neutrons at the start of each time zone when a coarse-mesh boundary is altered.
INITQ	Generates volume and surface integrals of inhomogeneous sources, normalizes sources, stores boundary sources in boundary flux arrays.

TABLE IX (continued)

Subroutine	Function
INITF	Calculates total delayed neutron fraction, multiplies delayed neutron spectra by λ_k, computes $\chi\ \nu\Sigma_f$ array for fission source and transposes for adjoint problems, calculates volume integral of fission source and normalizes fluxes.
	Computation Functions
OUTER	Performs the loop over the energy groups, calculates source to the group by call to SOURCE, calculates angular flux for the group by call to SWEEP, generates fission source on the fine mesh, calculates precursor concentrations by call to PCALC.
UNCOLL	Computes the uncollided flux and stores in LCM.
SOURCE	Calculates source to the group from inhomogeneous sources, fission and inscattering from other groups, calculates total source for rebalance.
SCALE	Multiplies the flux moments by $e^{\omega\Delta t}$ if the exponential extrapolation is in effect.
PCALC	Calculates the delayed neutron precursor concentrations on the fine mesh.
OREBAL	Performs outer rebalance of the angular flux and flux moments.
SWEEP	Performs sweep of the space-angle mesh for a group. Adds within-group scattering and fission to source, solves the 2x2 system for the cell-edge angular fluxes, performs fine-mesh rebalance, computes exponential extrapolation frequencies ω_i.
SETBC	Sets the angular flux boundary condition on either boundary. Called by SWEEP.
REBAL	Performs inversion of tridiagonal matrix for group fine-mesh rebalance factors.
	Output Edit Functions
FINAL	Controls edit output. Prints flux moments, angular fluxes, exponential extrapolation frequencies, fission rates, and precursor concentrations by call to EDIT; performs zone edits by call to ZEDIT, plots fluxes by call to PLOTTR, writes interface files by call to IFRITE.
EDIT	Prints flux moments, angular fluxes, exponential extrapolation frequencies, fission rates, and precursor concentrations.
ZEDIT	Calculates zone macroscopic activities, constituent activities, microscopic activities, and power densities.
	Service Routines
PRINTP	Prints input control integer and floating point variables.
MAPPER	Draws material map of system.
DUMPER	Reads or writes restart dump.
CLEAR	Clears an array to a specified value.
LOAD	Los Alamos data loader.
IFRITE	Writes standard interface files RTFLUX or ATFLUX and RAFLUX or AAFLUX.
PRNT	Prints output arrays in a down-the-page format.
WRITE	Routine for printing 1D, 2D, or 3D arrays, either integer or floating point.
REED	Handles all binary reading operations including rewind and LCM memory transfers.
RITE	Handles all binary writing operations including end-of-file and LCM memory transfers.
PLOTTR	Plots scalar flux on film file NFILM. Calls numerous system-dependent plotting routines.

TABLE X

RELATION OF PROBLEM VARIABLES TO PROGRAM MNEMONICS

Program Mnemonic	Subroutine	Problem Variable	Refer to
PN(NM,MM)	SNCON,SWEEP	$R_n(\underline{\Omega})$	Eqs. (10),(11)
C(IHM,MT)	SOURCE,SWEEP	$\sigma_a, \nu\sigma_f, \sigma, \sigma^n_{s,h\to g}$	Sec. II.B.1.
WGT(MM)	SNCON,SWEEP	w_m	Sec. II.B.3.
U(MM)	SNCON,SWEEP	μ_m	Sec. II.B.3.
WMU(MM)	SNCON,SWEEP	$w_m\ \mu_m$	Sec. II.B.3.
CT(IT)	INITAL,SWEEP	σ	Sec. II.B.1.
CS(IT)	INITAL,SWEEP	$\sigma^o_{s,g\to g}$	Sec. II.B.1.
BP(MM)	SNCON,SWEEP	$\alpha_{m+\frac{1}{2}}/w_m$	Sec. II.B.3.
BM(MM)	SNCON,SWEEP	$\alpha_{m-\frac{1}{2}}/w_m$	Sec. II.B.3.
FL(IM+1)	SWEEP,REBAL	$FL_{k\pm\frac{1}{2}}$	Eq. (55)
FR(IM+1)	SWEEP,REBAL	$FR_{k\pm\frac{1}{2}}$	Eq. (55)
AB(IM)	SWEEP,REBAL	AB_k	Eq. (55)
F(IM)	SWEEP,REBAL	f_k	Eq. (54)
Z(10,IT)	SWEEP,GEOFUN	z_i	Table V
V(2,IT)	SWEEP,GEOFUN	V-, V+	Table V
AI(IM+1)	SWEEP,GEOFUN	A-, A+	Table V
Q(NM,2,IT)	SOURCE,SWEEP	Source to group moments	Sec. II.C.
FLUX(NM,2,IT)	SWEEP	Flux moments	Sec. II.C.
S1,S2	SWEEP	$S_{i-\frac{1}{2}}, S_{i+\frac{1}{2}}$	Sec. II.C.
PSIB	SWEEP	ψ_b	Eq. (39)
AFE(NLEV,IT)	SWEEP	$\psi_{m\pm\frac{1}{2}}$	Sec. II.C.
AFC(2,IT)	SWEEP	$\psi_{i\pm\frac{1}{2}}$	Eq. (39)
AF1,AF2	SWEEP	$\psi_{i-\frac{1}{2}}, \psi_{i+\frac{1}{2}}$	Eq. (39)
KSTEP	MAIN	Time step index, j+1	Eq. (16)
RTIME	MAIN	Time variable, t^{j+1}	Sec. II.B.2.
PC(2,IT)	SOURCE,PCALC	Precursor concentrations	Eq. (16b)
RVT	OUTER,SWEEP	$1/v\Delta t$	Eqs. (18), (19)
ORSOR	SOURCE,OREBAL	Outer rebalance source	Eq. (59)
ORABS	SWEEP,OREBAL	Outer rebalance absorption	Eq. (59)
ORLEAK	SWEEP,OREBAL	Outer rebalance leakage	Eq. (59)
ORFACT	OREBAL	Outer rebalance factor	Eq. (58)
DELTAT	MAIN,SWEEP	Δt	Sec. II.B.2.
FREQ(IT)	SCALE,SWEEP	ω_i	Sec. II.D.5.a.
T1(IT)	SWEEP	$\frac{1}{v\Delta t} - \frac{\omega_-}{v}$	Sec. II.D.5.a.
T2(IT)	SWEEP	$\frac{1}{v\Delta t} + \frac{\omega_+}{v}$	Sec. II.D.5.2.

TABLE XI

CONTENTS OF BLANK COMMON BLOCK IA*

Position	Name	Pointer for Array	Remarks
1	ITH		Theory
2	ISCT		Scattering order
3	ISN		S_N order
4	IGM		Number of energy groups
5	IM		Number of coarse-mesh intervals
6	IBL		Left boundary condition indicator
7	IBR		Right boundary condition indicator
8	IGD		Number of delayed neutron groups
9	ISTART		Angular flux intial condition indicator
10	IQOPT		Source input option indicator
11	IGEOM		Geometry indicator
12	IQUAD		Source of S_N constants indicator
13	MT		Total number of materials
14	MTP		Number of cross-section materials from ISOTXS file
15	MCR		Number of cross-section materials from cards
16	MS		Number of mixture instructions
17	IHT		Position of total cross section in table
18	IHS		Position of self-scatter cross section in table
19	IHM		Cross-section table length
20	IDEN		Space-dependent density factor trigger
21	IQAN		Distributed source anisotropy order
22	IQL		Left boundary source trigger
23	IQR		Right boundary source trigger
24	IACC		Acceleration option indicator
25	IPCOPT		Precursor concentration initial condition indicator
26	I1		Initial flux print suppression trigger
27	I2		Time zone flux print trigger
28	IFISS		Fission fraction-type indicator
29	KP5		Flux components print trigger
30	ITN		Initial time step index for restart
31	ITLIM		Time limit for problem
32	I3		Cross-section print indicator
33	IFO		Interface file output trigger
34	I4		Time zone fission print trigger
35	I5		Source print trigger
36	I6		Fine-mesh geometry table print suppress indicator
37	ITXS		Time-dependent cross-section indicator
38	ITQ		Time-dependent source indicator
39	ITB		Time-dependent coarse-mesh boundary indicator
40	ITIDXS		Time-dependent cross-section i.d. indicator
41	ITFISS		Time-dependent fission fraction indicator

*Blank entries are available for future use.

TABLE XI (continued)

Position	Name	Pointer for Array	Remarks
42	ITVEL		Time-dependent velocities indicator
43	ITMIX		Time-dependent mixture instruction indicator
44	ITDEN		Time-dependent density factors indicator
45	ITLBDO		Time-dependent left albedo indicator
46	ITRBDO		Time-dependent right albedo indicator
47	ITDELY		Time-dependent delayed neutron parameters indicator
48	INDTS		Group-dependent time step indicator
49	IFCS		First collision source indicator
50	KP1		Delayed neutron precursor print trigger
51	KP2		Zone edit print trigger
52	KP3		Angular flux print trigger
53	KP4		Exponential extrapolation factors print trigger
54	IPLOT		Plotting option trigger
55			
56			
57			
58			
59			
60			
61			
62			
63			
64			
65			
66			
67			
68			
69			
70			
71			
72	NORM		Normalization amplitude
73	BHGT		Buckling height
74	BWTH		Buckling width
75			
76			
77			
78			
79			
80	RTIME		Problem real time
81	TIME		Execution or clock time
82			
83			
84			
85			
86			

TABLE XI (continued)

Position	Name	Pointer for Array	Remarks
87			
88			
89			
90			
91			
92			
93			
94			
95			
96			
97			
98			
99			
100	NLEV		Number of quadrature ξ levels
101	MIN		Total number of input cross-section blocks = MCR + MTP*(ISCT+1)
102			
103	IHF		Position of $\nu\sigma_f$ in cross-section table = IHT-1
104	IHA		Position of σ_a in cross-section table = IHT-2
105	MM		Number of quadrature angles
106	NM		Number of spherical harmonic and flux moments
107	NMQ		Number of distributed source moments
108	M2		MM/2
109	NN		ISN/2
110	IP		Number of coarse-mesh points = IM+1
111	IGP		IGM+1
112	IHMT		IHM*MT
113	ISCP		ISCT+1
114	M2P		M2+1
115			
116	ITP		Number of fine-mesh points = IT+1
117	IHTR		Position of σ_{tr} in cross-section table = IHT-3
118	IMGP		IM*IGM
119	IT		Number of fine-mesh intervals
120	IHNN		Position of $\sigma_{n,2n}$ in cross-section table = IHT-4
121	IPGP		IP*IGM
122	IFISP		Zone-dependent fission fraction trigger
123	LFLM		Last address of flux block
124			
125	KM		IM for zone-dependent fission fractions, 1 otherwise
126			
127	KEND		Last LCM position used
128	LAST		Last small core position used
129			

TABLE XI (continued)

Position	Name	Pointer for Array	Remarks
130			
131	LIHR	IHR(IM+1)	Number of fine-mesh intervals per coarse mesh
132	LW	W(MM)	Point weights
133	LU	U(MM)	Point cosines
134	LWM	WM(MM)	Point weights*cosines
135	LBP	BP(MM)	$\alpha_{m+\frac{1}{2}}/w_m$
136	LBM	BM(MM)	$\alpha_{m-\frac{1}{2}}/w_m$
137	LDM	MD(MM)	Reflected direction index
138			
139			
140	LUB	UB(ISN)	Level cosines
141	LWB	WB(ISN)	Level weights
142	LUSTRT	USTRT(NLEV)	Starting direction cosines
143	LUFW	UFW(NM)	Cylindrical geometry uncollided flux coefficients
144	LPN	P(NM,MM)	Spherical harmonic functions
145	LLI	LI(MM)	Level indices
146	LFT	FT(2*ISCT+1)	Factorials
147			
148			
149			
150	LC	C(IHM,MT)	Cross-section blocks for a group
151	LAAJ	AAJ(MT)	Effective absorption cross section
152	LCT	CT(IT)	Total cross section * density
153	LCS	CS(IT)	Self-scatter cross section * density
154	LCA	CA(IT)	Absorption cross section * density
155			
156	LDC	IDC(IM+1)	Cross-section identification number for each coarse-mesh interval
157	LMN	MIXNUM(MS)	Mixture numbers
158	LMC	MIXCOM(MS)	Mixture commands
159	LMD	MIXDEN(MS)	Mixture densities
160			
161	LDEN	DEN(IT)	Fine-mesh densities
162			
163			
164			
165			
166	LQ	Q(NM,2,IT)	Distributed source moments
167	LQR	QR(MM/2)	Right boundary source
168	LQL	QL(MM/2)	Left boundary source
169	LFL	FLUX(NM,2,IT)	Flux moments
170			
171			
172	LOMG	FREQ(IT)	Exponential extrapolation factors

TABLE XI (continued)

Position	Name	Pointer for Array	Remarks
173			
174			
175	LBL	BL(MM)	Left boundary flux
176	LBR	BR(MM)	Right boundary flux
177	LAFE	AFE(NLEV,IT)	Edge angular flux for angular extrapolation
178	LAFC	AFC(2,IT)	Mesh cell edge angular flux
179			
180			
181			
182	LPC	PC(2,IT)	Delayed neutron precursor concentrations
183			
184	LFISS	FISS(2,IT)	Fission rate
185	LLAM	LAM(KM,IGD)	Delayed neutron precursor decay constants
186	LBETA	BETA(KM,IGD)	Delayed neutron precursor fractions
187	LPS	PS(KM,IGD,IGM)	Delayed neutron precursor fission fractions
188	LRAD	RAD(IM+2)	Coarse-mesh boundary radii
189	LIDR	IDR(IT+2)	Coarse-mesh zone identifier on the fine mesh
190	LH	H(IM+1)	Fine-mesh Δr_i in each coarse mesh
191	LAI	AI(IT+1)	Fine-mesh area elements
192	LV	V(2,IT+1)	Fine-mesh volume elements
193	LT1	T1(IT) and T2(IT)	$(\frac{1}{v\Delta t} - \frac{\omega_-}{v})$ and $\sigma + \frac{1}{v\Delta t} + \frac{\omega_+}{v}$
194	LZ	Z(10,IT)	Finite element polynomials on the fine mesh
195			
196			
197	LR	R(IT+1)	Fine-mesh radii r_i
198			
199			
200	LRDA	RADA(IT+1)	Fine-mesh radii from previous time zone
201	LDEL	DEL(IM+1)	Coarse-mesh thickness
202			
203			
204			
205	LUFS	UFS(IGM)	Uncollided flux spectrum
206	LIUF	IUF(IGM)	Mesh position of uncollided flux
207	LIGT	IGTSF(IGM)	Number of time steps per group
208	LQG	QG(IGP)	Inhomogeneous source to a group
209	LFG	FG(IGP)	Fission source to a group
210			
211			
212			
213			
214			
215			
216			

TABLE XI (continued)

Position	Name	Pointer for Array	Remarks
217	LCHI	CHI(IM,IGM)	Fission matrix ($\chi\ \nu\sigma_f$) or fission fractions χ
218	LVEL	VEL(IGP)	Group speeds
219			
220	LLB	LB(IGP)	Left boundary group albedo
221	LRB	RB(IGP)	Right boundary group albedo
222	IGSV		Group index of v_{max}
223	IGLV		Group index of v_{min}
224	LBATA	BATA(KM)	Total delayed neutron fractions by zone
225			
226			
227	LF	F(IT)	Fine-mesh rebalance factors
228	LFR	FR(IT+1)	Fine-mesh boundary right flows
229	LFLL	FL(IT+1)	Fine-mesh boundary left flows
230	LAB	AB(IT)	Effective rebalance absorption
231	LQQ	QQ(IT)	Total rebalance source (fission + inscatter + inhomogeneous)
232			
233			
234	LHA	HA(IT)	Work vector for rebalance inversion
235	LGA	GA(IT)	Work vector for rebalance inversion
236	LFGG	FGG(IM,IGM)	Fission matrix $\chi\ \nu\sigma_f$
237	LSGG	SGG(IM,IGM)	Scattering matrix
238			
239			
240			
241			
242			
243			
244	LENC		Length of LCM cross-section block: LDC-LC
245	LENQ		Length of LCM inhomogeneous source block: LFL-LQ
246	LENF		Length of LCM flux block: LAFE-LFL
247	LENS		Length of LCM source to group block: NM*2*IT
248	LNAF		Length of LCM angular flux block: 2*IT
249	LNFS		Length of LCM fission spectrum: IM*IGM
250	LENPC		Length of LCM precursor concentration block: 2*IT
251			
252			
253	LNUF		Length of LCM uncollided flux block: IT
254			
255	KAFTST		Origin of LCM temporary starting direction angular flux array
256	KC		Origin of LCM cross-section array
257	KQ		Origin of LCM source array
258	KF		Origin of LCM flux array

TABLE XI (continued)

Position	Name	Pointer for Array	Remarks
259	KS		Origin of LCM source to group array
260	KAF		Origin of LCM angular flux array
261	KFS		Origin of LCM fission spectrum array
262	KPC		Origin of LCM precursor concentration array
263	KAFT		Origin of LCM temporary angular flux array
264	KAFST		Origin of LCM starting direction angular flux array
265	KF2		Origin of LCM scalar flux array from previous time step
266	KUF		Origin of LCM uncollided flux array
267	KCHI		Origin of LCM original fission fractions array
268	IGT or IGTSF		Number of time steps/group for a group
269	ALR		Right boundary albedo for a group
270	ALL		Left boundary albedo for a group
271	SUMMUL		$\sum_m w_m \mu_m$ for leftward directions
272	SUMMUR		$\sum_m w_m \mu_m$ for rightward directions
273			
274			
275			
276			
277			
278	NZEDS		Number of zone edits
279	LIDCA	IDCA(NCA)	Cross-section material i.d. numbers for constituent activities
280	LIDMA	IDMA(NMA)	Cross-section material i.d. numbers for microscopic activities
281	LACT	ACT(IHT,NZ)	Zone activities for a group
282	LTACT	TACT(IHT,NZ)	Group sum zone activities
283	LPOW	POW(NZ)	Zone power densities
284	LNEDZ	NEDZ(IT)	Zone identification numbers
285	NRECS		Number of records in a dump file for each time step
286	IPRNT		Print initialization trigger for subroutine PRNT
287	IUPTOT		Signed value of IHS
288	ORSOR		Outer rebalance source
289	ORLEAK		Outer rebalance leakage
290	ORABS		Outer rebalance absorption
291	G		Group index
292	IMOV		Plotting trigger
293	FMIN		Minimum scalar flux value for movie plot
294	FMAX		Maximum scalar flux value for movie plot
295	NSPMP		Number of time steps per movie plot
296	TFO		Total volume-energy integrated scalar flux at t=0
297	RVT		$1/v\Delta t$ for a group
298	DELTAT		Time step size Δt
299	KSTEP		Time step index
300	IFREQ		Exponential extrapolation trigger

TABLE XII

CONTENTS OF NAMED COMMON BLOCK/UNITS/

(The named common block UNITS contains the symbolic names of all input, output, and scratch devices required by TIMEX and which are set in the main program TIMEX.)

Position	Name	Contents and Remarks
1	NINP	Problem code-dependent decimal input
2	NOUT	Problem decimal output
3	NDMP1	First restart dump unit
4	NDMP2	Second restart dump unit (not used)
5	ISNCON	Interface form of S_N constants
6	ISOTXS	Interface form of multigroup cross-section file ISOTXS
7	IFIXSR	Interface form of inhomogeneous source (Q-source)
8	IAFLUX	Interface form of angular flux
9	ITFLUX	Interface form of total flux
10	NFILM	Plotting routine output
11	NEDIT	Scratch unit used for zone edit input
12	NEXTRA	Scratch unit used in subroutine LOAD
13	NTIMEX	Special angular flux file for TIMEX initial condition from ONETRAN steady-state calculation

4. Machine-Dependent Subprogram

a. LCM System Routines

LCM (large core memory) is a large bulk memory from which blocks of words may be quickly transferred to or from SCM (small core memory). This random bulk memory is accessed through two system routines -- ECRD (transfer LCM to SCM) and ECWR (transfers SCM to LCM) -- which process consecutive words of SCM and consecutive words of LCM given an SCM address and a pointer value for LCM. The pointer value given may be thought of as the index of a container array. To read from or write into a block of core, it is necessary to provide the read/write routines with the core origin, the LCM pointer value and the number of consecutive words to be transferred. For example, if we consider reading the entire FLUX block for group IG from LCM to SCM, we would have the FORTRAN IV statement

```
CALL REED(0,KF+(IG-1)*LENF,FLUX,LENF,1)
```

which is equivalent to

```
CALL ECRD(FLUX,KF+(IG-1)*LENF,LENF,IER).
```

In these statements FLUX is the SCM container array, KF+(IG-1)*LENF is the location of the first word of the IG^{th} group flux array in LCM, and LENF words are transferred. IER is an error indicator.

b. General System Routines

Additional system routines required by the code are SECOND (obtains current time), DATE1 (obtains current date), ATAN (arctangent), SQRT (floating-point square root), EXIT (returns control to system for next job), COS (cosine), SIN (sine), EXP (exponential), and ALOG (natural logarithm).

Use of the end-of-file test is made in INPUT1 to detect the last case of a sequence of cases. The test must be replaced by an equivalent statement to obtain a normal exit.

The subroutine PLOTTR, which plots the scalar flux on a film file NFILM, calls several LASL plotting subroutines. These 15 routines are described with comment cards in the code listing to facilitate the user's conversion of the routine to the plotting software of his installation.

B. External and Internal Data Files

All files used for input, output, and scratch data are referred to by symbolic name throughout the code. The user may easily change the physical unit assigned a file by modification of the symbolic name which is initialized in the main program of TIMEX. Table XIII indicates the files required by TIMEX.

C. Hardware Requirements

The TIMEX code does not require any special hardware. The LASL CDC 7600 provides 65K (decimal) SCM and 512K LCM 60-bit words. Only 370K LCM are available to the user with the operating system and buffers using the remainder. Type 7638 disk units provide 84 million decimal words of peripheral store per unit.

D. Software Requirements

1. CDC Machines

The code was designed to operate on the CDC 7600 under the CROS operating system[18] which was developed at Los Alamos. The system uses the CDC RUN compiler with a CDC optimizer attached. The disk units provide storage for input, output, scratch, and resident files.

TABLE XIII

TIMEX FILE REQUIREMENTS

Name	Logical Unit	Contents	Remarks
NINP	10	Problem code-dependent decimal input.	The user may wish to equate this file to the system input file.
NOUT	9	Problem decimal output.	The user should equate this file to the system decimal printed output file.
NDMP1	7	Restart dump.	This unit is used to receive the each restart dump written at various time steps. The unit must contain the restart dump information when the problem is restarted. Successive dumps will be written following the dump read for the desired time step (ISTART=+3) or the unit will be rewound and the dumps written from the beginning of the file (ISTART=-3).
NDMP2	5	Restart dump.	Second restart dump unit (not used).
NEXTRA	18	Scratch file.	The file is used in the decimal mode by subroutine LOAD for Hollerith conversions rather than the core-to-core conversions given by the FORTRAN statements of ENCODE and DECODE on CDC machines.
IAFLUX	31	Interface form of angular flux (either adjoint or regular).	The code requires that this unit be used when the initial flux is requested from the angular flux interface file. The unit is rewound and the records of the first file are used as the input flux. Output of the angular fluxes in interface form is also placed on this file. The file is rewound prior to processing the fluxes and an end-of-file is placed on the file after the last write. Data for one problem only are kept on this file.
ITFLUX	30	Interface form of total flux (either adjoint or regular).	The code requires that this unit be used when the initial flux is requested from the total flux interface file. The unit is rewound and the records of the first file are used as the input flux. The interface form of the total flux is prepared on this file as problem output by rewinding the file and writing the file in standard format. An end-of-file is placed on the file after the last write instruction.
ISNCON	32	Interface form of S_N constants.	This file is used only as input for the S_N quadrature constants.
IFIXSR	33	Interface form of both distributed and boundary sources.	This file is used as input for the cell-centered inhomogeneous source. Boundary sources (if any) are also obtained from this file.
ISOTXS	34	Interface form of the cross-section multigroup file ISOTXS.	This file is only used as input when cross sections are requested from an interface file library.
NFILM	12	Film file.	This file is used as output of the plotting subroutine PLOTTR. The LASL plotting software generates a magnetic tape that is used to generate film output by an FR-80 or SC-4020 film recorder. The PLOTTR routine could be modified by the user to generate CALCOMP plotter output.

TABLE XIII (continued)

Name	Logical Unit	Contents	Remarks
NTIMEX	15	TIMEX angular flux file.	This binary angular flux file is generated by the ONETRAN code to provide exact and consistent initial conditions for TIMEX.
NEDIT	13	Scratch file.	This file is used to store the zone edit input read with the initial problem input.

2. ONETRAN for the IBM-360

Although TIMEX was written for the CDC 7600, the coding was performed so that the conversion to the IBM-360 would involve as few changes as possible. Past experience has shown that the four-byte (single-precision) floating-point mode is adequate for most problems.

The major change made in the conversion of TIMEX is the treatment of peripheral storage. The vast amount of fast core available on the IBM-360 is one of the cheaper resources of that machine. Thus the data normally stored in LCM (large core memory) are stored directly after the A container array in fast core. The CDC 7600 system routines ECRD and ECWR in subroutines REED and RITE, respectively, are replaced by simple routines which move data to and from sections of the A container array. It is thus possible to keep the LCM pointer structure of the code with no change in logic and with a slight overhead in time for data movement.

In addition to the storage reorganization, the following changes are made to effect the IBM conversion of TIMEX:

1. The subroutine DATE1, called from INPUT1, must be provided by the user to return the date as an A8 word. A local system routine must be provided for SECOND to return the floating-point value of the current time in order for the periodic and time limit dump options to work.
2. A separate subroutine is provided to process the FIDO cross-section format. The CDC 7600 algorithm to read this format uses a rewind command, resulting in a prohibitively large amount of wait time on IBM systems.
3. Hollerith 6H constants throughout the code are typed as double precision (REAL*8).
4. The IF(EOF,NINP) CDC job termination test in INPUT1 is replaced with a read using the IBM END parameter.
5. Several options are present in subroutine REED to treat the reading of interface file identification records. The information in this identification record is presently bypassed by dummy reads.

E. Programming Considerations

1. Storage Management

a. Variable Dimensioning

A single container array, A, in common is used for the blocks of data required in executing a problem. The storage of all data is consecutive and compact in the A array so that the size of a problem is limited by the total storage required rather than by the size of individual parameters. A pointer word is associated with each data block and is used to index A to locate the block. For example, LFL is the first word address of the flux block in A and A (LFL) is the first word of the flux array. When subroutine calls are written, the address of a data block, say A(LFL), is passed through the argument call. In the subroutine the data block is variably dimensioned so that it may be easily indexed by its subscripts, e.g., FLUX(N,I,J).

b. Allocation of Large Core Memory (LCM)

The allocation of storage in large core memory (LCM) is handled in the same manner as core storage. Most of the group-dependent arrays are stored in LCM so the dimensionality is IGM times the core requirement of the array. For example, there are IGM*NM*2*IT LCM locations required for FLUX(NM,2,IT).

Certain blocks of data are stored contiguously in core so that they may be read in and out of LCM in a single stream. For example, the flux block includes FLUX(NM,2,IT), BL(MM), BR(MM),

and FREQ(IT). The first word of this block is LFL, and the last word is LAFE-1. The cross-section block includes the cross sections C(IHM,MT), the effective absorption cross section, AAJ(MT), the total cross section, CT(IT), the scattering cross section, CS(IT), and the absorption cross section CA(IT). The first word of this block is LC, and the last word is LQ-1. A complete list of LCM storage is given in Table XIV.

c. Computation of Required Storage

The easiest way to compute the storage required by a problem is to load the problem for a short run and let the code compute LAST, the amount of SCM and LASTEC, the amount of LCM. The computation is made very early in problem execution and this result is printed before most of the data is read. An approximate formula for LAST is

LAST=MT*IHM + IT*(36+4*NM+NLEV).

The amount of LCM is given by

LASTEC=IGM*(MT*IHM+MT+3*MM+6*IT+4*NM*IT+2*MM*IT+IM)+2*NM*IT+IGD*IT*2+Conditional Blocks,

where the conditional block sizes are

IT if ISTART=5

plus

(MM+NLEV)*2*IT if ITB=1

plus

IGM*NLEV*2*IT if IGEOM=2 or 3

plus

IGM if IFISS=1
IGM*IM if IFISS=2
IGM^2 if IFISS=3
IGM^2*IM if IFISS=4

} if ITXS,ITFISS, ITIDXS, or ITMIX ≠ 0.

TABLE XIV

LCM STORAGE PARAMETERS

LCM First Word Address	Length per Block	Number of Blocks	Contents
KC	LENC=IHM*MT+3*IT+MT	IGM	Cross-section blocks by group
KQ	LENQ=NM*2*IT+2*MM/2	IGM	Inhomogeneous distributed and boundary sources
KF	LENF=NM*2*IT+IT+2*MM	IGM	Scalar flux and moments, boundary fluxes, and frequency extrapolation factors
KAF	LNAF=2*IT	MM*IGM	Angular flux array by group and angle
KFS	LNFS=IGM*IM	IGM	χ or $\chi\ \nu\sigma_g$ array for each group
KF2	IT	IGM	Scalar flux from previous time step for exponential extrapolation
KUF	LNUF=IT	IGM	Uncollided flux
KS	LENS=NM*2*IT	1	Source to group array
KPC	LENPC=2*IT	IGD	Delayed neutron precursors
KAFT	LNAF=2*IT	MM	Temporary angular flux array for moving boundary interpolations. Stored only if ITB≠0.
KAFTST	LNAF=2*IT	NLEV	Temporary starting direction angular flux array for moving boundary interpolations. Stored only if ITB≠0.
KAFST	LNAF=2*IT	NLEV*IGM	Starting direction angular flux array by group
KCHI	LFISS=IGM or IGM*IM	1 or IGM	Original fission fraction (χ) array. May be group- and coarse-mesh-dependent. Stored only if ITXS,ITIDXS, or ITMIX≠0.

d. Temporary Storage Requirements

The amount of fast core storage actually calculated for LAST is the maximum of two quantities, the total SCM required for problem execution and temporary SCM required for problem input. Usually, the problem data requirement is much larger than the temporary storage requirement during input, but occasionally, the input cross-section requirement (IGM*IHM*ISCP)is largest.

At each output edit, temporary storage is required if interface file output is requested. This temporary storage, allocated in subroutine FINAL, is also usually less than the problem data storage. If this temporary storage exceeds the core storage size, the writing of the interface files is not performed.

e. Overstorage of Data in Core

In TIMEX a certain amount of overstorage is used to reduce the total amount of small core memory (SCM) required; i.e., more than one array may reside in the same SCM location as the problem progresses. This is done primarily with the CHI(IM, IGM) and FGG(IM,IGM) arrays. A similar overstorage is performed when the temporary storage is allocated for input in the INPUT2 subroutine.

2. Restart Tape Composition

The restart dump is composed of the following records for each time step: common block length LENIA, common block IA, data common block A, LCM data blocks in the order in which they appear in LCM, and the contents of the zone edit scratch file, NEDIT. Each restart dump contains the time step index, KSTEP, at which the dump was taken. The problem may be restarted at time step ITN only if a dump was taken at this time step when the problem was initially run. Both the reading and writing of the restart dumps is performed by subroutine DUMPER.

3. Standard Interface Files

The standard interface files read and written by TIMEX are Version III files.[3] The coding which processes these files is all written as separate subroutines. All files are rewound prior to either reading or writing so that the interface files for several problems may not be stacked on the same file. In the reading of the interface files, the first record containing the file identification data HNAME,(HUSE(I),I=1,2), IVERS is skipped by a dummy read statement. For input or output of the scalar or angular flux files, no physical unit distinction is made for regular or adjoint problems. If a standard interface file is used for an initial angular flux and a standard interface file output is requested, the input file information is destroyed. Since the discontinuous representation (two values per mesh cell) of the distributed source and fluxes is incompatible with the standard interface file (one value per mesh cell), only the cell-centered values of these quantities are read or written.

F. Time-Dependent Sources and Cross Sections

The TIMEX user is permitted time-dependent inhomogeneous sources and cross sections only in the sense that he may input new sources and cross sections at each time zone. In order to accurately model problems with time-dependent sources and cross sections, the user must specify one time step per time zone (NTS=1), and input the new sources and cross sections at each time step. This procedure is cumbersome, may require a large quantity of input if many time steps are desired, and seriously slows down the computation.

Three dummy subroutines and their appropriate CALLs have been placed in TIMEX to facilitate user modification of the code in order to run such problems. This dummy coding appears in subroutine SOURCE as comment cards. The three dummy subroutines and their functions are:

TDQF: Scales the inhomogeneous distributed source, Q(NM,2,IT), and the boundary sources (if any), QL(MM/2) and QR(MM/2), by a user-coded explicit time-dependent function. Since the boundary sources are also stored in the boundary flux arrays, BL(MM) and BR(MM), these must also be scaled.

TDXS: Scales the cross-section array C(IHM, MT), the total cross-section array, CT(IT), the self-scatter cross-section array, CS(IT), and the effective absorption cross-section array, CA(IT), by a user-coded explicit time-dependent function.

TDFS: Scales the fission array, CHI(IM,IGM)= $\chi_{h\to g}(\nu\sigma_f)_h$, by a user-coded explicit time-dependent function.

These dummy routines are called in subroutine SOURCE immediately after the appropriate arrays are read from LCM storage. Subroutine SOURCE calculates the

source to group g and thus these arrays read from LCM are for group g only.

G. TIMEX Problems with Feedback

Because of the wide variety of possible feedback functionals, no attempt has been made to include feedback effects directly into the TIMEX code. In order for a user to run problems including feedback effects, modification of the coding is required. These modifications may be quite simple or quite complicated, depending upon the nature of the feedback functional.

REFERENCES

1. T. R. Hill, "The Linear Discontinuous Finite Element Scheme in Time-Dependent Transport Calculations," Trans. Am. Nucl. Soc. 19, 228 (1975).
2. T. R. Hill, "ONETRAN: A Discrete Ordinates Finite Element Code for the Solution of the One-Dimensional Multigroup Transport Equation," Los Alamos Scientific Laboratory report LA-5990-MS (June 1975).
3. B. M. Carmichael, "Standard Interface Files and Procedures for Reactor Physics Codes, Version III," Los Alamos Scientific Laboratory report LA-5486-MS (February 1974).
4. W. W. Engle, Jr., "A User's Manual for ANISN, A One-Dimensional Discrete Ordinates Transport Code with Anisotropic Scattering," Union Carbide Corporation report K-1693 (March 1967).
5. "Guidelines for the Documentation and Recommended Programming Practices to Facilitate American Nuclear Society Standard 10.3," ANSI N 413 (August 1973).
6. G. I. Bell, G. E. Hansen, and H. A. Sandmeier, "Multitable Treatments of Anisotropic Scattering in S_n Multigroup Transport Calculations," Nucl. Sci. Eng. 28, 375 (1967).
7. B. G. Carlson and K. D. Lathrop, "Transport Theory - Method of Discrete Ordinates," Chapter III of Computing Methods in Reactor Physics (Gordon and Breach, NY, 1968), p. 173.
8. Ibid, p. 185.
9. Ibid, p. 211.
10. K. D. Lathrop, "DTF-IV - A FORTRAN IV Program for Solving the Multigroup Transport Equation with Anisotropic Scattering," Los Alamos Scientific Laboratory report LA-3373 (1965).
11. Wm. H. Reed, T. R. Hill, F. W. Brinkley, and K. D. Lathrop, "TRIPLET: A Two-Dimensional, Multigroup, Triangular Mesh, Planar Geometry, Explicit Transport Code," Los Alamos Scientific Laboratory report LA-5428-MS (October 1973).
12. Wm. H. Reed and K. D. Lathrop, "Truncation Error Analysis of Finite Difference Approximations to the Transport Equation," Nucl. Sci. Eng. 41, 237 (1970).
13. Wm. H. Reed and K. F. Hansen, "Alternating Direction Methods for the Reactor Kinetics Equations," Nucl. Sci. Eng. 41, 431 (1970).
14. Wm. H. Reed, "The Effectiveness of Acceleration Techniques for Iterative Methods in Transport Theory," Nucl. Sci. Eng. 45,245 (1971).
15. K. D. Lathrop and F. W. Brinkley, "TWOTRAN-II: An Interfaced, Exportable Version of the TWOTRAN Code for Two-Dimensional Transport," Los Alamos Scientific Laboratory report LA-4848-MS (July 1973).
16. G. I. Bell and S. Glasstone, Nuclear Reactor Theory (VanNostrand Reinhold, NY, 1970), p. 260.
17. Ibid, p. 264.
18. "Elementary Guide to the Control Data 7600," Ray Davenport, editor, Programmer's Information Manual, Vol. 5A, Los Alamos Scientific Laboratory (1972).

☆ US GOVERNMENT PRINTING OFFICE: 1976—677-343/91